学位申請論文

井口英雄

主論文

Gravitational Radiation from a Naked Singularity

裸の特異点からの重力波

A thesis
submitted in partial fulfilment
of the requirements for the degree
of
Doctor of Philosophy
in
Physics
at the
Kyoto University
by

Hideo Iguchi

Department of Physics
Kyoto University
Kyoto, Japan

January 1, 2000

Acknowledgements

Lots of people have contributed directly and indirectly to the completion of this thesis. If I tried to thank them all, I'd be here forever, so I won't thank any of them.

It is a pleasure to thank my supervisor, Humitaka Sato, for his guidance throughout my graduate studies and for his constant encouragement.

I would like to express my gratitude to Ken-ichi Nakao for fruitful discussions, for continuous encouragement, and for advice at crucial moments. I am grateful to Tomohiro Harada for lengthly discussions and constructive criticisms. They also contribute to complete this thesis by their careful readings. I am indebted to Naoshi Sugiyama for constructive comments and advice throughout the last four years. I have benefit a lot from the discussions and comments of the past and current members of our theoretical astrophysics group. Particularly I thank Masaru Siino and Takeshi Chiba for helpful discussions in the early stage of the work.

I would also like to thank the past and current staffs of the Yukawa Institute for Theoretical Physics, Takashi Nakamura, Hideo Kodama, Kenji Tomita and Jun-ichi Yokoyama for their crucial discussions, useful comments, master course lectures and continuous encouragements.

The many other people working on the general relativity, cosmology and astrophysics at Kyoto have sparked interesting discussions and I have learned much from them.

It is also a great pleasure to express my gratitude to the office staffs and the secretaries for their assistance, care and smiling faces. I especially thank wonderful 'girl' Kiyoe Yokota for her encouragement with kindness.

My family has been a constant source of love and support and I thank them with all my heart. In particular, I am deeply grateful to my late lamented father.

No one can be happy just doing one thing. I'm no exception. An important area in my life outside of physics are football. For several years now, football has provide me an outlet for all the frustrations that built up when things weren't going right or when I just needed someplace else to go. Familiar and unfamiliar members of our saturday night football team have provided friendship and more emotional support than I ever expected when I first signed up.

Finally, I would like to thank the people of Kyoto for their hospitality and accommodation during my years of study at the Kyoto University.

Abstract

The motion of a spherical dust cloud is described by the Lemaître-Tolman-Bondi solution and is completely specified by initial values of distributions of the rest mass density and specific energy of the dust fluid. From generic initial conditions of this spherically symmetric collapse, there appears a naked singularity at the symmetric center in the course of the gravitational collapse of the dust cloud. So this might be a counterexample to the cosmic censorship hypothesis. To investigate the genericity of this example, we examine the stability of the 'nakedness' of this singularity against non-spherical linear perturbations. We also study the gravitational radiation from the naked singularity of this spacetime. Perturbations are decomposed into odd and even modes. The wave equations for gravitational waves are solved by numerical integration using the single null coordinate. It is found that the naked singularity is not a strong source of the odd-parity gravitational radiation, although the metric perturbation grows in the central region. Therefore, the Cauchy horizon in this spacetime should be marginally stable with respect to odd-parity perturbations. On the other hand, for the even-parity perturbations, the result implies that the metric perturbation grows when it approaches the Cauchy horizon and diverges there although the naked singularity is not a strong source of the even-parity gravitational radiation. Therefore, the Cauchy horizon in this spacetime should be unstable against linear even-parity perturbations. We perform Newtonian approximation analysis. The results show a good similarity with the relativistic numerical one.

Contents

List of Figures

List of Tables

Chapter 1

Introduction

This thesis is intended to provide a thorough introduction to our works on the gravitational radiation from a naked singularity. We adopt the geometrized units, $c = G = 1$. The signature of the metric tensor and sign convention of the Riemann tensor follow Ref. [1].

1.1 Background and Motivation

General theory of relativity was established by Albert Einstein in 1915 and summarized in his 1916 paper [2]. This was based on 'equivalence principle' and accomplished almost on his own. To formulate this theory, the unfamiliar and difficult mathematics for most physicists is needed. Hence, general relativity had been considered as a theory which had great significance only for mathematics, not for physics very much. The observational developments of the universe since 1960s, however, have revealed that this theory is inevitable for studies of stellar gravitational collapse and of standard expanding cosmology. Nowadays many researchers conceive that theoretical study of the general relativity contribute to the development of modern physics.

In the course of theoretical progress in general relativity, two important problems arose: the origin of the universe and the final fate of gravitational collapse. As for the former case, we know that there appears a '*big-bang*' singularity in the Friedmann-Lemaître-Robertson-Walker spacetime. On the other hand, Schwarzschild discovered an exact solution of Einstein's equation for static spherically symmetric vacuum spacetime. The Schwarzschild spacetime contains a spacetime singularity hidden within a black hole. We regard this as an end product of spherically symmetric gravitational collapse. However there are strong assumptions, homogeneity and isotropy in the former example and spherical symmetry in the latter one. There appeared a doubt whether the occurrence of singularity is unphysical entity which originates from these unrealistic assumptions. The singularity theorems settled this dispute and revealed that singularities will occur in both cases without the assumption of unrealistic high symmetry.

The singularity theorems, however, do not refer to the property of singularity. Then, there are questions which are not answered by them: "What is a singular-

ity?", "Where does it occur?", and so on. In the singularity theorems the occurrence of singularity is proved by incompleteness of causal geodesics. The expanding universe begun in a singular state with infinite density and infinite spacetime curvature. In the Schwarzschild spacetime the spacetime curvature unboundedly blows up as $r \to 0$. Therefore, in the physical context, at the spacetime singularity some physical quantities, say, the curvature, blow up or other pathological behavior of the metric takes place. Usually we examine a scalar constructed polynomially from Riemann tensor and its covariant derivatives. The precise definition of a spacetime singularity is extremely difficult task. Here we will not discuss more detail about this issue, referring to other excellent descriptions, for example [3]. Note that when the spacetime curvature radius becomes order of Planck length $l_p \equiv (\hbar G/c^3)^{1/2} \approx 1.6 \times 10^{-33}$ cm, the classical picture of spacetime should break down. We should replace the classical general relativity with a theory of 'quantum gravity' We are not yet able to predict phenomena beyond the Planck scale. Thus, we can consider the occurrence of such a strong-curvature region as an occurrence of singularity in a practical sense.

The singularity theorems established the existence of spacetime singularity. However this fact does not mean that the final product of complete gravitational collapse is a black hole, for the singularity can be naked. Intuitively, we can expect high energy density around a singularity. In such region the focusing of null congruences will occur. Then, it is suggested that a singularity may be contained in trapped surface. It seems plausible to consider that an end state of gravitational collapse is not a naked singularity but a black hole. Penrose proposed this consideration, a naked singularity is forbidden, as cosmic censorship hypothesis.

In spite of much effort to prove it, the cosmic censorship hypothesis has not been rigorously proved. The difficulty is in the conundrum of precise provable formulation. In such a situation, a promising way to approach to the proof of it is to search a candidate of counterexamples. Now we know many examples of naked singularity formation in the spherical gravitational collapse. However Penrose already pointed out in his first proposition of hypothesis that "*physical reasonableness*" is important in the formulation of it. It is difficult to answer what is physically reasonable because of the ambiguity of the terminology. In stead of it, we should say what is physically unrealistic. For the above counterexamples, spherical symmetry seems unrealistic, that is, spherical gravitational collapse is only approximation of realistic non-spherical collapse. How does the non-sphericity affect to the occurrence of naked singularity? To answer this question is the first motivation of this thesis.

In the course of non-spherical gravitational collapse gravitational waves, in general, will be generated. If a naked singularity occurs in this collapse, we can observe gravitational waves from a naked singularity. These waves would be short wave length and may be strong. Can we expect the gravitational wave burst at the occurrence of naked singularity? To answer this question is the second motivation for us.

In the rest of this chapter, we briefly review the singularity theorems proved

by Penrose and Hawking. Then we propose rather precise formulations for cosmic censorship hypotheses. At last, we describe about investigations which are related to counterexamples.

We demonstrate the occurrence of naked singularity in the inhomogeneous spherically symmetric dust collapse in Chap. 2. This model is described by an exact solution of Einstein's equation, so-called, Lemaître-Tolman-Bondi (LTB) solution. It has been shown by many authors that the naked singularity should occur from generic initial density and velocity profile in the LTB spacetime.

As mentioned above, sphericity looks like unrealistic assumption. To investigate how non-sphericity affects to the occurrence of naked singularity in the LTB spacetime, we perform linear perturbation analysis. Perturbations are divided into odd (axial) mode and even (polar) mode. These two modes decouple in the linear order perturbation equations. Investigation for each modes is performed separately. The results of odd mode are summarized in Chap. 3. Chapter 4 takes our attention onto the even mode. These analysis were performed by numerical analysis. In Chap. 5 we try to realize the numerical results in the context of Newtonian approximation. These are original contribution. Chapter 6 summarizes the dissertation.

1.2 Existence of Spacetime Singularity

One of the most exciting developments of the study of general relativity is the proof of the singularity theorems by Penrose and Hawking [4, 5, 6]. Here we will sketch out those theorems following Hawking and Ellis [7].

The first theorem, which proves the occurrence of a singularity in a context relevant to gravitational collapse, was given by Penrose [4]. This theorem shows that a singularity must occur after a trapped surface has formed.

Theorem 1 (Hawking & Ellis *Theorem* 1)
Spacetime $(\mathcal{M}, g)$ *cannot be null geodesically complete if:*

1. $R_{ab}k^a k^b \geq 0$ *for all null vector* k^a*;*

2. *there is a non-compact Cauchy surface* $\mathcal{H}$ *in* $\mathcal{M}$*;*

3. *there is a closed trapped surface* $\mathcal{T}$ *in* $\mathcal{M}$*.*

This theorem contains unwanted hypothesis, condition (2), which implies that $\mathcal{M}$ is globally hyperbolic. To eliminate this condition we need some additional assumptions. Here we will merely quote a singularity theorem by Hawking and Penrose without detailed argument about elimination of hypothesis.

Theorem 2 (Hawking & Ellis *Theorem* 2)
Spacetime $(\mathcal{M}, g)$ *is not timelike and null geodesically complete if:*

1. $R_{ab}k^a k^b \geq 0$ *for every non-spacelike vector* k^a

2. *The generic conditions satisfied, i.e., every non-spacelike geodesic contains a point at which* $k_{[a}R_{b]cd[e}k_{f]}k^c k^d \neq 0$, *where* k^a *is the tangent vector to the geodesic.*

3. *The chronology condition holds on* $\mathcal{M}$.

4. *There exist at least one of the following:*

   (a) *a compact achronal set without edge,*

   (b) *a closed trapped surface,*

   (c) *a point p such that on every past (or every future) null geodesic from p the expansion of the null geodesics from p becomes negative.*

Condition (1) is satisfied for all plausible non-quantum matter. Condition (2) is serving only to rule out certain high symmetry. Condition (3), which means that there are no closed timelike curves, has no direct support but it seems to be reasonable to assume it. Condition (4a) is satisfied if the universe is compact. It is believed that condition (4b) is quite likely to be satisfied in gravitational collapse. It is also believed that condition (4c) is satisfied for any past-directed null cone in our universe from the fact that the expanding FLRW model is a very good approximation of our universe at least after the epoch of decoupling. Then this theorem gives us strong reason to believe the existence of the singularity in our universe.

Theorem 2 establishes the existence of singularities under very general conditions. However this theorem does not show whether singularity is in the future or the past. Next theorem shows that there is a singularity in the past.

Theorem 3 (Hawking & Ellis *Theorem* 3)
If

1. $R_{ab}k^a k^b \geq 0$ *for every non-spacelike vector* k^a;

2. *the strong causality condition holds on* $(\mathcal{M}, g)$;

3. *there is some past-directed unit timelike vector* w^a *at a point p and a positive constant b such that if* v^a *is the unit tangent vector to the past-directed timelike geodesics through p, then on each such geodesic the expansion* $\theta \equiv v^a{}_{;a}$ *of these geodesics becomes less than* $-3c/b$ *with a distance* b/c *from p, where* $c \equiv -w^a v_a$,

then there is a past incomplete non-spacelike geodesic through p.

Theorem 2 and 3 are the most useful theorem since their conditions are satisfied in a number of physical situations. However there exists a possibility that a closed timelike curve, violating causality conditions, occurs instead of singularity. There

is an opinion that it would be physically more objectable than a singularity. Nevertheless one would like to know whether such causality violations would prevent the occurrence of singularities. The following theorem shows that causality violations do not prevent the occurrence of singularities.

Theorem 4 (Hawking & Ellis *Theorem* 4)
Spacetime is not timelike geodesically complete if:

1. $R_{ab}k^a k^b \geq 0$ *for every non-spacelike vector* k^a*;*
2. *there exist a compact spacelike three-surface* $\mathcal{S}$ *(without edge);*
3. *the unit normals to* $\mathcal{S}$ *are everywhere converging (or everywhere diverging) on* $\mathcal{S}$*.*

Condition (2) may be interpreted as saying that the universe is spatially closed and condition (3) as saying that it is contracting (or expanding).

Thus the singularity theorems strongly suggest the existence of singularities in our universe and in generic continued gravitational collapse.

1.3 Cosmic Censorship Hypothesis

The singularity theorems revealed that the occurrence of singularities is a generic property of spacetime in general relativity. However, those theorems only prove the causally geodesic incompleteness of the spacetime and say nothing about the detailed features of the singularities themselves; for example, we do not get information from those theorems about whether the predicted singularity is naked or not. Naked means that the singularity is in principle observable. A singularity is a boundary of spacetime. Hence, in order to obtain a solution of hyperbolic field equations for matter, gauge fields and spacetime itself in the causal future of a naked singularity, we need to impose a boundary condition on it. However, we do not yet know physically reasonable boundary conditions on singularities and hence, to avoid this difficulty, the cosmic censorship hypothesis (CCH) proposed by Penrose [8, 9] is often adopted in the analysis of the physical phenomena of the strong gravitational fields. In spite of its importance, this hypothesis has remained unproved. Thus, the cosmic censorship hypothesis is the one of the most important unproved problems for classical theory of general relativity.

1.3.1 Formulation of Cosmic Censorship Hypothesis

Penrose asked, in his consideration of gravitational collapse theory [8], "Does there exist a 'cosmic censor' who forbids the appearance of naked singularities, clothing each one in an absolute event horizon?" The cosmic censorship hypothesis was presented at first like this. This statement is rather primitive and is not good for rigorous proof. Many researchers have proposed precise formulations to prove this

hypothesis ever since. Unfortunately no one has ever succeeded in the proof of any version of the CCH. Here we will formulate the CCH following Wald [10]. Some excellent reviews on the subject of CCH are written in recent years [11, 12, 13, 14, 15].

Weak cosmic censorship hypothesis states that all singularities of gravitational collapse are hidden within black holes. This statement means the future predictability of the spacetime outside the event horizon. To formulate it more precisely we need specify what conditions the matter fields must satisfy. We formulate a precise statement of weak CCH as follows:

Hypothesis 1.1 (Weak CCH) *Let (Σ, h_{ab}, K_{ab}) be an asymptotically flat initial data set for Einstein's equation with (Σ, h_{ab}) a complete Riemannian manifold. Let the matter sources be such that T_{ab} satisfies the dominant energy condition and the system of coupled Einstein-matter field equations is a quasilinear, diagonal, second order hyperbolic one. In addition let the initial data for the matter fields on Σ satisfy appropriate asymptotic falloff conditions at spatial infinity. Then the maximal Cauchy evolution of these initial data is an asymptotically flat, strongly predictable spacetime.*

Here Σ is a three-dimensional manifold, h_{ab} is a Riemann metric on Σ, and K_{ab} is a symmetric tensor field on Σ.

We call the singularity which is censored by weak CCH a *globally naked singularity*. The existence of black hole is proved by the weak CCH with the singularity theorem. The weak CCH is often assumed in theorems on general properties of a black hole, such as that it cannot bifurcate, that every trapped surface must be entirely contained within it and that the area of the event horizon cannot decrease with time.

To determine whether the weak CCH holds or not, the global properties of solutions to Einstein's equation would be needed. Such a global proof for the existence of solutions to the nonlinear hyperbolic equations is hard to establish for the poorness of mathematical techniques. Furthermore if the CCH is a principle of Nature, we should not give an observer at infinity special treatment. Then, the strong version of the CCH was first formulated by Penrose to prohibit a singularity visible to any observer [9]. It states that all physically reasonable spacetimes are globally hyperbolic. It is formulated more precisely as follows:

Hypothesis 1.2 (Strong CCH) *Let (Σ, h_{ab}, K_{ab}) be an asymptotically flat initial data set for Einstein's equation with (Σ, h_{ab}) a complete Riemannian manifold and with Einstein-matter field equations of the quasilinear, diagonal, second order hyperbolic system with T_{ab} satisfying the dominant energy condition. Then, if the maximal Cauchy development of this initial data is extendible, for each $p \in H^+(\Sigma)$ in any extension, either strong causality is violated at p or $\overline{I^-(p) \cap \Sigma}$ is noncompact.*

Here $H^+(S)$ is a future Cauchy horizon of the, closed, achronal set S and $I^-(S)$ is chronological past of the set S. And also $\bar{S}$ is the closure of the set S.

A singularity which is censored by strong CCH but not by weak one is called a *locally naked singularity.* Note that the violation of the CCH does not always mean the existence of the naked singularity. Also the strong CCH does not imply the weak one. This is because, if a singularity is formed from asymptotically flat initial data and it propagate out to null infinity destroying asymptotic flatness while preserving global hyperbolicity, this would violate weak CCH but not strong one.

Intuitively, it seems that singularities should be associated with high energy density. Around them null congruences focusing would occur. This suggest that singularities may be contained inside trapped surface. Thus any version of CCH looks like plausible. Some evidence in favor of CCH exists. For example, the linear stability of Schwarzschild black hole was analyzed [16, 17]. We are convinced of this stability. It was shown that impossibility of getting a extremal charged Kerr black hole to swallow too much charge or angular momentum by the analysis of test particle motion [18, 19]. There is also some evidence for instability of the inner horizon of the Reissner-Nordström spacetime and of the Kerr spacetime [20, 21, 22, 23, 24, 25].

There is no precise statement of the CCH which can be proved. In such a difficult situation for proof it is worth trying to obtain counterexamples. Much effort has been made to search for the naked singularity formation in gravitational collapse. We will introduce these counterexamples in Sec. 1.4.

At the last of this section, we provide the *hoop conjecture* which is originated from the doubts about general validity of CCH [26, 1]. It is formulated as follows:

Hoop conjecture 1 *Black holes with horizons form when and only when a mass M gets compacted into a region whose circumference in EVERY direction in $C \leq 4\pi M$.*

This conjecture states that if sufficiently elongated body collapses to singularity, it would be naked. A version of the "when" half of this conjecture can be established by the theorem of Schoen and Yau [27] if we assume the weak cosmic censorship.

1.4 Gravitational Collapse and Naked Singularity Formation

The first exact solution for Einstein's equation which denotes gravitational collapse is obtained by Oppenheimer and Snyder [28]. This solution relates to the collapse of a homogeneous spherically symmetric dust ball. It is well-known that the curvature singularity of this spacetime is not visible. So this model is an example of black hole formation.

The Oppenheimer-Snyder model is generalized by including density inhomogeneity. This solution was derived and examined in 1930s and 40s [29, 30, 31] and is often called the Lemaître-Tolman-Bondi (LTB) solution. The naked singularity formation in the LTB spacetime was first analyzed by Yodzis, Seifert and Müller

zum Hagen [32, 33]. They pointed out that there appear shell-crossing singularity in the course of the gravitational collapse in the LTB spacetime from generic initial data. They also analyzed a perfect fluid with bounded pressure and imperfect fluid with pressure bounded above in a certain way by the energy density. In the LTB spacetime, a naked shell-focusing singularity appears from generic initial data for spherically symmetric configurations of the rest mass density and specific energy of the dust fluid [34, 35, 36, 37]. This fact was first discovered numerically by Eardley and Smarr. Christodoulou investigated this issue analytically and some researchers followed him. The initial functions in the most general expandable form have been considered [38]. The matter content in this spacetime may satisfy even the dominant energy condition. These results are summarized as follows; in this spacetime, a naked singularity appears from generic initial data for spherically symmetric configurations of the rest mass density and specific energy of the dust fluid.

Ori and Piran numerically examined the structure of self-similar spherical collapse solutions for a perfect fluid with a barotropic equation of state [39, 40]. From the self-similarity this equation of state of the matter is restricted to the form $p = k\rho$. They showed that there is a globally naked singularity in a significant part of the space of self-similar solutions ($k \lesssim 0.0105$). Joshi and Dwivedi analytically investigated the self-similar spherically symmetric collapse of a perfect fluid with a similar equation of state [41]. Harada numerically investigated spherical collapse of a perfect fluid without the assumption of self-similarity [42]. He found that a globally naked, shell-focusing singularity can occur at the center from relativistically high-density, isentropic, and time symmetric initial data if the adiabatic index $\gamma \lesssim 1.01$. The results are free from the assumption of self-similarity. These results suggest that pressure can not always prevent naked singularity formation.

A spherical cloud of counterrotating particles was considered by Datta, Bondi, and Evans [43, 44, 45]. The causal structure of this spacetime was investigated by Harada, Iguchi and Nakao [46]. They obtained an explicit solution for metric functions using an elliptic integral. They also succeeded in giving an expression by elementary functions for marginally bound collapse with particular angular momentum distribution. Their main results are as follows. If the the specific angular momentum $L(r) = O(r^2)$ at $r \to 0$, no central singularity occurs. On the other hand, if the order of $L(r)$ is higher than that, a central singularity occurs and it can be naked. The spherical gravitational collapse of an imperfect fluid which has only tangential pressure are considered [47, 48, 49, 50, 51]. Magli solved an explicit solution with the mass-area coordinate. Harada, Nakao and Iguchi [51] investigated nakedness and curvature strength of the shell-focusing singularity in that spacetime.

Further the naked singularity produced by the gravitational collapse of radiation shells which is described by Vaidya spacetime were investigated [41]. Also more general matter case was investigated [52, 53].

Christodoulou gave a remarkably complete analysis of the singularities in spherically symmetric scalar field collapse [54, 55, 56, 57, 58]. He analytically proved

that naked singularity, which was referred to as "collapsed cone singularity", may arise from regular initial data and found that those solutions are not generic. He also showed for the collapse of the spherically symmetric scalar wave packet that sufficiently weak data evolve to a Minkowski-like spacetime and sufficiently strong data form a black hole.

Choptuik numerically analyzed what would happen between the weak and strong data in spherical scalar field collapse [59]. He discovered so-called "critical phenomena" in gravitational collapse in his numerical analysis. It was shown that the critical collapse forms a black hole with infinitesimal mass. This "zero-mass black hole" may be recognized as a naked singularity. Similar critical phenomena have been discovered for other matter models, say axisymmetric gravitational waves, a spherically symmetric radiation fluid, and so on.

Thus various types of matter content have been considered. However we do not have sufficient results to determine the role of the matter form in the naked singularity formation. We must continue the detailed investigation for the problem what type of matter fields are plausible for the formulation of the provable CCH.

As for the non-spherically symmetric collapse case, Szekeres discovered a class of exact solutions which describes the irrotational dust collapse with no Killing vector. This model is often said to be 'quasi-spherical' He found that shell-crossing singularity which occurs in this spacetime can be naked. Joshi and Krolak revealed that a shell-focusing naked singularity appears in this spacetime [60]. Global visibility of this singularity is recently analyzed [61].

Shapiro and Teukolsky numerically studied evolution of collisionless gas spheroids by fully general relativistic simulations [62, 63]. In their calculations, they evolved spacetimes describing collapsing gas spheroids using maximal time slicing. They found some evidences that the prolate spheroids with sufficiently elongated initial configurations and even with small angular momentum, may form naked singularities. More precisely, they found that when the spheroid was highly prolate a spindle singularity formed at the pole where they could not continue the numerical evolution. They also found that singular region extends outside the matter region by showing the Riemann invariant grows there. Then they searched for trapped surfaces and found their absence. They considered these results as indicating that the spindle might be a naked singularity. However the absence of the trapped surface on their maximal time slicing does not necessarily mean the singularity is indeed naked. To be established whether it is naked or not, we would need to investigate the region of the spacetime future of the singularity.

Wald and Iyer [64] proved that even in the Schwarzschild spacetime, it is possible to choose a time slice which comes arbitrarily close to the singularity, yet for which no trapped surfaces are found to its past. A simple analytical counterparts of the model of the prolate collapse numerically studied by Shapiro and Teukolsky is provided within the Gibbons-Penrose construction [65]. This construction considers a thin shell of null dust collapsing inward from past null infinity. Pelath, Tod, and Wald [66] gave an explicit example in which trapped surfaces are present on the shell, but none exist prior to the last flat slice, thereby explicitly showing that

the absence of trapped surfaces on a particular, natural slicing does not imply an absence of trapped surface in the spacetime.

Shapiro and Teukolsky also found that gravitational radiation carries away a negligible fraction ($\ll 1\%$) of the total mass energy by the time naked singularity forms in their numerical calculations. Intuitively at the formation of singularity, very short-wavelength disturbances of spacetime will be created. If there is no event horizon, these disturbances may propagate as gravitational radiation so that a naked singularity may be a strong source of very short wave length gravitational radiation. Nakamura, Shibata and Nakao [67] have suggested that a naked singularity may emit considerable gravitational wave radiation. This was proposed from the estimate of gravitational radiation from a spindle-like naked singularity. They modeled the spindle-like naked singularity formation in gravitational collapse by a sequence of general relativistic, momentarily static initial data for the prolate spheroid. It should be noted that their suggestion is controversial.

It has long been known that collapsing cylindrically symmetric fluids form naked singularities [26]. These examples are not considered as direct counterexamples to CCH because these spacetimes are not asymptotically flat. There is an expectation that the local behavior of prolate collapse to spindle singularity will be very similar to that of an infinite cylindrical one. Thus properties of the cylindrical collapse have been studied in this context. Apostolatos and Thorne [68] investigated the collapse of a counter-rotating dust shell cylinder and showed that rotation, even if it is infinitesimally small, can halt the gravitational collapse of the cylinder. Echeveria studied the evolution of a cylindrical dust shell analytically at late times and numerically for all times[69]. It was found that the shell collapse to form a strong singularity in finite proper time. The numerical results shows that a sharp burst of gravitational waves is emitted by the shell just before the singularity forms. Chiba [70] showed that the maximal time slicing never has singularity avoidance property in cylindrically symmetric spacetime and proposed a new kind of time slice which may be suitable to investigate the formation of a cylindrical singularity. He numerically investigated cylindrical dust collapse to see the role of gravitational waves and found that negligible gravitational wave is emitted during the free fall time.

In summary, there remains an important issue to formulate the CCH rigorously whether or not the spherical symmetry is essential to the occurrence of a naked singularity. Also it should be investigated whether or not a naked singularity, if such exists, is a strong source of gravitational radiation. These two points are the main theme of this thesis.

Chapter 2

Lemaître-Tolman-Bondi spacetime

It is difficult to solve the Einstein's equation for the dynamical system even when the system is assumed to be spherically symmetric. One of the exceptions is the exact solution for a dust fluid, which is a perfect fluid with zero pressure. The solution for the homogeneous spherical dust collapse was obtained by Oppenheimer and Snyder. This solution is the first model of black hole formation from gravitational collapse. Then this model supports the CCH.

This model can be generalized by relaxing the assumption of homogeneity for a density profile. The solution which describes the collapse of an inhomogeneous spherical dust cloud was derived more than fifty years ago and is often called the Lemaître-Tolman-Bondi (LTB) solution. This model has been studied by many researchers for simplicity and given us deep insight into the final fate of the gravitational collapse. It was found that shell-crossing and shell-focusing naked singularities occur from generic regular or smooth initial data. Hence, the LTB solution is considered as a candidate for a counterexample to the CCH. In this chapter we introduce LTB solution and give a brief review of the study of the naked singularity occurrence in this spacetime.

2.1 Spherically Symmetric Inhomogeneous Dust Collapse

Using the synchronous comoving coordinate system, the line element of the LTB spacetime can be expressed in the form

$$d\bar{s}^2 = \bar{g}_{\mu\nu}dx^\mu dx^\nu \equiv -dt^2 + A^2(t,r)dr^2 + R^2(t,r)(d\theta^2 + \sin^2\theta d\phi^2). \tag{2.1}$$

The stress-energy tensor for the dust fluid is

$$\bar{T}^{\mu\nu} = \bar{\rho}(t,r)\bar{u}^\mu\bar{u}^\nu, \tag{2.2}$$

where $\bar{\rho}(t,r)$ is the rest mass density and $\bar{u}^\mu$ is the 4-velocity of the dust fluid.

Then the Einstein equations and the equation of motion for the dust fluid reduce to the following simple equations

$$A = \frac{R'}{\sqrt{1+f(r)}}, \tag{2.3}$$

$$\bar{\rho}(t,r) = \frac{1}{8\pi}\frac{1}{R^2 R'}\frac{dF(r)}{dr}, \tag{2.4}$$

$$\dot{R}^2 - \frac{F(r)}{R} = f(r), \tag{2.5}$$

where $f(r)$ and $F(r)$ are arbitrary functions of the radial coordinate r, and the overdot and prime denote partial derivatives with respect to t and r, respectively. From Eq. (2.4), $F(r)$ is related to the Misner-Sharp mass function,[71] $m(r)$, of the dust cloud in the manner

$$m(r) = 4\pi \int_0^{R(t,r)} \bar{\rho}(t,r) R^2 dR = 4\pi \int_0^r \bar{\rho}(t,r) R^2 R' dr = \frac{F(r)}{2}. \tag{2.6}$$

Hence Eq. (2.5) might be regarded as the energy equation per unit mass. This means that the other arbitrary function, $f(r)$, is recognized as the specific energy of the dust fluid. The motion of the dust cloud is completely specified by the function, $F(r)$, (or equivalently, the initial distribution of the rest mass density, $\bar{\rho}$) and the specific energy, $f(r)$.

Equation (2.5) is integrated as,

$$t - t_0(r) = -\frac{R^{3/2}}{\sqrt{F}} G\left(-\frac{fR}{F}\right), \tag{2.7}$$

where $G(r)$ is a real positive function given by

$$G(y) \equiv \begin{cases} \dfrac{\arcsin\sqrt{y}}{y^{2/3}} - \dfrac{\sqrt{1-y}}{y}, & \text{for} \quad 0 < y \leq 1 \\ \dfrac{2}{3} & \text{for} \quad y = 0, \\ -\dfrac{\operatorname{arcsinh}\sqrt{-y}}{(-y)^{2/3}} - \dfrac{\sqrt{1-y}}{y} & \text{for} \quad y < 0, \end{cases} \tag{2.8}$$

and $t_0(r)$ is a constant of integration. Thus we have three arbitrary functions of r, $F(r)$, $f(r)$, and $t_0(r)$. Using the remaining coordinate freedom, i.e., the choice of scaling of r, we can reduce the number of such arbitrary functions. We rescale R like that it coincides with r at $t = 0$,

$$R(0,r) = r. \tag{2.9}$$

Then $t_0(r)$ becomes

$$t_0(r) = \frac{r^{3/2}}{\sqrt{F}} G\left(-\frac{fr}{F}\right) \tag{2.10}$$

2.2 Final Fate of Spherical Dust Collapse

We concentrate on the shell-focusing singularity. The nonextendibility beyond the shell-focusing singularity by the spherically symmetric spacetime with dust was shown by Eardley and Smarr. Equation (2.5) implies that every mass shell labeled by r which is initially collapsing inevitably results in a shell-focusing singularity if a shell-crossing singularity will not appear.

The shell-focusing singularity occurs when $R = 0$. Then, from Eq. (2.7), the singularity occurrence time is evaluated as $t = t_0(r)$. Whereas, the time of apparent horizon $t_{AH}(r)$ is estimated by the investigation of R along the out-going future-directed null geodesic. Along it we obtain

$$\frac{dR}{dt} = \dot{R} + R'\frac{dr}{dt} = \left(\frac{F(r)}{R} + f(r)\right)^{1/2} - (1 + f(r))^{1/2}, \tag{2.11}$$

where we use the inequality $\dot{R} < 0$ for collapsing phase and the relation for out-going null lines

$$\frac{dt}{dr} = A = \frac{R'}{\sqrt{1 + f(r)}}. \tag{2.12}$$

It follows that $dR/dt > 0, = 0, < 0$ according to whether $R > F, = F, < F$, respectively. Thus the apparent horizon is given by the curve $R = F$ which is the locus of turning points of the outgoing light rays. Using this relation and Eq. (2.7), we obtain

$$t_{AH} = t_0(r) - FG(-f). \tag{2.13}$$

Therefore the shell-focusing singularity at $r > 0$ is in the future of the apparent horizon. Thus only the shell-focusing singularity at $r = 0$ may become naked.

To decide whether the central singularity is naked or not, we should examine the existence of the future-directed out-going null geodesics which emanate from the central singularity. From the examination of the radial null geodesic equation, Christodoulou mathematically showed the appearance of central naked singularity first. To generalize this result some authors have been investigated in this direction. Here we show that the LTB solution from generic smooth initial data results in shell-focusing central naked singularity following Joshi and his coworkers. We derive the root equation which probes the naked singularity.

The future-directed out-going null geodesic equation (2.12) can be written in the form

$$\frac{dR}{d(r^\alpha)} = \frac{1}{\alpha r^{\alpha-1}}\left(R' + \dot{R}\frac{dt}{dr}\right) \tag{2.14}$$

The partial derivative of circumferential radius R with respect to the radial coordinate r is written as

$$R' = r^{\alpha-1} H(X, r), \tag{2.15}$$

where

$$H(x, r) = (\eta - \beta)\, x + \left\{\Theta - \left(\eta - \frac{3}{2}\beta\right) x^{3/2} G(-Px)\right\} \left\{P + \frac{1}{x}\right\}^{1/2}, \tag{2.16}$$

with

$$x = \frac{R}{r^\alpha}, \tag{2.17}$$

$$\eta(r) = \frac{rF'}{F}, \tag{2.18}$$

$$\beta(r) = \begin{cases} \dfrac{rf'}{f}, & \text{for} \quad f \neq 0 \\ 0, & \text{for} \quad f = 0 \end{cases} \tag{2.19}$$

$$p(r) = \frac{rf}{F}, \tag{2.20}$$

$$P(r) = pr^{\alpha-1}, \tag{2.21}$$

$$\Lambda(r) = \frac{F}{r^\alpha}, \tag{2.22}$$

$$\Theta(r) \equiv \frac{t_0' \sqrt{\Lambda}}{r^{\alpha-1}} = \frac{1 + \beta - \eta}{(1+p)^{1/2}\, r^{3(\alpha-1)/2}} + \frac{\left(\eta - \frac{3}{2}\beta\right) G(-p)}{r^{3(\alpha-1)/2}}. \tag{2.23}$$

Note that α is determined uniquely by the requirement that $\Theta(r)$ goes to a nonzero finite value in the limit $r \to 0$. Substituting Eqs. (2.5), (2.12), and (2.15) into Eq. (2.14), we obtain

$$\frac{dR}{d(r^\alpha)} = \frac{H(x, r)}{\alpha} \left(1 - \frac{\sqrt{f + \frac{\Lambda}{x}}}{\sqrt{1+f}}\right) \tag{2.24}$$

For out-going geodesics, both hands of the above equation should be positive.

The limiting value of x as $r \to 0$

$$x_0 = \lim_{r\to 0} \frac{R}{r^\alpha} = \lim_{r\to 0} \frac{dR}{d(r^\alpha)}, \tag{2.25}$$

gives the tangent of the out-going null geodesic at the singularity. Then we obtain the desired root equation from Eqs. (2.24) and (2.25) as

$$x_0 = \frac{H(x_0, 0)}{\alpha} \lim_{r\to 0} \left(1 - \frac{\sqrt{f + \frac{\Lambda}{x}}}{\sqrt{1+f}}\right) \tag{2.26}$$

If a real positive value x_0 satisfies this equation then the singularity will be naked.

If no real positive root of the above equation exists then singularity is not naked, and the collapse ends in a black hole. The existence of a real positive root depends on the model, i.e., the choice of the arbitrary functions $F(r)$ and $f(r)$.

To investigate the conditions for the appearance of naked singularity, we assume the arbitrary functions $F(r)$ and $f(r)$ as

$$F(r) = F_3 r^3 + F_5 r^5 + F_7 r^7 + \cdots, \tag{2.27}$$
$$f(r) = f_2 r^2 + f_4 f^4 + f_6 r^6 + \cdots. \tag{2.28}$$

This implies that the density field and specific energy field are initially not only regular but also smooth at the symmetric center. That is, the initial density and specific energy profiles are C^∞ on the entire real space r if they are extended to negative r as even functions. Hereafter we assume $F_3 > 0$, which ensures the positivity of the central energy density.

For the marginally bound $f(r) = 0$ case, when $F_5 < 0$, Eq. (2.26) has a real positive root

$$x_0 = \left(-\frac{F_5}{2F_3}\right), \tag{2.29}$$

with $\alpha = 7/3$. From Eq. (2.4) the condition $F_5 < 0$ means $\bar{\rho}''(0,0) < 0$. Therefore, there exists naked singularity in the marginally bound collapse with $\bar{\rho}''(0,0) < 0$ initially. On the other hand, if $F_5 = 0$, that is $\bar{\rho}''(0,0) = 0$, it is easily found that the root equation (2.26) has no real positive root for any $\alpha > 1$. For a homogeneous cloud, which is expressed by the marginally bound Oppenheimer-Snyder solution, the singularity is covered by an event horizon because of $F_5 = 0$.

For the collapse that is not marginally bound, we should include the specific energy function $f(r)$ in the analysis. In this case,the function $\Theta(r)$ depends on the functions β, p, and $G(-p)$ in addition to the function η. To investigate the root equation (2.26), we need limiting formula of $\Theta(r)$ as $r \to 0$. Then we express $\Theta(r)$ as

$$\Theta(r) = \frac{Q(r)}{r^{3(\alpha-1)/2}}, \tag{2.30}$$

where

$$Q(r) = Q_2 r^2 + Q_4 r^4 + \cdots. \tag{2.31}$$

The coefficient Q_2 is given by[1]

$$Q_2 = \frac{2}{\left(1+\frac{f_2}{F_3}\right)^{1/2}}\left(\frac{f_4}{f_2} - \frac{F_5}{F_3}\right) + \left(2\frac{F_5}{F_3} - 3\frac{f_4}{f_2}\right) G\left(-\frac{f_2}{F_3}\right) \tag{2.32}$$

[1]The expression for Q_2 given by Singh and Joshi is not correct. The complete expression is given by Jhingun and Joshi as Eq. (17.46) in [38]. However there contains apparent misprint.

If Q_2 is positive, then the root equation (2.26) has real positive root

$$x_0 = \left(\frac{3Q_2}{4}\right)^{2/3}, \tag{2.33}$$

with $\alpha = 7/3$. Therefore the singularity is naked when Q_2 takes a positive value.

Singh and Joshi [72] and Jhingun, Joshi and Singh [73] also investigate more general class in which $F(r)$ and $f(r)$ are of the form

$$F(r) = F_3 r^3 + F_4 r^4 + F_5 r^5 + F_6 r^6 + F_7 r^7 + \cdots, \tag{2.34}$$

$$f(r) = f_2 r^2 + f_3 r^3 + f_4 f^4 + f_5 r^5 + f_6 r^6 + \cdots. \tag{2.35}$$

This choice corresponds to the initial density and specific energy distributions which are not C^∞ on the entire real space r if they are extended to negative r as even functions. They found that a naked singularity also occurs from generic initial data in this extended space of data. They also showed that, for $F_3 > 0$, $F_4 = F_5 = 0$ and $F_6 < -\frac{26+15\sqrt{3}}{2} F_3^{5/2}$ for marginally bound collapse, Eq. (2.26) has a real positive root x_0 with $\alpha = 3$ and hence the singularity is naked. x_0 is given by the root of some quartic equation.

2.3 Summary

The numerous investigation for the final fate of the inhomogeneous spherical dust collapse show that this collapse results in a shell-focusing central naked singularity from generic initial data. However, it is not so plausible for a counterexample to the CCH for its non-generic character. At first, we should be more careful of the choice of matter model. The dust fluid, which is treated in the LTB solution, is a perfect fluid with null pressure. In realistic situations, it is expected that pressure is not negligible. Therefore it would be much significant to study examples with a more suitable form of matter. As has been quoted in Chap. 1, various examinations on this concern exist. Also, the assumption of spherical symmetry is a matter of grave concern. The physically reasonable gravitational collapse model should contain non-spherical nature in it. Only a few studies of non-spherical collapse have been carried out. Another extraordinally consideration for a naked singularity is about the way to observe it. Particle creation in the LTB spacetime which comes from quantum effect in curved spacetime was considered [74]. In it, the authors shows that the radiation on future null infinity tends to infinity as the Cauchy horizon is approached. Gravitational radiation should be produced in the generic non-spherical gravitational collapse. I and my collaborators investigated linear non-spherical perturbations of the LTB spacetime to settle the problems on the effect of nonsphericity and on the production of gravitational radiation in the occurrence of naked singularity. The results of our investigations will be described in the following three chapters.

Chapter 3

Odd-parity Perturbation of LTB Spacetime

As mentioned in the previous chapter, central shell-focusing naked singularities should occur from 'generic' initial data in the LTB spacetime. There remain some unrealistic assumptions to state generic initial data, e.g., pressureless dust matter, spherical symmetry, and so on. Here we consider whether the spherical symmetry is essential to the occurrence of the shell-focusing naked singularity in the LTB spacetime. At the same time, we investigate whether the naked singularity can be a strong source of gravitational wave burst. For this purpose, we introduce a non-sphericity into the LTB spacetime by the linear perturbation method. Cunningham, Price and Moncrief studied linear perturbations of Oppenheimer-Snyder collapse [75, 76, 77]. Seidel and his coworkers extended this work [78, 79, 80]. They investigated a variety of collapse models based on a May-White hydrodynamic code [81]. The angular dependence of perturbations is decomposed into series of tensorial spherical harmonics. Spherical harmonics are called even-parity if they have parity $(-1)^l$ under spatial inversion and odd-parity if they have parity $(-1)^{l+1}$. Even and odd perturbations decouple each other in the linear perturbation analysis.

At first, because of the simplicity of the equations, we consider odd-parity modes of these perturbations in the marginally bound LTB spacetime and examine the stability of the 'nakedness' of that naked singularity against those linear perturbations. We also attempt to investigate whether the naked singularity is a strong source of gravitational radiation of this mode.

In this chapter we mainly follow Iguchi, Nakao, and Harada [82] and Iguchi, Harada, and Nakao [83].

3.1 Basic equations

We consider the evolution of odd-parity perturbations of the LTB spacetime up to linear order. We follow the gauge-invariant formalism for a general spherically symmetric spacetime established by Gerlach and Sengupta [84, 85]. We will describe their formalism briefly in Appendix A. For the odd-parity mode, there are 2 gauge-invariant metric variables k_a and 3 matter variables L_a and L, where subscript a

refers to t and r

In the LTB case, the odd-parity gauge-invariant matter variables become

$$L_0 = \bar{\rho}(t,r)U(t,r) \qquad \text{and} \qquad L_1 = L = 0, \tag{3.1}$$

where $U(t,r)$ represents the perturbation of the 4-velocity as $\delta u_\mu = (0,0,U(t,r)S_A)$. Because there is no odd-parity scalar harmonics, the density perturbation does not exist. The evolution equation for the matter variable (A.29) is

$$\partial_t \left(AR^2 L_0 \right) = 0. \tag{3.2}$$

This equation is easily integrated, and we obtain

$$L_0 = \frac{1}{AR^2}\frac{dJ(r)}{dr}, \tag{3.3}$$

where $J(r)$ is an arbitrary function depending only on r. From Eqs. (2.4), (3.1), and (3.3), we obtain the relation

$$\begin{aligned} U(t,r) &= 8\pi\sqrt{1+f(r)}\frac{dJ(r)/dr}{dF(r)/dr} && (3.4)\\ &\equiv U(r), && (3.5) \end{aligned}$$

so $U(t,r)$ is independent of the time coordinate t. We introduce a gauge-invariant variable for the metric as

$$\psi_s \equiv \frac{1}{A}\left[\partial_t\left(\frac{k_1}{R^2}\right) - \partial_r\left(\frac{k_0}{R^2}\right)\right] \tag{3.6}$$

Using this, the linearized Einstein equations become

$$\begin{aligned} \partial_t\left(Ak_0\right) - \partial_r\left(\frac{k_1}{A}\right) &= 0, && (3.7)\\ \partial_r\left(R^4\psi_s\right) + A\left(l-1\right)\left(l+2\right)k_0 &= 16\pi AR^2 L_0, && (3.8)\\ \partial_t\left(R^4\psi_s\right) + \frac{1}{A}\left(l-1\right)\left(l+2\right)k_1 &= 0. && (3.9) \end{aligned}$$

From these equations we obtain wave equation for the odd-parity perturbation as

$$\begin{aligned} \partial_t\left(\frac{A}{R^2}\partial_t\left(R^4\psi_s\right)\right) &- \partial_r\left(\frac{1}{AR^2}\partial_r\left(R^4\psi_s\right)\right) + \left(l-1\right)\left(l+2\right)A\psi_s \\ &= -16\pi\partial_r\left(\frac{1}{AR^2}\frac{dJ}{dr}\right) \end{aligned} \tag{3.10}$$

Let us consider the regularity conditions for the background metric functions and gauge-invariant perturbations at $r = 0$. Hereafter we restrict ourselves to the

axisymmetric case, i.e., $m = 0$. Note that this restriction does not lose generality of our analysis. Further we consider only the case in which the spacetime is regular before the occurrence of the singularity. This means that, before the naked singularity formation, the metric functions, $R(t,r)$ and $A(t,r)$, behave near the center in the manner

$$R \longrightarrow R_c(t)r + O(r^3), \tag{3.11}$$
$$A \longrightarrow R_c(t) + O(r^2). \tag{3.12}$$

To investigate the regularity conditions of the gauge-invariant variables, k_a and L_0, we follow Bardeen and Piran [86]. The results are given by

$$L_0 \longrightarrow L_c(t)r^{l+1} + O(r^{l+3}), \tag{3.13}$$
$$k_0 \longrightarrow k_{0c}(t)r^{l+1} + O(r^{l+3}), \tag{3.14}$$
$$k_1 \longrightarrow k_{1c}(t)r^{l+2} + O(r^{l+4}). \tag{3.15}$$

From Eqs.(3.6), (3.11), (3.12), (3.14) and (3.15), we find that ψ_s behaves near the center as

$$\psi_s \longrightarrow \psi_{sc}(t)r^{l-2} + O(r^l) \qquad \text{for } l \geq 2, \tag{3.16}$$
$$\psi_s \longrightarrow \psi_{sc(t)}r + O(r^3) \qquad \text{for } l = 1. \tag{3.17}$$

In the case of $l \geq 2$, the coefficient, $\psi_{sc}(t)$, is related to $R_c(t)$ and $k_{0c}(t)$ in the manner

$$\psi_{sc}(t) = -(l-1)\frac{k_{0c}(t)}{R_c^3(t)}. \tag{3.18}$$

From the above equations, we note that only the quadrupole mode, $l = 2$, of ψ_s does not vanish at the center.

3.2 Perturbation of Riemann Tensor

In this section, we consider the perturbation of the Riemann tensor, $R_{\mu\nu\sigma}{}^{\lambda}$, of the LTB space-time to investigate the relation between the singularity formation and the perturbations. The Riemann tensor is decomposed into the Ricci tensor, $R_{\mu\nu}$, and the Weyl tensor,

$$C_{\mu\nu\sigma\lambda} = R_{\mu\nu\sigma\lambda} + \{g_{\mu[\lambda}R_{\sigma]\nu} + g_{\nu[\sigma}R_{\lambda]\mu}\} + \frac{1}{3}Rg_{\mu[\sigma}g_{\lambda]\nu}. \tag{3.19}$$

We shall give them in the form of the components of the following tetrad basis,

$$e^{\mu}_{(t)} = \left(1, 0, 0, -\frac{h_0 P_{l,\theta}}{R^2 \sin\theta}\right), \tag{3.20}$$

$$e^{\mu}_{(r)} = \left(0, \frac{1}{A}, 0, -\frac{h_1 P_{l,\theta}}{AR^2 \sin\theta}\right), \tag{3.21}$$

$$e^{\mu}_{(\theta)} = \left(0, 0, \frac{1}{R}, -\frac{h_2}{2R^3 \sin^2\theta}\left(\sin\theta P_{l,\theta,\theta} - \cos\theta P_{l,\theta}\right)\right), \tag{3.22}$$

$$e^{\mu}_{(\phi)} = \left(0, 0, 0, \frac{1}{R\sin\theta}\right), \tag{3.23}$$

where $P_l(\cos\theta)$ is the Legendre polynomial and the comma followed by θ denotes a derivative with respect to θ. The Weyl tensor is then decomposed into the so-called electric part, $E_{\alpha\beta}$, and magnetic part, $B_{\alpha\beta}$, which are defined as

$$E_{\alpha\beta} \equiv C_{\alpha\mu\beta\nu} e^{\mu}_{(t)} e^{\nu}_{(t)}, \tag{3.24}$$

$$B_{\alpha\beta} \equiv \frac{1}{2}\epsilon_{\alpha\sigma}{}^{\mu\nu} C_{\mu\nu\beta\lambda} e^{\sigma}_{(t)} e^{\lambda}_{(t)}, \tag{3.25}$$

where $\epsilon_{\mu\nu\alpha\beta}$ is the 4-dimensional skew tensor. In the background LTB space-time, the Ricci tensor has a non-zero value in the region of non-vanishing rest mass density, $\bar{\rho} \neq 0$, through the Einstein equations and also the electric part has a non-zero value. On the other hand, the magnetic part is identically equal to zero in the background LTB space-time. However, when axisymmetric odd-parity metric perturbations exist, the Riemann tensor is perturbed and the magnetic part may also have a non-vanishing value.

The perturbation of the Ricci tensor is expressed by the matter perturbation through the Einstein equations as

$$\delta(R_{(t)(\phi)}) = \frac{8\pi}{R} L_0 P_{l,\theta} = \frac{8\pi}{AR^3}\frac{dJ}{dr} P_{l,\theta}, \tag{3.26}$$

and the other components vanish, where we have used Eq.(3.3) in the last equality. The perturbations of the tetrad components of the electric part are given in the form

$$\delta(E_{(r)(\phi)}) = \frac{1}{2}\left[\frac{1}{AR^3}(l-1)(l+2)k_1 + R(\partial_t R)\psi_s\right]\sin\theta P_{l,\theta}, \tag{3.27}$$

$$\delta(E_{(\theta)(\phi)}) = \frac{1}{2AR^2}\left[\partial_t\left(\frac{k_1}{A}\right) - (\partial_t A)k_0\right]\left(\sin\theta P_{l,\theta,\theta} - \cos\theta P_{l,\theta}\right), \tag{3.28}$$

and the other components vanish. The perturbations of the tetrad components of the magnetic part are obtained in the form

$$\delta(B_{(r)(r)}) = \frac{1}{2} l(l+1)\psi_s P_l, \tag{3.29}$$

$$\delta(B_{(r)(\theta)}) = \frac{1}{4AR^3}\left[R^2\left(R^2\psi_s\right)' - A(l-1)(l+2)k_0\right] P_{l,\theta}, \tag{3.30}$$

$$\delta(B_{(\theta)(\theta)}) = -\frac{1}{AR^2}\left[R\left(\frac{k_0}{R}\right)' + \left(\frac{\dot{R}}{R} - \frac{\dot{A}}{A}\right)k_1 + \frac{1}{2}AR^2\psi_s\right]P_{l,\theta,\theta}$$
$$-\frac{1}{2AR^2}\left[R\left(\frac{k_0}{R}\right)' + \left(\frac{\dot{R}}{R} - \frac{\dot{A}}{A}\right)k_1 + AR^2\psi_s\right]l(l+1)P_l, \quad (3.31)$$

$$\delta(B_{(\phi)(\phi)}) = -\frac{1}{AR^2}\left[R\left(\frac{k_0}{R}\right)' + \left(\frac{\dot{R}}{R} - \frac{\dot{A}}{A}\right)k_1 + \frac{1}{2}AR^2\psi_s\right]\cot\theta P_{l,\theta}$$
$$-\frac{1}{2AR^2}\left[R\left(\frac{k_0}{R}\right)' + \left(\frac{\dot{R}}{R} - \frac{\dot{A}}{A}\right)k_1 + AR^2\psi_s\right]l(l+1)P_l, \quad (3.32)$$

and the other components vanish.

Now we will investigate the behavior of the Ricci and Weyl tensors near the center where the naked singularity appears. From the regularity conditions (3.11)-(3.18), we can see that the perturbations of the Ricci and Weyl tensors obtained in the above behave near the center in the manner

$$\delta(R_{(t)(\phi)}) \longrightarrow \frac{8\pi}{R_c}L_c P_{l,\theta} r^l, \quad (3.33)$$

for the Ricci tensor, and

$$\delta(E_{(r)(\phi)}) \longrightarrow \frac{1}{2R_c^4}(l-1)\left[(l+2)k_{1c} - R_c\frac{dR_c}{dt}k_{0c}\right]P_{l,\theta}r^{l-1}, \quad (3.34)$$

$$\delta(E_{(\theta)(\phi)}) \longrightarrow \frac{1}{2R_c^4}\left[(l+2)k_{1c} - R_c\frac{dR_c}{dt}k_{0c}\right](P_{l,\theta,\theta} - \cot\theta P_{l,\theta})r^{l-1}, \quad (3.35)$$

$$\delta(B_{(r)(r)}) \longrightarrow -\frac{1}{2R_c^3}(l-1)l(l+1)k_{0c}P_l r^{l-2}, \quad (3.36)$$

$$\delta(B_{(r)(\theta)}) \longrightarrow -\frac{1}{2R_c^3}(l-1)(l+1)k_{0c}P_{l,\theta}r^{l-2}, \quad (3.37)$$

$$\delta(B_{(\theta)(\theta)}) \longrightarrow -\frac{1}{2R_c^3}(l+1)k_{0c}(P_{l,\theta,\theta} + lP_l)r^{l-2}, \quad (3.38)$$

$$\delta(B_{(\phi)(\phi)}) \longrightarrow -\frac{1}{2R_c^3}(l+1)k_{0c}(\cot\theta P_{l,\theta} + lP_l)r^{l-2}, \quad (3.39)$$

for the Weyl tensor of $l \geq 2$. For the $l = 1$ mode, we find

$$\delta(E_{(r)(\phi)}) \longrightarrow \frac{1}{2}\frac{dR_c}{dt}\psi_{sc}r^2\sin\theta, \quad (3.40)$$

$$\delta(B_{(r)(r)}) \longrightarrow -\psi_{sc}r\cos\theta, \quad (3.41)$$

$$\delta(B_{(r)(\theta)}) \longrightarrow \frac{1}{4}\psi_{sc}r\sin\theta, \quad (3.42)$$

$$\delta(B_{(\theta)(\theta)}) \longrightarrow \frac{1}{2}\psi_{sc}r\cos\theta, \quad (3.43)$$

$$\delta(B_{(\phi)(\phi)}) = \delta(B_{(\theta)(\theta)}). \quad (3.44)$$

From the above equations, we see that the perturbations of the tetrad components of the Ricci and Weyl tensors, except for the quadrupole mode, $l = 2$, of the magnetic part, $B_{\alpha\beta}$, identically vanish at the center. This means that the central naked singularity formation is affected only by the quadrupole mode up to linear order. Therefore, hereafter we shall consider the quadrupole mode only. It is also shown that ψ_s is closely connected to the tetrad components of the magnetic part of the Weyl tensor.

3.3 Numerical Methods and Results

We numerically solve the wave equation (3.10) in the case of marginally bound collapse, $f(r) = 0$, and the quadrupole mode, $l = 2$. At first, we investigate the purely gravitational wave case and next we include the matter perturbations.

3.3.1 Methods

By virtue of the relation $f(r) = 0$, we can easily integrate Eq. (2.5) and obtain

$$R(t,r) = \left(\frac{9F}{4}\right)^{1/3} [t_0(r) - t]^{2/3}, \tag{3.45}$$

where $t_0(r)$ is an arbitrary function of r. The naked singularity formation time is $t_0 = t_0(0)$. Using the freedom for the scaling of r, we choose $R(0,r) = r$. This scaling of r corresponds to the following choice of $t_0(r)$:

$$t_0(r) = \frac{2}{3\sqrt{F}} r^{3/2} \tag{3.46}$$

Here note that, from Eq. (2.3), the background metric variable, A, is equal to R' Then, the wave equation (3.10) becomes

$$\begin{aligned} \ddot{\psi}_s - \frac{1}{R'^2}\psi_s'' &= \frac{1}{R'^2}\left(6\frac{R'}{R} - \frac{R''}{R'}\right)\psi_s' - \left(6\frac{\dot{R}}{R} + \frac{\dot{R}'}{R'}\right)\dot{\psi}_s \\ &\quad -4\left[\frac{\dot{R}'}{R'}\frac{\dot{R}}{R} + \frac{1}{2}\left(\frac{\dot{R}}{R}\right)^2\right]\psi_s - \frac{16\pi}{R'R^2}\left(\frac{r^2\rho(r)U(r)}{R'R^2}\right)', \end{aligned} \tag{3.47}$$

where $\rho(r) = \bar{\rho}(0,r)$ is the density profile at $t = 0$. We solve this partial differential equation numerically.

We have a disadvantage when we use the (t,r) coordinate system, because of the restriction on the region in which we can numerically construct the solution of the wave equation, (3.10). Therefore, instead of the (t,r) coordinate system, we introduce a single-null coordinate system, $(u,\tilde{r})$, where u is an outgoing null coordinate and chosen so that it agrees with t at the symmetric center and we choose $\tilde{r} = r$. We perform the numerical integration along two characteristic directions.

The transformation matrix is formally expressed in the form

$$d\tilde{r} = dr, \tag{3.48}$$
$$du = (\partial_t u)_r\, dt + (\partial_r u)_t\, dr. \tag{3.49}$$

Because u is the out-going null coordinate, the following relation holds,

$$\frac{(\partial_t u)_r}{(\partial_r u)_t} = -\frac{1}{R'}. \tag{3.50}$$

Using these relations, we obtain the line element of the 2-dimensional sub-space-time, (t, r), in the following new form

$$ds^2_{(2)} = -\alpha^2 du^2 - 2\alpha R' du d\tilde{r}, \tag{3.51}$$

where we have introduced

$$\alpha \equiv \frac{1}{(\partial_t u)_r} \tag{3.52}$$

By using this new coordinate system, $(u, \tilde{r})$, Eq. (3.47) is expressed in the form

$$\begin{aligned}\frac{d\phi_s}{du} &= -\frac{\alpha}{R}\left[3R' + \frac{1}{2}R\dot{R}\dot{R}' - \frac{5}{4}\dot{R}^2 R'\right]\psi_s \\ &\quad -\frac{\alpha}{2}\left[\frac{R''}{R'^2} - \frac{2}{R}\left(1 - \dot{R}\right)\right]\phi_s - \frac{8\pi\alpha}{R}\partial_r\left(\frac{r^2\rho(r)U(r)}{R'R^2}\right),\end{aligned} \tag{3.53}$$
$$\partial_{\tilde{r}}\psi_s = \frac{1}{R}\phi_s - 3\frac{R'}{R}\left(1 + \dot{R}\right)\psi_s, \tag{3.54}$$

where the ordinary derivative on the left-hand side of Eq. (3.53) and the partial derivative on the left-hand side of Eq. (3.54) are given by

$$\frac{d}{du} = \partial_u + \frac{d\tilde{r}}{du}\partial_{\tilde{r}} = \partial_u - \frac{\alpha}{2R'}\partial_{\tilde{r}} = \frac{\alpha}{2}\partial_t - \frac{\alpha}{2R'}\partial_r, \tag{3.55}$$
$$\partial_{\tilde{r}} = -\frac{(\partial_r u)_t}{(\partial_t u)_r}\partial_t + \partial_r = R'\partial_t + \partial_r, \tag{3.56}$$

respectively. Also, ϕ_s is defined by Eq. (3.54). We integrate Eq. (3.53) using the scheme of an explicit first order difference equation. We use the trapezoidal rule,

$$\psi_{sj+1} = \psi_{sj} + \frac{\Delta r'}{2}\left((\partial_{r'}\psi_s)_j + (\partial_{r'}\psi_s)_{j+1}\right), \tag{3.57}$$

to integrate Eq. (3.54).

For the boundary condition at the center we demand that ψ_s behaves as $\psi_{sc}(t) + \psi_{s2}(t)r^2$ on a surface of t = const. We numerically realize this condition by two-step interpolation. First the values of ψ_s are derived at two points on the surface of t = const from the interpolation on the slices of u = const. Next, using these

two values, the central value of ψ_s is derived from the interpolation on the slice of $t = \text{const}$. Another way to determine the central value of ψ_s is as follows. We first obtain the central value of ϕ_s from Eq. (3.53). From Eq. (3.54) and the boundary conditions, the relation of ψ_s and ϕ_s at the center is given by

$$\phi_s = 3\partial_{r'} R\psi_s. \tag{3.58}$$

Using this relation the central value of ψ_s is obtained. In our numerical analyses the results of these two methods agree well.

The numerical code used here was checked in the Minkowski spacetime. We compared the numerical results with the analytic solutions described in Sec. 3.3.2. Also, the numerical results shown here were almost independent of the number of grid points.

3.3.2 Purely Gravitational Wave case

For the first step we perform the analysis of the perturbations without matter matter perturbations, i.e., $U(r) = 0$, in order to isolate the effects of pure gravitational waves.

We adopt the following initial rest mass density profile so that the central naked singularity appears;

$$\bar{\rho}(0,r) = \begin{cases} \rho_0[1 - 2(r/r_b)^2 + (r/r_b)^4] & \text{for} \quad 0 \le r \le r_b \\ 0 & \text{for} \quad r > r_b, \end{cases} \tag{3.59}$$

where ρ_0 is a positive constant and r_b denotes the radial coordinate at the surface of the dust cloud. The total (gravitational) mass of the dust cloud is

$$M = m(r_b) = \frac{32\pi}{105}\rho_0 r_b^3. \tag{3.60}$$

The time of the central naked singularity formation is

$$t = t_0(0) = \frac{1}{\sqrt{6\pi\rho_0}}. \tag{3.61}$$

Whether the naked singularity is global or local is determined by a non-dimensional constant $\rho_0 r_b^2$. It is known that the singularity is globally naked for sufficiently small $\rho_0 r_b^2$ [35, 72]. However, the critical value of $\rho_0 r_b^2$ can not be obtained explicitly. Hence, after $\rho_0 r_b^2$ is given, we have to investigate whether the central naked singularity is global or local, by numerically solving the future directed null ray from the central naked singularity. Here we consider two cases. One is that of $\rho_0 r_b^2 = 3 \times 10^{-2}$, which corresponds to a globally naked singularity, and the other is that of $\rho_0 r_b^2 = 3 \times 10^{-1}$, which corresponds to a locally naked one.

In the globally naked case, the initial radius of the dust cloud and the time of

the central naked singularity formation are given by

$$\frac{R(0,r_b)}{M} = \frac{r_b}{M} = \frac{105}{32\pi\rho_0 r_b^2} \cong 34.8, \tag{3.62}$$

$$\frac{t_0(0)}{M} = \frac{105}{32\sqrt{6}\pi^{3/2}(\rho_0 r_b^2)^{3/2}} \cong 46.3. \tag{3.63}$$

On the other hand, in the locally naked case, they are given by

$$\frac{R(0,r_b)}{M} = \frac{r_b}{M} \cong 3.48, \tag{3.64}$$

$$\frac{t_0(0)}{M} \cong 1.46. \tag{3.65}$$

The initial conditions which we consider are a Gaussian-shaped wave packet with respect to the coordinate, r',

$$\psi_s|_{u=u_0} = \psi_s^i \exp\left[-\frac{(r'-r_c')^2}{2\sigma^2}\right], \tag{3.66}$$

where ψ_s^i, σ, and r_c' are constants and characterize the amplitude, width and initial position of the initial wave packet, respectively. The initial null hypersurface, $u = u_0$, is chosen so that it includes a world point $(t,r) = (0,0)$, except for the analysis of the scattered waves which will be discussed in this section.

We investigate models with three different initial positions of the wave packet, i.e., r_c' in Eq.(3.66), on the initial null hypersurface. In Case 1, the wave packet reaches the center of the dust cloud before the formation of the central naked singularity. In Case 2, a significant portion of the wave packet hits the central naked singularity. In Case 3, the packet does not hit the central naked singularity but reaches the Cauchy horizon associated with it. Fig.3.1 shows these situations schematically. In each case, the value of ψ_s at the center is plotted as a function of the coordinate time, t, in Fig.3.2 for the globally naked case and in Fig.3.3 for the locally naked case. Note that it is impossible to perform the numerical calculation in the causal future of the central naked singularity. Therefore we plot ψ_s at the center only before the occurrence of the central naked singularity. Although such a difficulty exists, we find that violent growth of the amplitude of ψ_s is not observed near the central naked singularity and Cauchy horizon associated with it.

Next we show the dependence of ψ_s at the center on the width of the initial wave packet. Fig.3.4 depicts ψ_s at the center for various widths of packets in Case 2. It is found that the amplitude of ψ_s with smaller initial width becomes larger at the center. The relation between the width, σ, and the maximal value of $|\psi_s|$ at the center is shown in Fig.3.5. We find that there is the following power-law relation

$$|\psi_s|_{r=0} \propto \sigma^{-3} \tag{3.67}$$

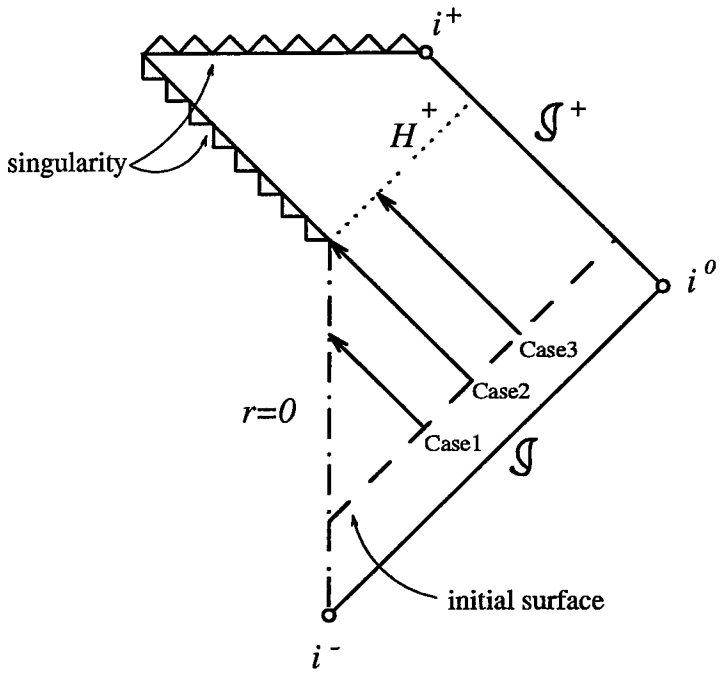

Figure 3.1: Conformal diagram of the LTB space-time with a globally naked singularity. $i^+(i^-)$ denotes future (past) timelike infinity respectively, while i^0 denotes spacelike infinity. $\mathcal{J}^+(\mathcal{J}^-)$ denotes future (past) null infinity respectively. The dotted line H^+ indicates a future Cauchy horizon associated with the central naked singularity. The broken line is a null hypersurface on which we put initial wave packets. The initial positions of the wave packets are classified into Cases 1-3. For the locally naked singularity case, the Cases 1-3 are defined in the same manner as the globally naked case.

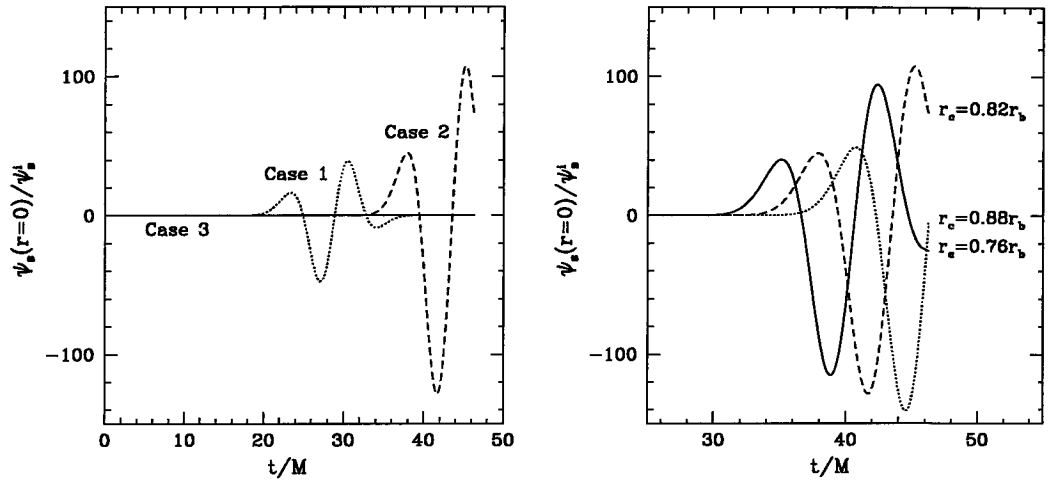

(a) Case1,2,3 (b) Case2

Figure 3.2: Plots of the gauge-invariant variable, ψ_s, at the center, $r = 0$, with an initial width $\sigma = 0.05r_b$ for the Cases 1-3 for globally naked cases. In (a), the dotted line denotes Case 1 ($r'_c = 0.5r_b$), the broken line shows Case 2 ($r'_c = 0.82r_b$), and the solid line denotes Case 3 ($r'_c = 1.2r_b$). In (b), the results of Case 2 are shown in more detail. The broken line in (b) is the same as the broken line in (a). The solid and dotted lines show the cases that the wave packets were put on the initial surface at $r'_c = 0.76r_b$ and at $r'_c = 0.88r_b$, respectively.

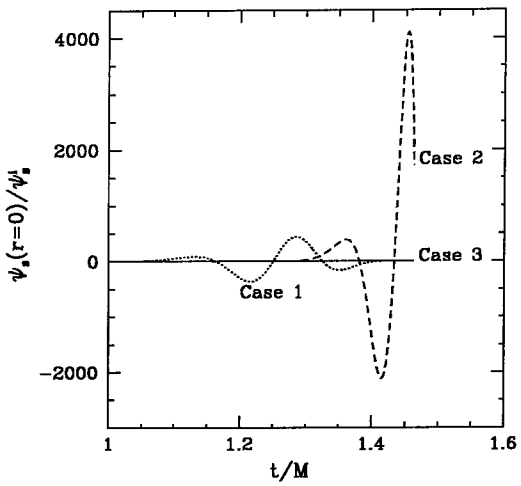

Figure 3.3: Plots of the gauge-invariant variable, ψ_s, at the center, $r = 0$, with an initial width $\sigma = 0.02r_b$ for Cases 1-3 for locally naked cases. The dotted, broken, and solid lines denote Case 1 ($r'_c = 0.28r_b$), Case 2 ($r'_c = 0.38r_b$), and Case 3 ($r'_c = 0.58r_b$), respectively.

We also observe the time dependence of ψ_s along the line of a constant circumferential radius outside the dust cloud. Since we would like to see the effect of the central naked singularity on ψ_s, we consider the globally naked case only. We set up an initial wave packet of $\sigma = 0.05r_b$ at $R = 100M$ on the initial null hypersurface which does not include the space-time point $(t, r) = (0, 0)$ but is chosen so that the wave packet will reach the neighborhood of the central naked singularity.

The results are shown in Fig.3.6 in which ψ_s at $R = 100M$ is plotted as a function of t. Note that the point, $R = 100M$, is located in the vacuum region which is the Schwarzschild space-time by Birkhoff's theorem. Hence the value of t along the curve of $R = 100M$ agrees with that of the usual static time coordinate of the Schwarzschild space-time.

In Fig.3.6(a), the solid line corresponds to Case 1 while the broken line is for Case 2. The dotted line denotes the result for Case 3. The left-hand peaks in Fig.3.6(a) correspond to the initial incident waves. On the other hand, the right-hand peaks of Cases 1 and 2 in this figure correspond to the scattered outgoing waves. In Case 3, the right-hand peak does not exist and this is because, in this case, almost all portions of the incident waves enter into the Cauchy horizon associated with the central naked singularity and hence it is impossible to follow numerically the scattered waves in the causal future of the central naked singularity. Fig.3.6(b) shows detailed behavior of the scattered ψ_s for Case 2. It is a most important fact seen in these figures that the amplitude of the scattered waves is almost the same as that of the initial incident waves in Cases 1 and 2.

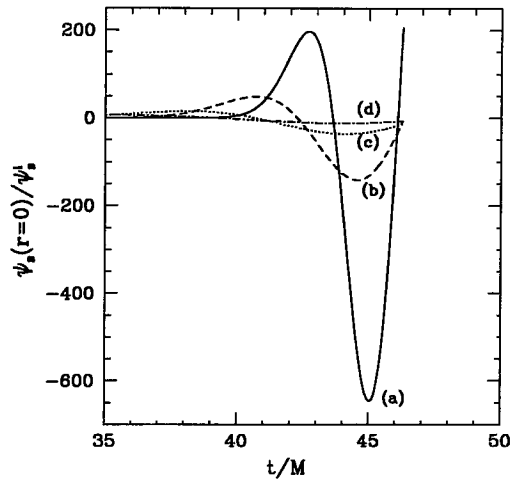

Figure 3.4: Plots of the gauge-invariant variable, ψ_s, at the center, $r = 0$, in the LTB space-time for various widths of initial wave packets. The wave packets are put at $r = 0.88r_b$ on the initial null surface. The widths of initial wave packets are varied from $0.03r_b$ to $0.12r_b$. The solid line (a) corresponds to the wave form of the wave packet with the initial width $\sigma = 0.03r_b$. The broken line (b) is that of the initial width $\sigma = 0.05r_b$ while the dotted line (c) corresponds to that of the initial width $\sigma = 0.08r_b$. The broken dotted line (d) is that of the initial width $\sigma = 0.12r_b$.

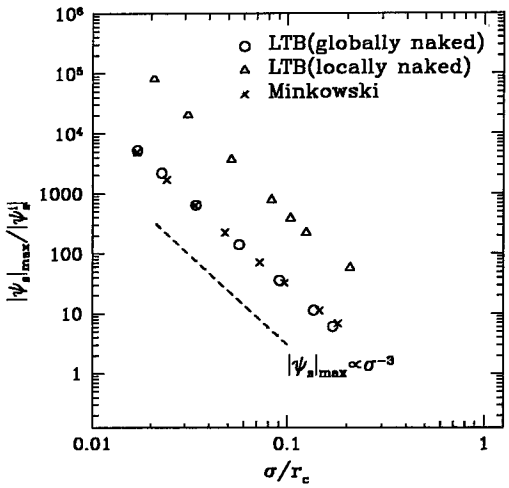

Figure 3.5: The relation between the widths of initial wave packets and the maximal values of $|\psi_s|$ at the center, $r = 0$. The results for the case of the LTB space-time with globally naked singularity are marked by open circles. The results of the locally naked case are marked by the triangles. The results of the Minkowski space-time are marked by cross marks. The broken line denotes the relation, $|\psi_s|_{max} \propto \sigma^{-3}$.

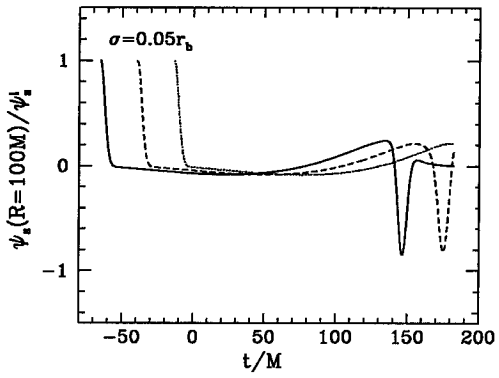

(a) Case 1,2,3

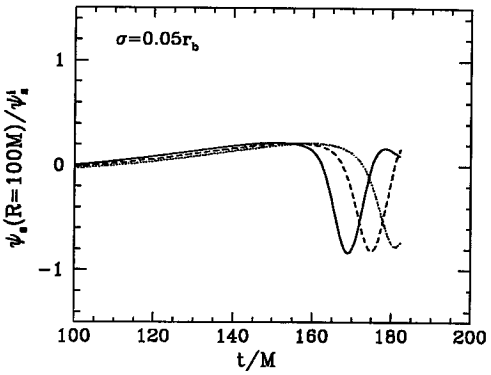

(b) Case 2

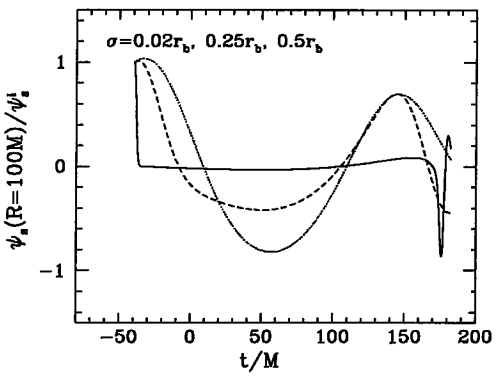

(c) $\sigma = 0.02 - 0.5 r_b$ in Case2

Figure 3.6: Plots of ψ_s with an initial width $\sigma = 0.05 r_b$ at $R = 100M$ as a function of time, t, in the LTB space-time. In (a), the solid line shows the result for the case with an initial time when we put the wave packet on the initial surface $t_i/M = -65.310$ (Case1), the broken line is for $t_i/M = -38.529$ (Case2), the dotted line is for $t_i/M = -13.610$ (Case3). (b) depicts the details of the Case2. The solid line shows the plot of ψ_s with the initial time, $t_i/M = -34.336$, the broken line is for $t_i/M = -38.529$, the dotted line is for $t_i/M = -44.677$. We find no diverging tendency of the gauge-invariant ψ_s when it approaches the Cauchy horizon. In (c), we vary the width of the initial wave packet in Case2. The solid line is a plot of $\sigma = 0.02 r_b$, the broken line is the case of the initial width $\sigma = 0.25 r_b$, the dotted line is that of $\sigma = 0.5 r_b$.

In order to investigate the effect of the wavelength of ψ_s, we perform the numerical integration for Case 2 but with different initial widths of wave packets. The results of narrower ($\sigma = 0.02r_b$) and broader ($\sigma = 0.25r_b$ and $0.5r_b$) widths than the case plotted in Fig.3.6(a) and (b) are shown in Fig.3.6(c). The narrower wave is similar to $\sigma = 0.05r_b$ while the broader packets have different forms of scattered waves from the narrower one. However, in both cases, the amplitude of the scattered wave is not so different from the incident one.

Next, in order to isolate the effect of the spacetime curvature on the propagation of gravitational waves, we compare the analytic solution in the Minkowski spacetime with the results of the LTB space-time obtained in the above. In the Minkowski case, since $R(t,r) = r$, Eq.(3.47) becomes

$$\partial_t^2\psi_s - \partial_r^2\psi_s = \frac{6}{r}\partial_r\psi_s. \tag{3.68}$$

The solution of this equation which is regular at $r = 0$ is obtained in the form

$$\begin{aligned}\psi_s &= 3\frac{f(t-r) - f(t+r)}{r^5} + 3\frac{f^{(1)}(t-r) + f^{(1)}(t+r)}{r^4} \\ &\quad + \frac{f^{(2)}(t-r) - f^{(2)}(t+r)}{r^3},\end{aligned} \tag{3.69}$$

where $f(x)$ is an arbitrary function and $f^{(n)}(x)$ denotes the n-th order derivative of $f(x)$ with respect to x. We set the following initial wave packet on the null hypersurface, $t = r$,

$$\psi_s = \exp\left[-\frac{(r-r_c)^2}{2\sigma^2}\right] \tag{3.70}$$

Using the above solution, we compare the evolution of wave forms in the Minkowski space-time with that in the LTB space-time. The initial wave packet in the LTB space-time has been given by Eq.(3.66) as a function of the coordinate radius, r' However, note that r' does not agree with the circumferential radius, R, in this case but in the Minkowski case, the coordinate radius, r, agrees with the circumferential radius, R. Since the circumferential radius, R, is tightly connected with the behavior of the amplitude of the wave, we should set the same initial data with respect to R both for the LTB and Minkowski cases. Hence first we plot the initial wave packet (3.66) as a function of R/M on the initial null hypersurface and then the values of σ and r_c in Eq.(3.70) are adjusted so that the initial wave form fits well with that of the LTB case.

First we consider the evolution of ψ_s at the center. Using Eqs.(3.69) and (3.70), we obtain ψ_s at the center in the form

$$\psi_s(t,0) = \left[1 - \frac{1}{\sigma^2}\left(\frac{t}{2} - r_c\right)\frac{t}{2} - \frac{1}{4\sigma^2}\left(\frac{t}{2}\right)^2 + \frac{1}{4\sigma^4}\left(\frac{t}{2} - r_c\right)^2\left(\frac{t}{2}\right)^2\right.$$

$$+\frac{1}{20\sigma^4}\left(\frac{t}{2}-r_c\right)\left(\frac{t}{2}\right)^3-\frac{1}{60\sigma^6}\left(\frac{t}{2}-r_c\right)^3\left(\frac{t}{2}\right)^3\Bigg]$$
$$\times\exp\left[-\frac{1}{2\sigma^2}\left(\frac{t}{2}-r_c\right)^2\right] \tag{3.71}$$

The parameters, σ and r_c, in Eq.(3.70) are chosen so that the initial wave packets fit well with those of the Cases 1 and 2 of Fig3.2. The results are given in Fig.3.7(a) and (b), respectively, and in this figure, we also plot the results for the corresponding cases of the LTB space-time. It should be noted that there is scarcely any difference between the wave forms of the Minkowski and LTB cases.

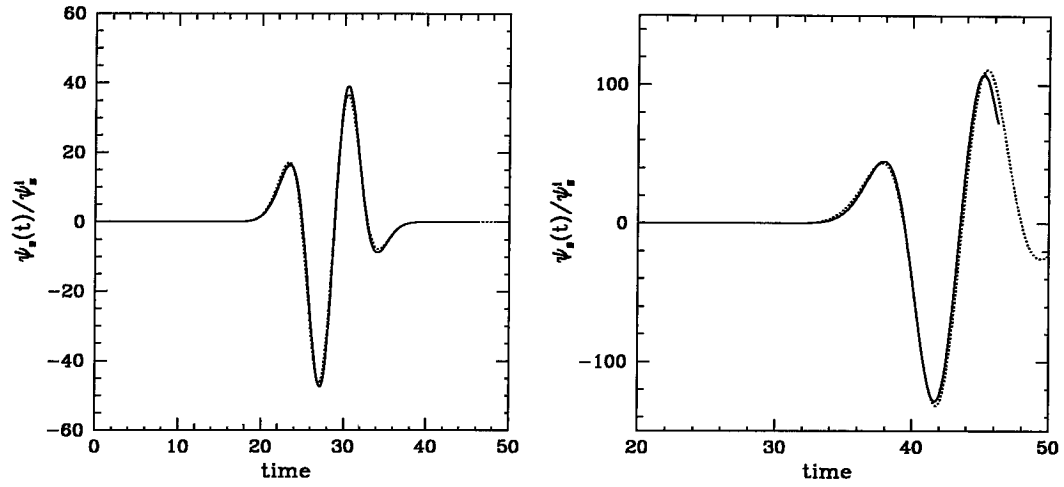

(a) Case 1 (b) Case 2

Figure 3.7: Results of the comparison of the wave forms at the center. In (a), the solid line shows the LTB case, as a function of t/M, that is the same as the Case 1 in Fig.3.2(a). The dotted line shows the corresponding one of the Minkowski case, as a function of t, where $\sigma = 1.18$ and $r_c = 13.9$. In (b), the LTB case is the solid line and Case 2 in Fig.3.2(a). The Minkowski case is the dotted line where $\sigma = 1.25$ and $r_c = 21.4$.

Next we consider the behavior of ψ_s at a finite circumferential radius which agrees with the numerical value of $R = 100M$ in the LTB case. Here the wave form is obtained numerically by the same procedure as in the LTB case. The result is shown in Fig.3.8. We also plot the corresponding case of the LTB space-time in the same figure. We find that there is a little difference of the phase between the Minkowski and LTB cases. However, the behavior of ψ_s in the Minkowski case is

basically the same as that in the LTB case. The effect due to the dust cloud and the existence of the central naked singularity on the propagation of ψ_s is rather small.

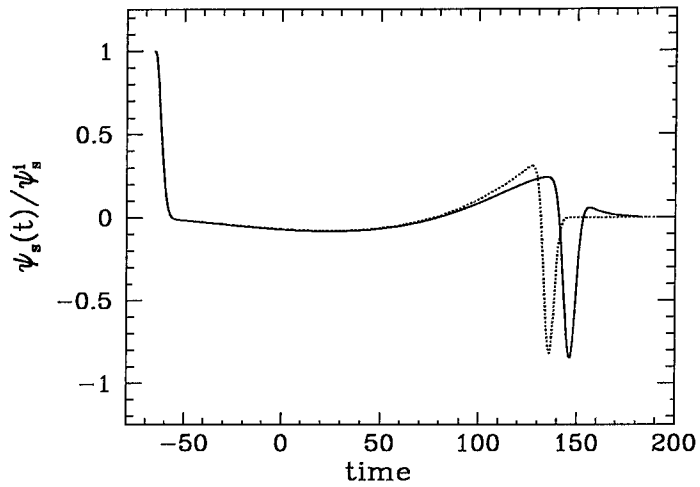

Figure 3.8: Wave forms along the constant circumferential radius both for the Minkowski and LTB cases are plotted. The solid line shows the LTB case, as a function of t/M, that is identical with Case 1 in Fig.3.6 (a). The dotted line shows the corresponding one of the Minkowski case, as a function of t, where $\sigma = 1.33$ and $r_c = 100$.

We consider the relation between the maximum value of $|\psi_s|$ observed at the center and the width, σ, of an initial wave packet in the Minkowski space-time. This relation is obtained from Eq.(3.71). The results are also shown in Fig.3.5. The power-law relation Eq.(3.67) is also valid in the Minkowski case. From Eq.(3.69), ψ_s is approximately proportion to $1/r^3$ except for the region of $r > \sigma$ around the center. If the initial amplitude of the wave packet has a value ψ_i at $r = r_c$, then the value of ψ_s at $r = \sigma$ is roughly estimated as $\psi_i \times (\sigma/r_c)^{-3}$. This will be the reason why the relation (3.67) holds in the Minkowski space-time. As we have discussed above, ψ_s behaves outside the Cauchy horizon of the LTB space-time in approximately the same manner as in the Minkowski space-time. Therefore it would be also the reason why the relation (3.67) holds in the LTB space-time.

As a result, we conclude that even in the neighborhood of the central naked singularity and of the Cauchy horizon associated with it, the metric perturbation, ψ_s, does not show any peculiar behavior. However, we should note that ψ_s does not vanish in the neighborhood of the central naked singularity although it is well-behaved. Therefore, the formation process of the central naked singularity is *marginally stable* against the odd-parity metric perturbations.

Table 3.1: Parameters of initial density profiles, power law indices and damped oscillation frequencies. d.o.f denotes damped oscillation frequency.

	final state	ρ_0	r_1	r_2	n	power index	d.o.f
(a)	globally naked	1×10^{-2}	0.25	0.5	2	5/3	—
(b)	locally naked	1×10^{-1}	0.25	0.5	2	5/3	$0.37+0.089i$
(c)	black hole	2×10^{-2}	2	0.4	4	—	$0.37+0.089i$

3.3.3 Including Matter Perturbations

When the matter perturbation exists, the source term in the wave equation (3.47) does not vanish. In the previous subsection, we have found that the homogeneous solution of the wave equation (3.47) does not show any violent behavior. So, if the solution with nonvanishing source term shows divergent behavior, it does not depend on the choice of initial data for ψ_s because the divergent behavior is due to the particular solution part. Here we assume ψ_s vanishes on the initial null hypersurface.

We adopt the initial rest mass density profile

$$\rho(r) = \rho_0 \frac{1 + \exp\left(-\frac{1}{2}\frac{r_1}{r_2}\right)}{1 + \exp\left(\frac{r^n - r_1^n}{2r_1^{n-1}r_2}\right)}, \tag{3.72}$$

where ρ_0, r_1 and r_2 are positive constants and n is a positive even integer. As a result the dust fluid spreads all over the space. However, if $r \gg r_1, r_2$, then $\rho(r)$ decreases exponentially, so that the dust cloud is divided into the core part and the envelope which would be considered as the vacuum region essentially. We define a core radius as

$$r_{\rm core} = r_1 + \frac{r_2}{2}. \tag{3.73}$$

If we set $n = 2$, there appears a central naked singularity. This singularity becomes locally or globally naked depending on the parameters (ρ_0, r_1, r_2). However, if the integer n is greater than 2, the final state of the dust cloud is a black hole independently of the parameters. Then we consider three different density profiles connected with three types of the final state of the dust cloud, globally and locally naked singularities and a black hole. The outgoing null coordinate u is chosen so that it agrees with the proper time at the symmetric center. Therefore, even if the black hole background is considered, we can analyze the inside of the event horizon. Corresponding parameters are given in Table 3.1. Using this density profile, we numerically calculate the total gravitational mass of the dust cloud M. In our calculation we adopt the total mass M as the unit of the variables.

The source term of Eq. (3.53),

$$S(t,r) = -\frac{8\pi\alpha}{R}\partial_r\left(\frac{r^2\rho(r)U(r)}{(\partial_r R)R^2}\right), \tag{3.74}$$

is determined by $U(r)$. As mentioned above, the constraints on the functional form of $U(r)$ are given by the regularity condition of L_0. From Eq. (3.76), $U(r)$ should be proportional to r^{l+1} toward the center. We localize the matter perturbation near the center to diminish the effects of the initial ingoing waves. Therefore we define $U(r)$ such that

$$r^2\rho(r)U(r) = \begin{cases} U_0\left(\frac{r}{r_b}\right)^5\left(1-\left(\frac{r}{r_b}\right)^2\right)^5 & \text{for} \quad 0 \le r \le r_b, \\ 0 & \text{for} \quad r > r_b, \end{cases} \tag{3.75}$$

where U_0 and r_b are arbitrary constants. In our numerical calculation we chose r_b as $r_{\rm core}/2$. This choice of r_b has no special meaning, and the results of our numerical calculations are not sensitive to it.

Before the detailed explanation of the numerical results, we comment on the behavior of the matter perturbation variable L_0 around a naked singularity on the slice $t = t_0$. The regularity conditions of L_0 and $\bar{\rho}$ determine the behavior of $U(r)$ near the center as

$$U(r) \propto r^{l+1} \tag{3.76}$$

This property does not change even if a central singularity appears. However, the r dependence of R and A near the center changes at that time. Assuming a rest mass density profile of the form

$$\rho(r) = \rho_0 + \rho_n r^n + \cdots , \tag{3.77}$$

we obtain the relation

$$t_0(r) \propto t_0 + t_n r^n \tag{3.78}$$

from Eqs. (2.4) and (3.46), where n is a positive even integer. After substituting this relation into Eq. (3.45), the lowest order term is absent from the square brackets of it. Then we obtain the behavior of R and A around the central singularity as

$$R(t_0, r) \propto r^{1+\frac{2}{3}n}, \tag{3.79}$$

and

$$A(t_0, r) \propto r^{\frac{2}{3}n} \tag{3.80}$$

on the slice $t = t_0$. As a result, we obtain the r dependence of L_0 around the center when the naked singularity appears as

$$L_0(t_0, r) \propto r^{l-2n+1} \tag{3.81}$$

For example, if $l = 2$ and $n = 2$, then L_0 is inversely proportional to r and diverges toward the central naked singularity. Therefore the source term of the wave equation is expected to have a large magnitude around the naked singularity. Thus the metric perturbation variable ψ_s as well as matter variable L_0 may diverge toward the naked singularity.

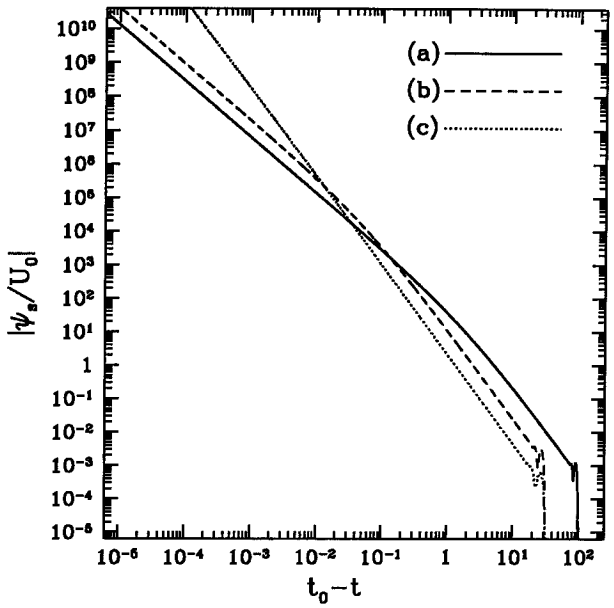

Figure 3.9: Plots of ψ_s at the center as a function of the time coordinate t. The solid line represents the globally naked case (a), the dashed line represents the locally naked case (b), and the dotted line represents the black hole case (c).

First we observe the behavior of ψ_s at the center. The results are plotted in Fig. 3.9. The initial oscillations correspond to the initial ingoing waves. After these oscillations, ψ_s grows proportional to $(t_0 - t)^{-\delta}$ for the naked singularity cases near the formation epoch of the naked singularity. For the case of black hole formation, ψ_s exhibits power-law growth in the early part. Later its slope gradually changes but it grows faster than in the case of the naked singularity. For the naked singularity cases, the power-law indices δ are determined by $(t_0 - t)\dot{\psi}_s/\psi_s$ locally. The results are shown in Fig. 3.10. From this figure we read the final indices as 5/3 for both naked cases. Therefore the metric perturbations diverge at the central naked singularity.

We also observe the wave form of ψ_s along the line of a constant circumferential radius outside the dust cloud. The results are shown in Figs. 3.11–3.13. Figure 3.11 displays the wave form of the globally naked case (a), Fig. 3.12 displays the wave form of the locally naked case (b), and Fig. 3.13 displays the wave form of the black hole case (c). The initial oscillations correspond to the initial ingoing waves. In the case of a locally naked singularity and black hole formation, damped oscillations dominate the gravitational waves. We read the frequencies and damping rates of these damped oscillations from Figs. 3.12 and 3.13 and give them in terms of complex frequencies as $0.37 + 0.089i$ for locally naked and black hole cases. These

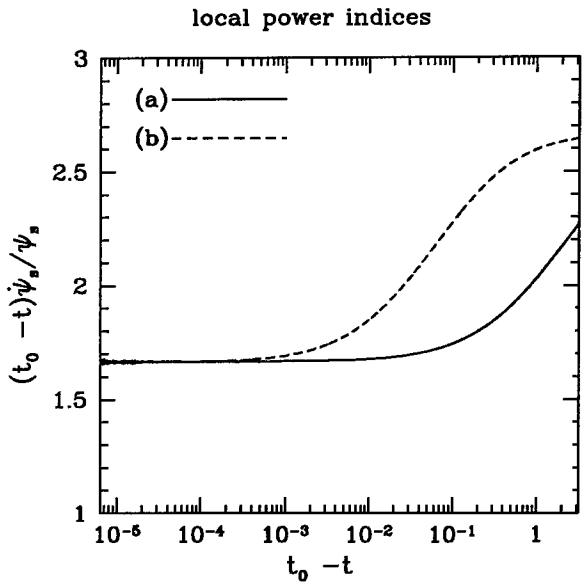

Figure 3.10: Plots of the local power indices $(t_0 - t)\dot{\psi}_s/\psi_s$. The solid line corresponds to the globally naked case (a), and the dashed line corresponds to the locally naked case (b). Both of them approach a value near 5/3.

agree well with the fundamental quasi-normal frequency of the quadrupole mode ($2M\omega = 0.74734 + 0.17792i$) of a Schwarzschild black hole given by Chandrasekhar and Detweiler [87]. In the globally naked singularity case (a), we did not see this damped oscillation because of the existence of the Cauchy horizon. In all cases the gravitational waves generated by matter perturbations are at most quasi-normal modes of a black hole, which is generated outside the dust cloud. Therefore intense odd-parity gravitational waves would not be produced by the inhomogeneous dust cloud collapse. We should not expect that the central extremely high density region can be observed by this mode of gravitational waves.

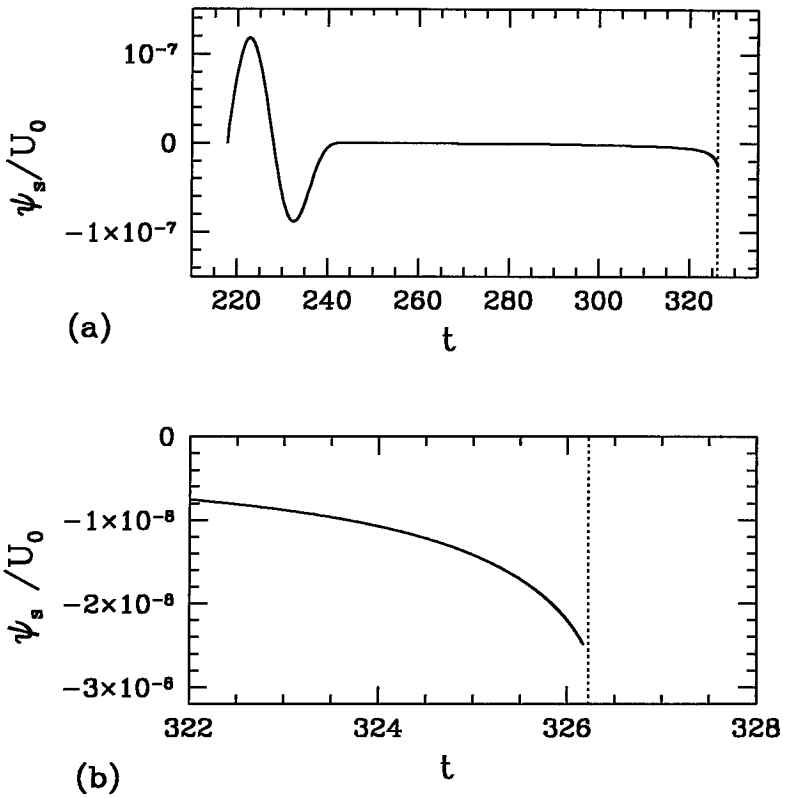

Figure 3.11: Plots of ψ_s for the globally naked case (a) at $R = 100$. In (a) the left hand side oscillation originates from the initial ingoing wave. In (b) we magnify the the right-hand edge, which is just before the Cauchy horizon. The dotted lines represent the time at which the observer at $R = 100$ intersects the Cauchy horizon, which is determined by numerical integration of the null geodesic equation from the naked singularity.

We can calculate the radiated power of the gravitational waves and thereby grasp the physical meaning of the gauge-invariant quantities. The result is de-

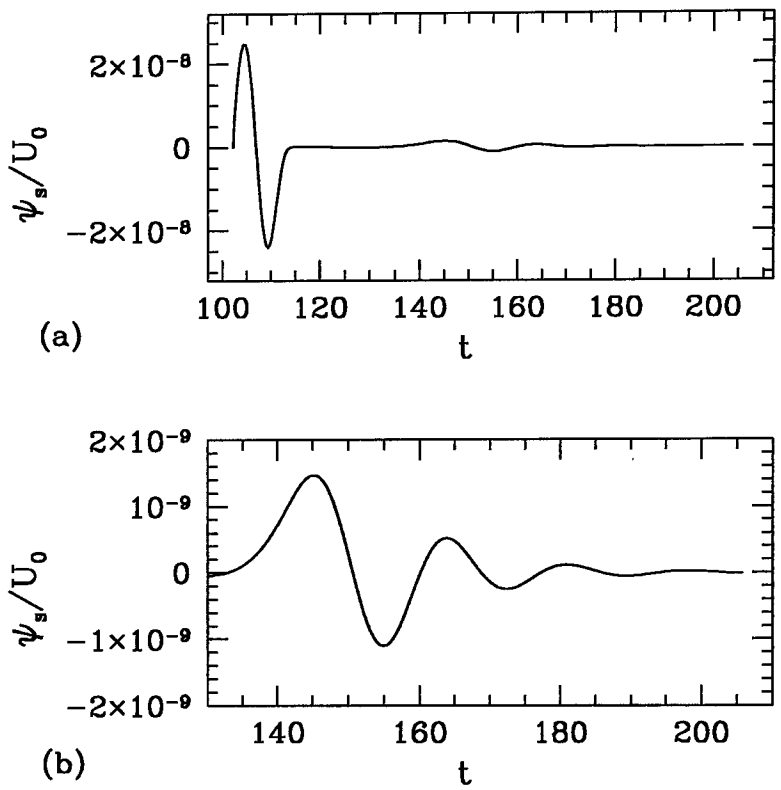

Figure 3.12: Plots of ψ_s for the locally naked case (b) at $R = 100$. In (a) the left hand side oscillation originates from the initial ingoing wave. After this oscillation, the damped oscillation dominates, and this part of the wave form is magnified in (b).

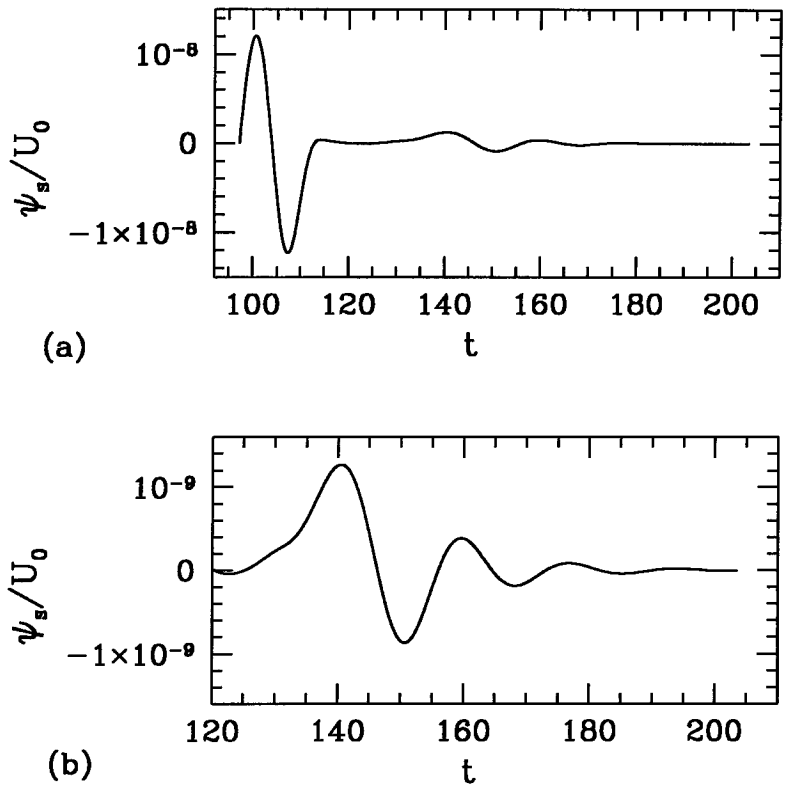

Figure 3.13: Plots of ψ_s for the black hole case (c) at $R = 100$. In (a) the left-hand side oscillation originates from the initial ingoing wave. After this oscillation, the damped oscillation dominate, as depicted in (b).

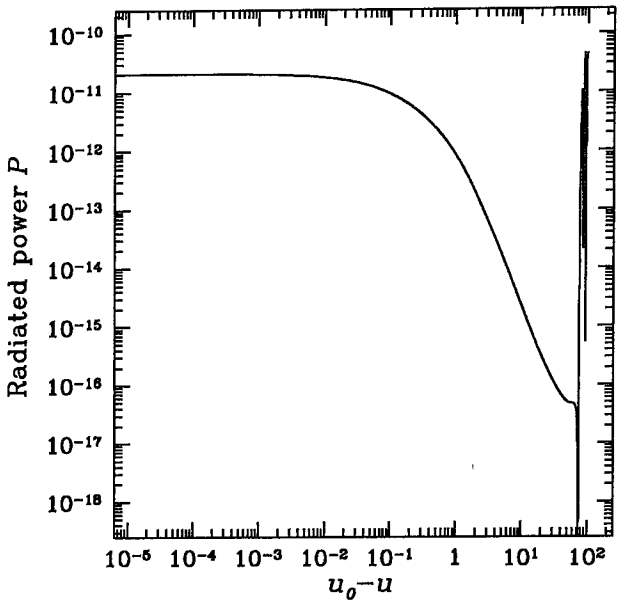

Figure 3.14: Plots of the radiated power P for globally naked case (a) at $R = 100$. The horizontal axis is the out-going null coordinate u. At the Cauchy horizon, this coordinate has the value u_0.

scribed in Appendix B. Using Eqs. (3.9) and (B.24), the radiated power P of quadrupole mode is denoted as

$$P = \frac{3}{32\pi} R'^2 \left[\partial_\tau \left(R^3 \psi_s\right)\right]^2 \tag{3.82}$$

Fig. 3.14 shows the time evolution of the radiated power P The radiated power also has a finite value at the Cauchy horizon. The total energy radiated by the odd-parity quadrupole gravitational waves during the dust collapse would not diverge.

3.4 Discussion

First we consider the behavior of the source term $S(t, r)$ around the naked singularity. From the regularity conditions and Eqs. (3.76), (3.79), and (3.80), the asymptotic behavior of the source term is obtained as

$$S(t, r) \propto r^{l-1} \tag{3.83}$$

for $t < t_0$ and

$$S(t, r) \propto r^{l-\frac{8}{3}n-1}, \tag{3.84}$$

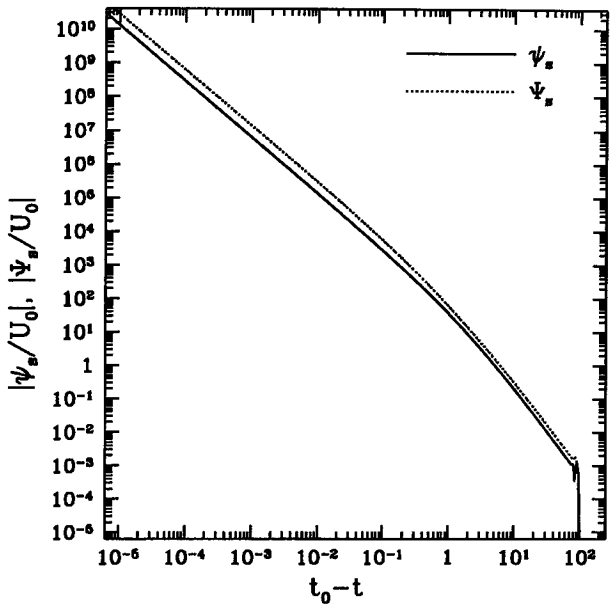

Figure 3.15: Plots of ψ_s and the estimated value Ψ_s at the center for the globally naked case (a). The solid line represents the ψ_s, and the dotted line represents the estimated value Ψ_s. Both lines exhibit power-law behavior with power indices 5/3.

at $t = t_0$. For example, in the case $l = 2$ and $n = 2$, the source term behaves on $t = t_0$ as

$$S(t, r) \propto r^{-13/3}, \tag{3.85}$$

and then it diverges at the center. Thus the divergency of ψ_s at the center originates from the source term. To confirm this, we numerically integrate the source term along the ingoing null lines with respect to u and estimate the central value of ϕ_s. We define this 'estimated' value as

$$\Phi_s \equiv \int S(t, r) du. \tag{3.86}$$

Using Eq. (3.58) we can define the estimated value of ψ_s as

$$\Psi_s \equiv \frac{\Phi_s}{3\partial_r R}. \tag{3.87}$$

We plot it in Fig. 3.15 together with the corresponding ψ_s. The estimated value has the same power-law index of ψ_s. We conclude that the behavior of ψ_s is determined by the source term in the dust cloud.

We next consider the stability of the Cauchy horizon. We found that the metric

perturbation produced by the source term does not propagate outside the dust cloud, except for quasi-normal ringing. The source term, which controls ψ_s, does not diverge at the Cauchy horizon. Therefore ψ_s should not diverge at the Cauchy horizon and should not destroy it. Then, even if odd-parity perturbations are considered, it will not be the case that the LTB spacetime loses its character as a counterexample to CCH due to Cauchy horizon instability. Also, it does not seem that such collapse is a strong source of gravitational waves.

Here we have dealt with the marginally bound case. For the case of non-marginally bound collapse, the condition of the appearance of the central naked singularity is slightly different from that in the above case [72, 73] and hence there is the possibility that the behavior of ψ_s in this case is different from that in the marginally bound case. However, it is well known that the limiting behavior of the metric as $t \to t_0(r)$ is common for all the cases:[88]

$$R \approx \left(\frac{9F}{4}\right)^{1/3} (t_0 - t)^{2/3}, \quad A \approx \left(\frac{2F}{3}\right)^{1/3} \frac{t_0'}{\sqrt{1+f}} (t_0 - t)^{-1/3} \tag{3.88}$$

We conjecture that the results of the perturbed analysis for the non-marginal collapse would be similar to the results for the marginal bound.

3.5 Summary

We have studied the behavior of the odd-parity perturbations in the LTB spacetime. For the quadrupole mode, where gravitational waves exist, we have numerically investigated the wave equation.

We have derived the wave equation for the gauge-invariant variable, ψ_s. From the analysis of the regularity for ψ_s and the perturbations of the Riemann tensor, only the quadrupole mode, $l = 2$, of ψ_s and of the magnetic part of the Weyl tensor does not vanish at the symmetric center of the background LTB space-time, where a naked singularity appears in the course of the gravitational collapse of the dust cloud. Therefore this quadrupole mode is the most important for the stability analysis of naked singularity formation in the LTB space-time. Then we have performed numerical experiments on how a Gaussian-shaped incident wave packet behaves under this wave equation for the $l = 2$ mode without matter perturbations. From those numerical experiments, we have obtained the following results. When this wave packet approaches the center, its amplitude becomes larger but finite. The amplitude at the center depends on the width of the initial wave packet according to a power law. On the other hand, when the incident wave packet initially located outside the dust cloud returns back to the same circumferential radius as the initial one, the amplitude of the returned wave is almost equal to that of the incident one.

In order to reveal the characteristic effects of the LTB space-time on the behavior of ψ_s, we have also investigated ψ_s in the Minkowski space-time. Then we

have found that in the outside of the Cauchy horizon associated with the central naked singularity, the behavior of ψ_s in the LTB space-time seems to be not so different from that in the Minkowski space-time at least except for the extreme neighborhood of the naked singularity. Therefore the power-law dependence in the LTB space-time described above is basically realized by the analytical discussion about the case of the Minkowski space-time. Further the propagation effect due to the existence of the dust cloud and the occurrence of the central naked singularity is rather small. In other words, there is no peculiar behavior of ψ_s even in the neighborhood of the central naked singularity. However, it should be noted that the odd-parity metric perturbation does not vanish in the neighborhood of the central naked singularity and Cauchy horizon associated with it. As a result, we conclude that the central naked singularity formation in the LTB space-time is 'marginally' stable against the odd-parity metric perturbations.

For the case of naked singularity formation, the gauge-invariant metric variable, ψ_s, diverges according to a power law with power index 5/3 at the center. This power index is closely related to the behavior of the matter perturbation around the center. We have also observed ψ_s at a constant circumferential radius. For the globally naked case, we cannot see intense gravitational waves propagated from the center just before the crossing of the Cauchy horizon. For the locally naked case, we have confirmed that there exist quasi-normal oscillations. As a result, we conclude that the type of singularity changes due to the odd-parity perturbation because ψ_s diverges at the center. However, the Cauchy horizon is still marginally stable against odd-parity perturbations even when we include matter perturbations.

At the final stage of the collapse, the effects of the rotational motion are important and the centrifugal force might dominate the radial motion. If this is true, the central singularity would disappear when an odd-parity matter perturbation is introduced. For the dipole mode, such a situation seems to be inevitable. However, we should note that it is a non-trivial and open question how non-linear asphericity affects the final fate of the singularity-formation process. Further, in the case of initially sufficiently small aspherical perturbations, the radius of spacetime curvature at the center might reach the Planck length, and hence there is still the possibility that the naked singularity is formed there in a practical sense. However, as our present analysis has revealed, since the Cauchy horizon is stable with respect to odd-parity linear perturbations, there is little possibility that this collapse is a strong source of odd-parity gravitational waves.

Chapter 4

Even-parity Perturbation of LTB Spacetime

We have analyzed the behavior of odd-parity perturbations in the LTB spacetime in Chap. 3. At the case of the odd-parity perturbation, however, the evolution of the matter perturbation decouples from the evolution of the metric perturbation, while the even-parity matter perturbation couples to the metric part. Therefore an even mode seems to be more essential. Particularly, the existence of matter perturbation seems to play a significant role in the evolution of perturbations. Thus, to investigate the generation of gravitational waves in LTB spacetime we should analyze even-parity perturbations. Generally, there are more gauge invariants for even-parity perturbations than for odd-parity ones. Equations for perturbations are also more complicated.

Here we investigate the behavior of the even-parity quadrupole metric and matter perturbations in the marginally bound LTB background. We numerically solve the time evolutions of the gauge invariant metric variables. We show that some of metric perturbation variables and Weyl scalar diverge at the Cauchy horizon but the energy flux does not. In this chapter we follow Iguchi, Harada, and Nakao [89].

4.1 Basic Equations

We consider the evolution of even-parity perturbations of the LTB spacetime to linear order. We follow the gauge-invariant formalism established by Gerlach and Sengupta [84, 85] which is described in Appendix A. Here we restrict our numerical investigation to the quadrupole mode in the marginally bound background. We derive the perturbed equations in that case.

There are 4 gauge-invariant metric variables, k_{ab} and k, and 7 matter variables, T_{ab}, T_a, T^2, and T^3, where a refers to t, r. The energy density $\bar{\rho}$ is perturbed by adding the scalar term $\delta\rho Y$, while the 4-velocity $\bar{u}_\mu$ is perturbed by adding the term

$$\delta u_\mu = (V_0(x^d)Y, V_1(x^d)Y, V_2(x^d)Y_{,A}). \tag{4.1}$$

The normalization for the 4-velocity yields the relation $\bar{u}^\mu \delta u_\mu = 0$. This relation implies that V_0 vanishes exactly. Then there are only three matter perturbation

variables,

$$T_{00} = \delta\rho(t,r), \tag{4.2}$$
$$T_{01} = \bar{\rho}V_1(t,r), \tag{4.3}$$
$$T_0 = \bar{\rho}V_2(t,r). \tag{4.4}$$

The others exactly vanish:

$$T_{11} = T_1 = T^3 = T^2 = 0. \tag{4.5}$$

Now we can write down the perturbed Einstein field equations for the background LTB spacetime. The resulting linearized Einstein equations are given in Appendix C.

We have obtained seven differential equations, (C.1)–(C.7), for seven variables (four metric and three matter). The right-hand sides of four of these equations vanish exactly. Then we can obtain the behavior of the metric variables through the integration of them. We transform these equations into more favorable forms. From Eq. (A.26),

$$k_{00} = \frac{1}{R'^2}k_{11}. \tag{4.6}$$

Using this relation and the remaining equations whose r.h.s. vanish, we obtain evolution equations for gauge-invariant metric variables as

$$\begin{aligned} -\ddot{q} + \frac{1}{R'^2}q'' &= \frac{4}{R^2}q + \left(\frac{2}{RR'} + \frac{R''}{R'^3}\right)q' + 3\frac{\dot{R}'}{R'}\dot{q} + 4\left(\frac{\dot{R}}{R} - \frac{\dot{R}'}{R'}\right)\dot{k} \\ &\quad + \frac{2}{R'^3}\left(-\dot{R}'' - \frac{2R'^2\dot{R}}{R^2} - \frac{R''\dot{R}}{R} + \frac{2R'\dot{R}'}{R} + \frac{2R''\dot{R}'}{R'}\right)k_{01} \\ &\quad + \frac{2}{R'^3}\left(-\dot{R}' + \frac{R'\dot{R}}{R}\right)k_{01}', \end{aligned} \tag{4.7}$$

$$\ddot{k} = -\frac{2}{R^2}q - \frac{q'}{RR'} + \frac{\dot{R}}{R}\dot{q} - 4\frac{\dot{R}}{R}\dot{k} + \frac{2}{RR'}\left(-\frac{\dot{R}'}{R'} + \frac{\dot{R}}{R}\right)k_{01}, \tag{4.8}$$

$$\dot{k}_{01} = -\frac{\dot{R}'}{R'}k_{01} - q', \tag{4.9}$$

where $q \equiv k - k_{00}$. If we solve these three equations for some initial data and for the appropriate boundary conditions, we can follow the full evolution of the metric perturbations. When we substitute these metric perturbations into Eqs. (C.1), (C.2) and (C.4), the matter perturbation variables $\delta\rho, V_1$ and V_2, respectively, are obtained.

We can also investigate the evolution of the matter perturbations from the

linearized conservation equations $\delta(T^{\mu\nu}{}_{;\nu}) = 0$. They reduce to

$$\left(\frac{\delta\rho}{\bar{\rho}}\right) = \frac{1}{\bar{\rho}R^2R'}\left(\frac{R^2\bar{\rho}}{R'}(k_{01}+V_1)\right)' - \frac{6}{R^2}V_2 - \dot{k} - \frac{3}{2}\left(\dot{k}-\dot{q}\right), \quad (4.10)$$

$$\dot{V}_1 = -\frac{1}{2}(k'-q'), \quad (4.11)$$

$$\dot{V}_2 = -\frac{1}{2}(k-q). \quad (4.12)$$

Integration of these equations gives us the time evolution of the matter perturbations. We can check the consistency of the numerical calculation by comparison of these variables and those obtained from Eqs. (C.1), (C.2) and (C.4).

To constrain the boundary conditions in our numerical calculation, we should consider the regularity conditions at the center. These conditions are obtained from requiring that all tensor quantities be expandable in non-negative integer powers of locally Cartesian coordinates near the center.[86] The detailed derivation of these conditions is too complicated to be presented here. We simply quote the results. The regularity conditions for the metric perturbations are

$$k \sim k_0(t)r^2, \quad q \sim q_0(t)r^4, \quad k_{01} \sim k_0(t)r^3. \quad (4.13)$$

For the matter perturbations, the regularity conditions at the center are

$$\delta\rho \sim \delta\rho_0(t)r^2, \quad V_1 \sim V_{10}(t)r, \quad V_2 \sim V_{20}(t)r^2 \quad (4.14)$$

Therefore all the variables we need to calculate vanish at the center.

4.2 Numerical method and results

We numerically solved the wave equations (4.7)–(4.9). Following the method of previous chapter, we transformed the wave equation (4.7) into the out-going single-null coordinate system. In this section, we present this coordinate transformation and explain our background and initial data of the perturbations. In the later half of this section, we give our numerical results.

4.2.1 Numerical method

In the previous section it was shown that the perturbation variables q, k and k_{01} vanish at the center. A careful treatment of the differential equations may be required near the center for proper propagation through the center. Hence we define the new variables

$$\tilde{q} = qR'^7/R^4, \quad \tilde{k} = kR'^4/R^2, \quad \tilde{k}_{01} = k_{01}R'^5/R^3 \quad (4.15)$$

Table 4.1: Parameters of initial density profiles and damped oscillation frequencies, where $M = 1$.

	final state	ρ_0	r_1	r_2	n	damped oscillation frequency
(a)	globally naked	1×10^{-2}	0.25	0.5	2	—
(b)	locally naked	1×10^{-1}	0.25	0.5	2	$0.36+0.096i$
(c)	black hole	2×10^{-2}	2	0.4	4	$0.36+0.093i$

These new variables are not identically zero at the regular center and do not diverge when they approach the central singularity because of the suppression factor R' We rewrite Eqs. (4.7)–(4.9) in terms of these new variables.

Next we perform a coordinate transformation for Eq. (4.7) from the synchronous comoving coordinate system (t, r) to the single-null coordinate system $(u, \tilde{r})$, where u is the outgoing null coordinate and $\tilde{r} = r$. We perform the numerical integration of this equation along two characteristic directions. Therefore we use a double null grid in the numerical calculation. Whereas we integrate Eqs. (4.8) and (4.9) along the direction $r = \text{const}$. (Detailed explanations of the single-null coordinate used in our calculation is given in INH.) As a result, we obtain the first order differential equations

$$\frac{1}{\alpha}\frac{d}{du}X = a_1 X + a_2 W + a_3 Z + a_4 \tilde{k} + a_5 \tilde{q}, \tag{4.16}$$

$$\dot{W} = b_1 X + b_2 W + b_3 Z + b_4 \tilde{k} + b_5 \tilde{q}, \tag{4.17}$$

$$\dot{Z} = c_1 X + c_2 W + c_3 Z + c_4 \tilde{k} + c_5 \tilde{q}, \tag{4.18}$$

$$\dot{\tilde{k}} = d_1 X + d_2 W + d_3 Z + d_4 \tilde{k} + d_5 \tilde{q}, \tag{4.19}$$

$$\partial_{\tilde{r}} \tilde{q} = e_1 X + e_2 W + e_3 Z + e_4 \tilde{k} + e_5 \tilde{q}, \tag{4.20}$$

where we have introduced X and W, which are defined by Eqs. (4.20) and (4.19), respectively, and

$$Z \equiv \tilde{k}_{01} - \frac{R}{R'}\tilde{q}. \tag{4.21}$$

The coefficients $a_1, a_2, \cdots$ are shown in Appendix C. Equations (4.16) and (4.20) are integrated along the double-null grid. We integrate Eq. (4.16) using the scheme of an explicit first order difference equation, and we use the trapezoidal rule to integrate Eq. (4.20). Equations (4.17)–(4.19) are integrated along the timelike directions $r = \text{const}$ using a first order difference method. We interpolate variables to estimate the right-hand sides of Eqs. (4.17)–(4.19) at the same radial coordinate r on the previous out-going null slice.

We adopt Eq. (3.72) in Sec. 3 as the initial rest mass density profile. Using this density profile, we numerically calculate the total gravitational mass of the dust cloud M. In our calculation we adopt the total mass M as the unit of the variables.

We give the numerical results from the initial conditions for the perturbations

$$X = \frac{\partial_{\tilde{r}}\tilde{q} - (e_3 Z + e_5 \tilde{q})}{e_1}, \tag{4.22}$$

$$W = -d_5 \tilde{q}, \tag{4.23}$$

$$Z = 4\frac{R}{\dot{R}R'}\tilde{q}, \tag{4.24}$$

$$\tilde{k} = -\frac{(3R'b_1 + b_5 - b_2 d_5)\tilde{q}}{b_4}, \tag{4.25}$$

$$\tilde{q} = \left(1 + \left(\frac{r}{r_3}\right)^2\right)^{-\frac{5}{2}} \frac{R^2}{\dot{R}^2} b_4, \tag{4.26}$$

on the initial null surface. Here $\dot{\tilde{k}}$ vanishes on this surface and $\dot{W}$ and $\dot{Z}$ are diminished near the center. We chose $r_3 = 0.3 r_{\text{core}}$. The main results of our numerical investigation do not depend on the detailed choice of the initial conditions.

4.2.2 Results

First we observe the behavior of the metric variables q, k, k_{01} and the Weyl scalar, which corresponds to out-going waves,

$$\Psi_4 \equiv C_{\mu\nu\rho\sigma} n^\mu \bar{m}^\nu n^\rho \bar{m}^\sigma \tag{4.27}$$

$$= -\frac{3}{32}\sqrt{\frac{5}{\pi}} \sin^2\theta \frac{k_{01} - (k-q)R'}{R^2 R'}, \tag{4.28}$$

where

$$n^\mu = \left(\frac{1}{2}, -\frac{1}{2R'}, 0, 0\right) \tag{4.29}$$

$$\bar{m}^\nu = \left(0, 0, \frac{1}{\sqrt{2}R}, -\frac{i}{\sqrt{2}R\sin\theta}\right), \tag{4.30}$$

outside the dust cloud. The results are plotted in Fig. 4.1. We can see that the metric variables q, k_{01} and the Weyl scalar Ψ_4 diverge when they approach the Cauchy horizon. The asymptotic power indices of these quantities are about ~ 0.88. On the other hand the metric quantity k does not diverge when it approaches the Cauchy horizon. The energy flux is computed by constructing the Landau-Lifshitz pseudotensor. We can calculate the radiated power of gravitational waves from this. The result is given in Appendix B. For the quadrupole mode, the total radiated power becomes

$$P = \frac{3}{8\pi}k^2 \tag{4.31}$$

The radiated power of the gravitational waves is proportional to the square of k. Therefore the system of spherical dust collapse with linear perturbations cannot

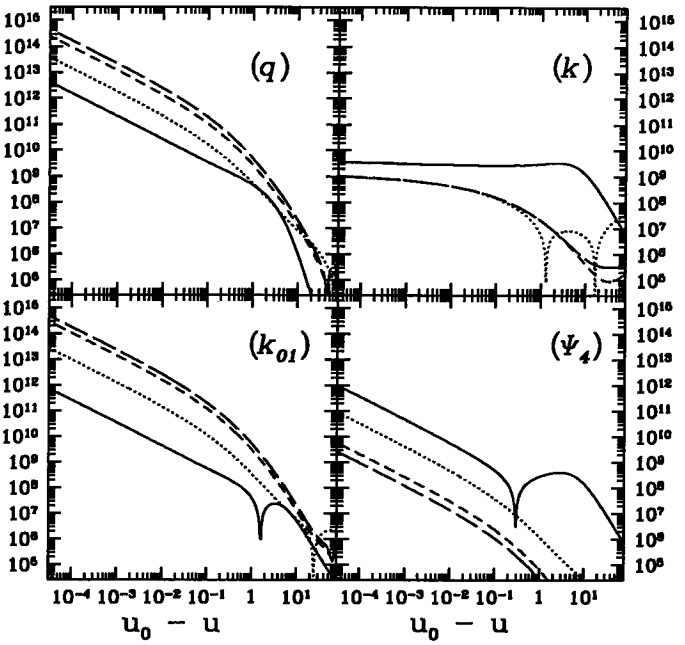

Figure 4.1: Plots of perturbed variables q, k, k_{01} and the Weyl scalar Ψ_4 at constant circumferential radius R. The results for $R = 1$, $R = 10$, $R = 100$, and $R = 200$ are plotted. The solid lines represent the results for $R = 1$, the dotted lines for $R = 10$, the dashed lines for $R = 100$, and the long dashed lines for $R = 200$. $u = u_0$ corresponds to the Cauchy horizon.

be expected as a strong source of gravitational waves.

Second we observe the perturbations near the center. The results are plotted in Figs. 4.2 and 4.3. In these figures we plot the perturbations at $t - t_0(0) = -10^{-1}$, -10^{-2}, -10^{-3}, -10^{-4}, and 0. Before the formation of the naked singularity, the perturbations obey the regularity conditions at the center. Each line in these figures displays this dependence if the radial coordinate is sufficiently small. In this region, we can also see that all the variables grow according to power-laws on the time coordinate along the lines of $r = \text{const}$. The asymptotic behavior of perturbations near the central naked singularity is summarized as follows:

$$q \propto \Delta t^{-2.1} r^4, \quad k \propto \Delta t^{-1.4} r^2, \quad k_{01} \propto \Delta t^{-1.0} r^3,$$
$$\frac{\delta\rho}{\bar{\rho}} \propto \Delta t^{-1.6} r^2, \quad V_1 \propto \Delta t^{-0.4} r, \quad V_2 \propto \Delta t^{-0.4} r^2,$$

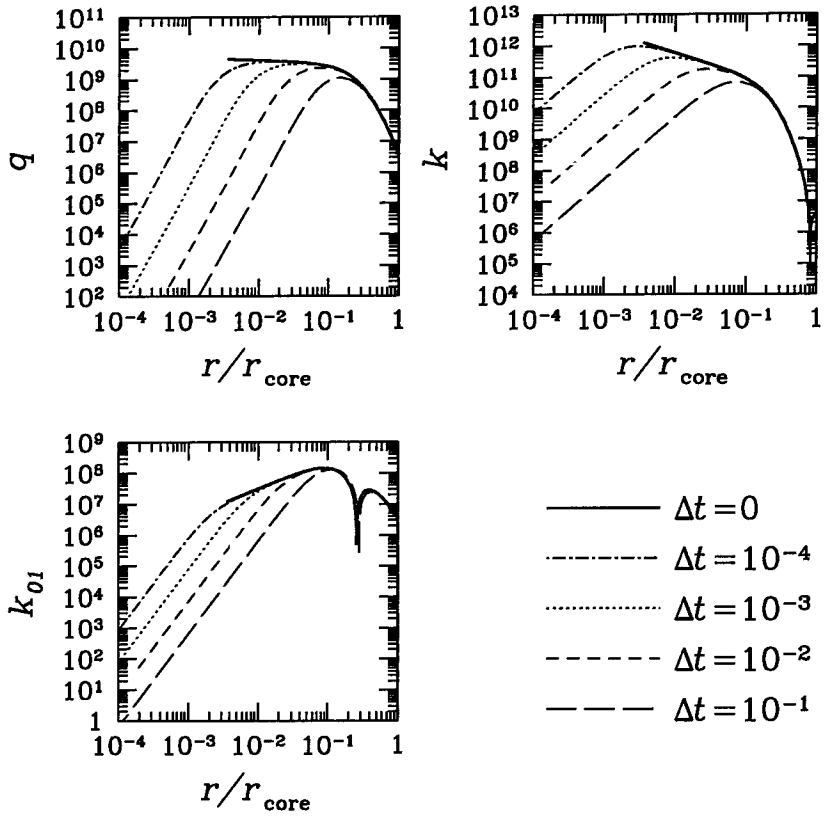

Figure 4.2: Plots of perturbed variables q, k and k_{01} near the center. The values for $\Delta t = t_0 - t = 10^{-1}, 10^{-2}, 10^{-3}, 10^{-4}, 0$ are plotted. The solid lines represent the results for $\Delta t = 0$, the long dashed lines for $\Delta t = 10^{-1}$, the dashed lines for $\Delta t = 10^{-2}$, the dotted lines for $\Delta t = 10^{-3}$, and the dotted dashed lines for $\Delta t = 10^{-4}$

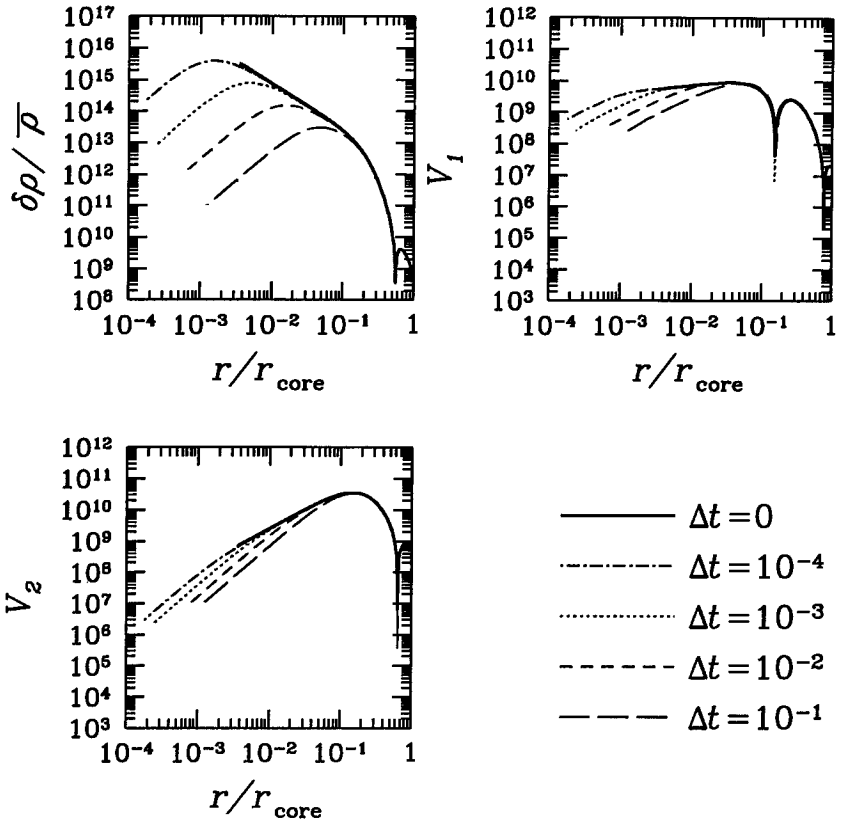

Figure 4.3: Plots of perturbed variables $\delta\rho, V_1$, and V_2 near the center. The values for $\Delta t = 10^{-1}, 10^{-2}, 10^{-3}, 10^{-4}$, and 0 are plotted. The solid lines represent the results for $\Delta t = 0$, the long dashed lines for $\Delta t = 10^{-1}$, the dashed lines for $\Delta t = 10^{-2}$, the dotted lines for $\Delta t = 10^{-3}$, and the dotted dashed lines for $\Delta t = 10^{-4}$

where $\Delta t = t_0(0) - t$. On the time slice at $\Delta t = 0$, perturbations behave as

$$q \propto r^{-0.09}, \quad k \propto r^{-0.74}, \quad k_{01} \propto r^{0.92},$$
$$\frac{\delta\rho}{\bar{\rho}} \propto r^{-1.4}, \quad V_1 \propto r^{0.25}, \quad V_2 \propto r^{1.3}$$

On this slice k and $\delta\rho/\bar{\rho}$ diverge and q diverges weakly when they approach the central singularity. On the other hand, k_{01} and V_2 go to zero and V_1 vanishes slowly.

In cases of a locally naked singularity and black hole formation, we expect to observe damped oscillation in the asymptotic region outside the dust cloud, as in the odd parity case. The results are plotted in Fig. 4.4. These figures show that damped oscillations are dominant. We read the frequencies and damping rates of these damped oscillations from Fig. 4.4 and give them in terms of complex

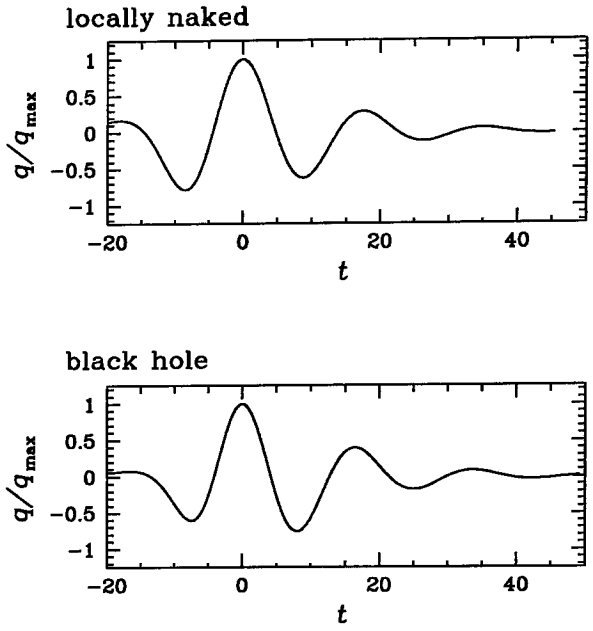

Figure 4.4: Plots of perturbed variables q at constant circumferential radius $R = 100$ in the locally naked and black hole cases. q is normalized with respect to its maximum value, and the origin of the time variable is adjusted to coincide with the time when q is maximum.

frequencies as $0.36+0.096i$ and $0.36+0.093i$ for locally naked and black hole cases, respectively. These results agree well with the fundamental quasi-normal frequency of the quadrupole mode ($2M\omega = 0.74734 + 0.17792i$).[87]

The numerical accuracy of our calculations was checked with the equations that were not used for the derivation of Eqs. (4.7)–(4.9), e.g., Eq. (C.4). We define the maximum relative error $\mathcal{E}$ as

$$\mathcal{E} \equiv \frac{\left| -2\frac{R^3}{R'^8}X + 2\frac{R^2}{R'^4}W + \frac{R^3}{R'^6}\left(6\frac{R''}{R'^2} - \frac{3}{R} - 7\frac{\dot{R}}{R} + 8\frac{\dot{R}'}{R'}\right)Z \right.}{\Sigma|\text{each term of numerator}|} \\ \left. -\frac{R^3}{R'^7}\partial_{\bar{r}}Z + \frac{R^2}{R'^4}\left(4\frac{\dot{R}}{R} - 6\frac{\dot{R}'}{R'}\right)\tilde{k} + 16\pi\bar{\rho}V_2 \right| . \quad (4.32)$$

We calculated this quantity on the last null surface where the matter variable V_2 is obtained from the integration of Eq. (4.12) using a method similar to that used for Eqs. (4.17)–(4.19). The results are displayed in Fig. 4.5. Except the region of small r say, ($r < 3 \times 10^{-4}$), this value is less than 0.01. Both the numerator and denominator of Eq. (4.32) vanish at the center. Therefore it seems difficult to estimate the numerical errors from Eq. (4.32) when r is small.

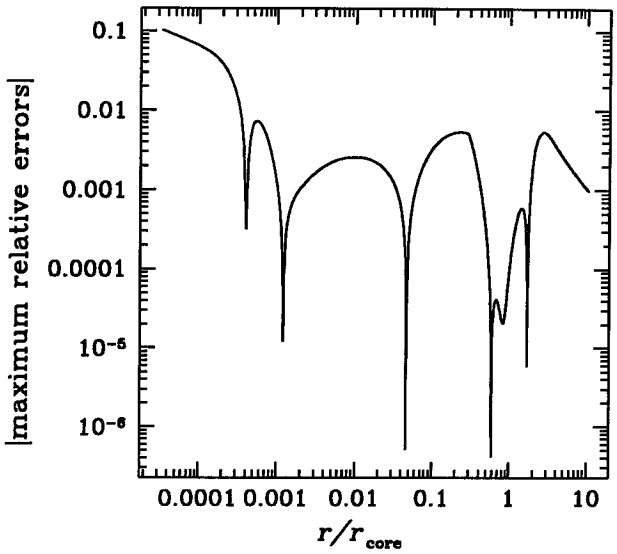

Figure 4.5: Maximum relative errors on the last null slice.

4.3 Discussions

In this section we consider the physical interpretation of our numerical results for even-parity perturbations. The divergence behavior of the perturbations implies that the linear perturbation analysis near the Cauchy is invalid. This fact shows that aspherical effects are important in the naked singularity formation.

To consider where these effects are important and what would happen in this region, we should discuss our results more carefully. The perturbations grow according to power-laws and diverge only at the Cauchy horizon. Therefore, except for the region very near the Cauchy horizon, the perturbations are finite and small when we choose sufficiently small initial values. This means that the central region can reach an extremely high density before the breakdown of the linear perturbation analysis. While in the region of spacetime just before the Cauchy horizon, aspherical property becomes important for the dynamics of the spacetime. Our results suggest that the Cauchy horizon is unstable and that a singularity appears along it.

The naked singularity of the LTB spacetime is considered as a massless singularity. Gravitational waves, even if they have finite energy, would affect the naked singularity. To investigate this effect we should consider back-reaction of the gravitational waves.

4.4 Summary

We have studied the behavior of even-parity perturbations in the LTB spacetime. We have numerically solved the linearized Einstein equations for gauge-invariant variables in the case of the quadrupole mode and marginally bound background. We have constructed a numerical code which solves the perturbation equations on an out-going single null coordinate. For the globally naked case, the perturbed variables q, k_{01} and the Weyl scalar Ψ_4 grow as powers of $(u_0 - u)$ outside the dust cloud, where the power index is approximately -0.88. Then the Cauchy horizon of this spacetime is unstable with respect to linear even-parity perturbations. On the other hand, the perturbed variable k is finite just before the crossing of the Cauchy horizon. The energy flux, which is proportional to the square of k, is also finite. Therefore inhomogeneous aspherical dust collapse is not expected to be a strong source of gravitational wave bursts.

We have investigated the asymptotic behavior of perturbations near a central naked singularity. If the radial coordinate is sufficiently small, the dependence on it is determined by the regularity conditions at the center. Our numerical results show this dependence. The time dependence is an inverse power-law in Δt. At the time of naked singularity formation, q, k and $\delta\rho/\bar{\rho}$ diverge when they approach the central singularity, while k_{01}, V_1 and V_2 do not.

For the cases of locally naked and black hole formation, there appear the damped oscillations outside the dust cloud. This is consistent with the fundamental quasi-normal frequency of the quadrupole mode of a Schwarzschild black hole.

Chapter 5

Newtonian Analysis of Gravitational Waves around a Naked Singularity

---

In the previous chapter we have numerically shown that some perturbed variables and Weyl scalar grow according to the power of $u_0 - u$ outside the dust cloud, whereas perturbed variable k and energy flux are finite. Here we attempt to explain these properties by analytical treatment. To do so, we perform Newtonian approximation and estimate gravitational waves by quadrupole formula. For the globally naked case, the inequality $R < F$ is satisfied outside the Cauchy horizon except for the center in the dust cloud. Then the gravitational potential $|\Phi|$ and the velocity v of each dust shell component satisfy the relations

$$|\Phi| \sim v^2 \sim \dot{R}^2 \sim \frac{F}{R} < 1. \tag{5.1}$$

Thus the relativistic effects may be small. The results show a good similarity.

5.1 Newtonian Background Metric and Coordinate System.

First, we make relations between the Eulerian, Lagrangian and synchronous-comoving (SC) coordinate systems in the Newtonian approximation clear. In the Newtonian approximation, the maximal time slicing condition and the Eulerian coordinate are often adopted; the line element is assumed to be the following form:

$$ds_E^2 = -(1 + 2\Phi_N)\, dT^2 + dR^2 + R^2 d\Omega^2, \tag{5.2}$$

where Φ_N is Newtonian gravitational potential and we have adopted the spherical-polar coordinate system as a spatial coordinates.

For the purpose to follow the motion of a dust sphere, the Lagrangian coordinate is more suitable. The transformation matrix between the above coordinate system

and the Lagrangian one is given by

$$dT = d\tau, \tag{5.3}$$
$$dR = (\partial_\tau R)_x d\tau + (\partial_x R)_\tau dx. \tag{5.4}$$

Then the line element in the Lagrangian coordinate system is obtained as

$$\begin{aligned} ds_L^2 &= -\left\{1 + 2\Phi_N - (\partial_\tau R)_x^2\right\} d\tau^2 + 2(\partial_\tau R)_x (\partial_x R)_\tau d\tau dx \\ &\quad + (\partial_x R)_\tau^2 dx^2 + R^2(\tau, x) d\Omega^2 \end{aligned} \tag{5.5}$$

In the Lagrangian coordinate system, the equations for the circumferential radius, Newtonian gravitational potential and the dust fluid are given by

$$(\partial_\tau R)_x^2 = f(x) + \frac{F(x)}{R}, \tag{5.6}$$
$$(\partial_x \Phi_N)_\tau = \frac{(\partial_x R)_\tau}{2R^2} F(x), \tag{5.7}$$
$$F(x) = 8\pi \int_0^x \bar{\rho}(\tau, y)(\partial_y R)_\tau R^2 dy. \tag{5.8}$$

where $f(x)$ is an arbitrary function and $F(x)$ is also regarded as an arbitrary function which determines an initial configuration of the density $\bar{\rho}$ of the dust fluid.

In the LTB solution, the SC coordinate system is usually adopted for combinience. We should note that the SC coordinate system is different from the Lagrangian one. The transformation matrix between the SC coordinate system and Lagrangian one is given by

$$dt = \left\{1 + \Phi_N - \frac{1}{2}(\partial_\tau R)_x^2\right\} d\tau - (\partial_\tau R)_x (\partial_x R)_\tau dx, \tag{5.9}$$
$$dr = dx. \tag{5.10}$$

The derivative of the circumferential radius R with respect to the Lagrangian time coordinate τ is written as

$$(\partial_\tau R)_x = (\partial_\tau t)_x (\partial_t R)_r + (\partial_\tau r)_x (\partial_r R)_t = \left\{1 + \Phi_N - \frac{1}{2}(\partial_\tau R)_x^2\right\} (\partial_t R)_x. \tag{5.11}$$

In the Newtonian approximation, expansion parameter ϵ is the ratio between typical speed of the system and speed of light. The order-counting is given as follows:

$$R = O(\epsilon^0), \quad (\partial_x R)_\tau = O(\epsilon^0), \quad (\partial_\tau R)_x = O(\epsilon), \quad \text{and} \quad \Phi_N = O(\epsilon^2). \tag{5.12}$$

Then the line element in the SC coordinate system up to the Newtonian order is

written as

$$ds^2_{SC} = -dt^2 + (\partial_\tau R)^2_t dr^2 + R^2 d\Omega^2. \tag{5.13}$$

Further we obtain the equations up to the Newtonian order in the SC coordinate system are given in the completely same form as that in the Lagrangian one:

$$(\partial_t R)^2_\tau = f(r) + \frac{F(r)}{R}, \tag{5.14}$$

$$F(r) = 8\pi \int_0^r \bar{\rho}(\tau, y)(\partial_\tau R)_t R^2 dy. \tag{5.15}$$

Here note that in the SC coordinate system, the Newtonian gravitational potential Φ_N does not appear. The above equation is the Newtonian order equations of the LTB space-time, which are completely the same form as the relativistic one.

5.2 Perturbation

We consider non-spherical perturbations in a system of a spherically symmetric dust ball. First, we consider perturbations in the Eulerian coordinate system. The line element is written as

$$ds^2_E = -\left(1 + 2\Phi_N + 2\delta\Phi_N\right) dT^2 + dR^2 + R^2 d\Omega^2, \tag{5.16}$$

where $\delta\Phi_N$ is a perturbation of the Newtonian gravitational potential. Using the transformation matrix (5.3) and (5.4), we obtain the perturbed line element by using the background Lagrangian coordinate system:

$$\begin{aligned} ds^2_L &= -\left\{1 + 2\Phi_N + 2\delta\Phi_N - (\partial_\tau R)^2_x\right\} d\tau^2 + 2(\partial_\tau R)_x (\partial_x R)_\tau d\tau dx \\ &+ (\partial_x R)^2_\tau dx^2 + R^2 d\Omega^2. \end{aligned} \tag{5.17}$$

Hereafter we discuss the behaviors of perturbations in this coordinate system. The density ρ and 4-velocity u^μ are written in the form

$$\rho = \bar{\rho}(1 + \delta_\rho), \tag{5.18}$$

$$u^\mu = \bar{u}^\mu + \delta u^\mu, \tag{5.19}$$

where $\bar{\rho}$ and $\bar{u}^\mu$ are the background quantities. By definition, the components of the background 4-velocity is given by

$$(\bar{u}^\mu) = \left(\bar{u}^0, 0, 0, 0\right) \tag{5.20}$$

From the normalization of the 4-velocity, we find

$$\delta u^0 = \delta\Phi_N + (\partial_\tau R)_x (\partial_x R)_\tau \delta u^1 \tag{5.21}$$

The order-counting with respect to the expansion parameter of the Newtonian

approximation is given by

$$\delta u^0 = O(\epsilon^2), \quad \delta u^\ell = O(\epsilon), \quad \delta_\rho = O(\epsilon^0) \quad \text{and} \quad \delta\Phi_N = O(\epsilon^2). \tag{5.22}$$

Then the equations for the perturbations are given by

$$\partial_\tau \delta_\rho + \frac{1}{\bar{\rho}\sqrt{\bar{\gamma}}}\partial_\ell\left(\bar{\rho}\sqrt{\bar{\gamma}}\delta u^\ell\right) = 0, \tag{5.23}$$

$$\partial_\tau \delta u_\ell + \partial_\ell \delta\Phi_N = 0, \tag{5.24}$$

$$\frac{1}{\sqrt{\bar{\gamma}}}\partial_\ell\left(\sqrt{\bar{\gamma}}\bar{\gamma}^{\ell m}\partial_m \delta\Phi_N\right) - 4\pi\bar{\rho}\delta_\rho = 0, \tag{5.25}$$

where

$$\sqrt{\bar{\gamma}} \equiv (\partial_x R)_\tau R^2 \sin\theta, \tag{5.26}$$

and $\bar{\gamma}^{\ell m}$ is a contravariant component of the background 3-metric.

Here we focus on the axisymmetric even modes of perturbations. Hence the perturbations are expressed in the form

$$\delta_\rho = \sum_l \Delta_{\rho(l)}(\tau, x) P_l(\cos\theta), \tag{5.27}$$

$$\delta\Phi_N = \sum_l \Delta_{\Phi(l)}(\tau, x) P_l(\cos\theta), \tag{5.28}$$

$$\delta u_1 = \sum_l U_{x(l)}(\tau, x) P_l(\cos\theta), \tag{5.29}$$

$$\delta u_2 = \sum_l U_{\theta(l)}(\tau, x) \frac{d}{d\theta} P_l(\cos\theta), \tag{5.30}$$

$$\delta u_3 = 0. \tag{5.31}$$

From Eqs.(5.23), (5.24) and (5.25), we obtain

$$\partial_\tau \Delta_{\rho(l)} + \frac{1}{F'}\partial_x\left(\frac{F'}{R'^2}U_{x(l)}\right) - l(l+1)\frac{U_{\theta(l)}}{R^2} = 0, \tag{5.32}$$

$$\partial_\tau U_{x(l)} + \partial_x \Delta_{\Phi(l)} = 0, \tag{5.33}$$

$$\partial_\tau U_{\theta(l)} + \Delta_{\Phi(l)} = 0, \tag{5.34}$$

$$\frac{1}{R'R^2}\partial_x\left(\frac{R^2}{R'}\partial_x \Delta_{\Phi(l)}\right) - l(l+1)\frac{\Delta_{\Phi(l)}}{R^2} - 4\pi\bar{\rho}\Delta_{\rho(l)} = 0, \tag{5.35}$$

where $R' \equiv (\partial_x R)_\tau$ and $F' \equiv dF/dx$.

Hereafter we focus on the case where the background is marginally bound. The solution of the background is given in the form

$$R(\tau, x) = \left(\frac{9F}{4}\right)^{\frac{1}{3}} [\tau_R(x) - \tau]^{\frac{2}{3}}, \tag{5.36}$$

where

$$\tau_R(x) = \frac{2}{3\sqrt{F}} x^{\frac{3}{2}} \tag{5.37}$$

The background variables are written in the form of Taylor series

$$F = x^3 \left(\frac{4}{9} + \sum_{n=1}^{\infty} F_{(n)} x^{2n} \right), \tag{5.38}$$

$$\tau_R = 1 + \sum_{n=1}^{\infty} \tau_{R(n)} x^{2n}, \tag{5.39}$$

$$R = x \sum_{n=0}^{\infty} R_{(n)}(\tau) x^{2n}, \tag{5.40}$$

$$\bar{\rho} = \sum_{n=0}^{\infty} \bar{\rho}_{(n)}(\tau) x^{2n} \tag{5.41}$$

Here we choose a normalization factor of F so that τ_R is equal to unity at the origin. On the other hand, the perturbation variables are written in the form

$$\Delta_\rho = x^2 \sum_{n=0}^{\infty} \Delta_{\rho(n)}(\tau) x^{2n}, \tag{5.42}$$

$$\Delta_\Phi = x^2 \sum_{n=0}^{\infty} \Delta_{\Phi(n)}(\tau) x^{2n}, \tag{5.43}$$

$$U_x = x \sum_{n=0}^{\infty} U_{x(n)}(\tau) x^{2n}, \tag{5.44}$$

$$U_\theta = x^2 \sum_{n=0}^{\infty} U_{\theta(n)}(\tau) x^{2n}. \tag{5.45}$$

We introduce the following hatted variables:

$$F'\Delta_\rho = x^4 \hat{\Delta}_\rho, \tag{5.46}$$

$$F'U_x = x^3 \hat{U}_x, \qquad F'U_\theta = x^4 \hat{U}_\theta, \tag{5.47}$$

$$\Delta_\Phi = x^2 \hat{\Delta}_\Phi. \tag{5.48}$$

To obtain the solution of Eq.(5.35), we introduce the following variable,

$$\Delta_\Phi = \frac{\varpi(\tau, x)}{R^3}. \tag{5.49}$$

Substituting the above form of Δ_Φ into Eq.(5.35), we obtain the equation for ϖ as

$$\frac{\partial}{\partial x} \left(\frac{1}{R' R^4} \frac{\partial \varpi}{\partial x} \right) = \frac{F'\Delta_\rho}{2R^3} \tag{5.50}$$

Integrating the above equation, we obtain

$$\frac{\partial \varpi}{\partial x} = -\frac{1}{2} R' R^4 \int_x^\infty dx_1 \frac{F'(x_1)}{R^3(\tau, x_1)} \Delta_\rho(\tau, x_1), \tag{5.51}$$

where we have chosen the integration constant so that $\partial\varpi/\partial x$ is finite for $x \to \infty$. Further integration leads to

$$\begin{aligned}
\varpi(\tau, x) &= -\frac{1}{2}\int_0^x dx_1 R'(\tau, x_1) R^4(\tau, x_1) \int_{x_1}^\infty dx_2 \frac{F'(x_2)}{R^3(\tau, x_2)} \Delta_\rho(\tau, x_2) \\
&= -\frac{1}{2}\int_0^x dx_1 R'(\tau, x_1) R^4(\tau, x_1) \int_x^\infty dx_2 \frac{F'(x_2)}{R^3(\tau, x_2)} \Delta_\rho(\tau, x_2) \\
&\quad -\frac{1}{2}\int_0^x dx_2 \frac{F'(x_2)}{R^3(\tau, x_2)} \Delta_\rho(\tau, x_2) \int_0^{x_2} dx_1 R'(\tau, x_1) R^4(\tau, x_1) \\
&= -\frac{1}{10}\left\{ R^5 \mathcal{A}(\tau, x) + x^7 \mathcal{B}(\tau, x) \right\}
\end{aligned} \tag{5.52}$$

where

$$\mathcal{A}(\tau, x) \equiv \int_x^\infty dx_1 \frac{F'(x_1)}{R^3(\tau, x_1)} \Delta_\rho(\tau, x_1), \tag{5.53}$$

$$\mathcal{B}(\tau, x) \equiv \frac{1}{x^7}\int_0^x dx_1 F'(x_1) \Delta_\rho(\tau, x_1) R^2(\tau, x_1), \tag{5.54}$$

and we have chosen the integration constant so that q vanishes at the origin, $x = 0$. Hence $\hat{D}_\Phi$ and $\hat{\Delta}_\Phi$ are written as

$$\hat{\Delta}_\Phi = -\frac{1}{10}\left\{ \left(\frac{R}{x}\right)^2 \mathcal{A} + x^2 \left(\frac{x}{R}\right)^3 \mathcal{B} \right\}, \tag{5.55}$$

$$\hat{D}_\Phi = -\frac{R'}{10}\left\{ 2\left(\frac{R}{x}\right) \mathcal{A} - 3x^2 \left(\frac{x}{R}\right)^4 \mathcal{B} \right\} \tag{5.56}$$

5.3 Quadrupole Moment

Hereafter we focus on the quadrupole mode $l = 2$. The mass quadrupole moment Q_{ij} is then given as

$$Q_{ij} \equiv \int \rho \left(X_i X_j - \frac{1}{3} R^2 \delta_{ij} \right) d^3X = \frac{4\pi}{15} Q(T) \mathrm{diag}[-1, -1, 2], \tag{5.57}$$

where

$$Q(T) \equiv \int_0^\infty \bar{\rho} \Delta_\rho R^4 dR = \frac{1}{8\pi} \lim_{x \to \infty} x^7 \mathcal{B}(\tau, x). \tag{5.58}$$

As well known, the gravitational waves h_{ij} at the null infinity is given by

$$h_{ij} \longrightarrow \frac{1}{R}\left(\frac{d^2Q_{ij}(Y)}{dY^2}\right)_{Y=T-R} \tag{5.59}$$

Hence the Weyl scalar Ψ_4 is proportional to the fourth order derivative of $Q(T-R)$ with respect to the Newtonian time T

By the transformation matrix Eqs.(5.3) and (5.4), the derivative $(\partial/\partial T)_R$ is rewritten by use of the independent variables of the Lagrangian coordinates as

$$\left(\frac{\partial}{\partial T}\right)_R = \left(\frac{\partial}{\partial \tau}\right)_x - \frac{\dot{R}}{R'}\left(\frac{\partial}{\partial x}\right)_\tau, \tag{5.60}$$

where $\dot{R} \equiv (\partial_\tau R)_x$. Then for a finite function $\mathsf{f}(x)$ with sufficiently rapid fall off for $r \to \infty$, we find that

$$\begin{aligned}\frac{d}{dT}\int_0^\infty \mathsf{f} dR &= \int_0^\infty \left(\frac{\partial \mathsf{f}}{\partial T}\right)_R dR = \int_0^\infty \left\{\left(\frac{\partial \mathsf{f}}{\partial \tau}\right)_x - \frac{\dot{R}}{R'}\left(\frac{\partial \mathsf{f}}{\partial x}\right)_\tau\right\} R' dx \\ &= \int_0^\infty \left(R'\frac{\partial \mathsf{f}}{\partial \tau} + \dot{R}'\mathsf{f}\right) dx - \left[\dot{R}\mathsf{f}\right]_0^\infty = \int_0^\infty \frac{\partial}{\partial \tau}(R'\mathsf{f}) dx. \end{aligned} \tag{5.61}$$

Using the above formula, we obtain

$$\frac{d^m Q}{dT^m} = \int_0^\infty \frac{\partial^m}{\partial \tau^m}\left(\bar{\rho}\Delta_\rho R' R^4\right) dx = \frac{1}{8\pi}\int_0^\infty F' \frac{\partial^m}{\partial \tau^m}\left(\Delta_\rho R^2\right) dx. \tag{5.62}$$

5.4 Analytic Estimate of the Asymptotic Behavior

From Eqs.(5.33) and (5.34), we find

$$\partial_\tau\left(U_x - \partial_x U_\theta\right) = 0. \tag{5.63}$$

Hence U_x is written in the form

$$U_x = \partial_x U_\theta + C_x(x). \tag{5.64}$$

Here we assume that C_x vanishes because it will not play an important role. This makes us to focus on only Δ_ρ and U_θ.

The numerical calculation in Chap. 4 revealed that the perturbation variables $\delta\rho/\bar{\rho}$, V_1, and V_2 grow in accordance with power laws near the center. Then we assume that perturbation variables $\hat{\Delta}_\rho$ and $\hat{U}_\theta$ grow at the origin $x = 0$ as

$$\hat{\Delta}_\rho \propto (1-\tau)^{-p} \quad \text{and} \quad \hat{U}_\theta \propto (1-\tau)^{-q}, \tag{5.65}$$

where p and q are positive numbers. The perturbation variables becomes infinite only at the origin at $\tau = 1$, while these do not elsewhere at this moment. Further, the perturbation variables are regular everywhere before the central singularity formation. These results imply that the perturbation variables take the following forms

$$\hat{\Delta}_\rho = C_\rho(\tau, x)\left[\tau_\rho(x) - \tau\right]^{-p}, \tag{5.66}$$

$$\hat{U}_\theta = C_\theta(\tau, x)\left[\tau_\theta(x) - \tau\right]^{-q}, \tag{5.67}$$

where the functions, τ_ρ, τ_θ, C_ρ and C_θ are assumed to be everywhere regular. Hence those functions are written in the form of the Taylor series around $(\tau, x) = (1, 0)$ as,

$$\tau_\rho(x) = 1 + \sum_{m=1}^{\infty} \tau_{\rho(m)} x^{2m}, \tag{5.68}$$

$$\tau_\theta(x) = 1 + \sum_{m=1}^{\infty} \tau_{\theta(m)} x^{2m}, \tag{5.69}$$

$$C_\rho(\tau, x) = \sum_{m=0}^{\infty}\sum_{n=0}^{\infty} C_{\rho(m,n)}(1-\tau)^m x^{2n}, \tag{5.70}$$

$$C_\theta(\tau, x) = \sum_{m=0}^{\infty}\sum_{n=0}^{\infty} C_{\theta(m,n)}(1-\tau)^m x^{2n}, \tag{5.71}$$

where $\tau_{\rho(1)}$ and $\tau_{\theta(1)}$ should be positive for the perturbation variables should be regular everywhere before the central singularity formation.

Now our present purpose is to estimate the power p, q and the contribution of the central singularity formation to the quadrupole moment. For this purpose, we introduce two infinitesimal parameters, ϵ and κ, and assume

$$\Delta\tau \equiv 1 - \tau = O(\epsilon) \qquad \text{and} \qquad x = O(\kappa), \tag{5.72}$$

Further introduce a new variable w defined by

$$w \equiv \left(\frac{\tau_{R(1)}}{\Delta\tau}\right)^{\frac{1}{2}} x = O(\epsilon^{-\frac{1}{2}}\kappa). \tag{5.73}$$

First, in order to find p and q we focus our attention on the region in which the parameters ϵ and κ satisfy the following relation,

$$0 < \kappa^4 \ll \epsilon \ll \kappa^2 \tag{5.74}$$

The above equation implies $\kappa^{-1} \gg \epsilon^{-\frac{1}{2}}\kappa \gg 1$ and hence w is large number in this

region. Then we cam write the perturbation variables as

$$\hat{\Delta}_\rho = \frac{C_{\rho(0,0)}}{\beta_\rho^p \Delta\tau^p w^{2p}} \left\{ 1 - \frac{p}{\beta_\rho w^2} + \mathcal{O}(\kappa^2) \right\}, \tag{5.75}$$

$$\frac{\partial \hat{\Delta}_\rho}{\partial \tau} = \frac{pC_{\rho(0,0)}}{\beta_\rho^{p+1} \Delta\tau^{p+1} w^{2(p+1)}} \left\{ 1 - \frac{p+1}{\beta_\rho w^2} + \mathcal{O}(\kappa^2) \right\}, \tag{5.76}$$

$$\hat{U}_\theta = \frac{C_{\theta(0,0)}}{\beta_\theta^q \Delta\tau^q w^{2q}} \left\{ 1 - \frac{q}{\beta_\theta w^2} + \mathcal{O}(\kappa^2) \right\}, \tag{5.77}$$

and the background variables as

$$\frac{R}{x} = \Delta\tau^{\frac{2}{3}} w^{\frac{4}{3}} \left\{ 1 + \frac{2}{3w^2} + \mathcal{O}(\kappa^2) \right\}, \tag{5.78}$$

where

$$\beta_\theta \equiv \frac{\tau_{\theta(1)}}{\tau_{R(1)}} \quad \text{and} \quad \beta_\rho \equiv \frac{\tau_{\rho(1)}}{\tau_{R(1)}} \tag{5.79}$$

To obtain $\hat{\Delta}_\Phi$, we consider the functions $\mathcal{A}$ and $\mathcal{B}$. Using Eqs.(5.75) and (5.78), they are estimated as

$$\begin{aligned}
\mathcal{A} &= \left(\int_x^{\Lambda_1} + \int_{\Lambda_1}^{\infty} \right) dy \frac{y^4}{R^3} \hat{\Delta}_\rho \\
&= \frac{C_{\rho(0,0)}}{\tau_{R(1)} \beta_\rho^p \Delta\tau^{p+1}} \int_w^{\left(\frac{\tau_{R(1)}}{\Delta\tau}\right)^{\frac{1}{2}} \Lambda_1} \frac{dz}{z^{2p+3}} \left\{ 1 - \frac{2\beta_\rho + p}{\beta_\rho z^2} + \mathcal{O}(\kappa^2) \right\} \\
&\quad + F_1(\infty) - F_1(\Lambda_1) \\
&= \frac{C_{\rho(0,0)}}{2\tau_{R(1)} \beta_\rho^p \Delta\tau^{p+1} w^{2(p+1)}} \left\{ \frac{1}{p+1} - \frac{2\beta_\rho + p}{(p+2)\beta_\rho w^2} + \mathcal{O}(\kappa^2) \right\},
\end{aligned} \tag{5.80}$$

and

$$\begin{aligned}
\mathcal{B} &= \frac{1}{x^7} \left(\int_0^{\Lambda_2} + \int_{\Lambda_2}^{x} \right) dy y^4 \hat{\Delta}_\rho R^2 \\
&= \frac{1}{x^7} \left[F_2(\Lambda_2) - F_2(0) + \frac{C_{\rho(0,0)}}{\beta_\rho^p \tau_{R(1)}^{\frac{7}{2}} \Delta\tau^{p-\frac{29}{6}}} \right. \\
&\quad \left. \times \int_{\left(\frac{\tau_{R(1)}}{\Delta\tau}\right)^{\frac{1}{2}} \Lambda_2}^{w} \frac{dz}{z^{2p-\frac{26}{3}}} \left\{ 1 + \frac{4\beta_\rho - 3p}{3\beta_\rho z^2} + \mathcal{O}(\kappa^2) \right\} \right] \\
&= \frac{C_{\rho(0,0)}}{\beta_\rho^p \Delta\tau^{p-\frac{4}{3}} w^{2p-\frac{8}{3}}} \left\{ \frac{3}{29-6p} + \frac{4\beta_\rho - 3p}{(23-6p)\beta_\rho w^2} + \mathcal{O}(\kappa^2) \right\},
\end{aligned} \tag{5.81}$$

where Λ_1 and Λ_2 are constant numbers of order κ,

$$F_1(z) \equiv \int^z dy \frac{y^4}{R^3}\hat{\Delta}_\rho, \tag{5.82}$$

$$F_2(z) \equiv \int^z dy y^4 \hat{\Delta}_\rho R^2, \tag{5.83}$$

and we have used

$$F_1(\infty) = F_2(0) = 0, \tag{5.84}$$

$$F_1(\Lambda_1) = -\frac{C_{\rho(0,0)}\Lambda_1^2}{2(\tau_{R(1)}\Lambda_1^2)^2(\tau_{\rho(1)}\Lambda_1^2)^p}\left\{\frac{1}{p+1} - \frac{1}{p+2}\left(\frac{2}{\tau_{R(1)}} + \frac{p}{\tau_{\rho(1)}}\right)\frac{\Delta\tau}{\Lambda_1^2} + \mathcal{O}(\kappa^2)\right\}, \tag{5.85}$$

$$F_2(\Lambda_2) = C_{\rho(0,0)}\Lambda_2^7\frac{(\tau_{R(1)}\Lambda_2^2)^{\frac{4}{3}}}{(\tau_{\rho(1)}\Lambda_2^2)^p}\left\{\frac{3}{29-6p} + \frac{1}{23-6p}\left(\frac{4}{\tau_{R(1)}} - \frac{3p}{\tau_{\rho(1)}}\right)\frac{\Delta\tau}{\Lambda_2^2} + \mathcal{O}(\kappa^2)\right\}. \tag{5.86}$$

Hence from Eqs.(5.55), (5.78), (5.80) and (5.81), we obtain

$$\begin{aligned}\hat{\Delta}_\Phi = {} & \frac{C_{\rho(0,0)}}{12\tau_{R(1)}\beta_\rho^p\Delta\tau^{p-\frac{1}{3}}w^{2p-\frac{2}{3}}(p+1)(p+2)(6p-23)(6p-29)} \\ & \times\Big\{21(p+2)(6p-23) - 2(78p^2-221p+107)\frac{1}{w^2} \\ & -21p(p+1)(6p-29)\frac{1}{\beta_\rho w^2} + \mathcal{O}(\kappa^2)\Big\}.\end{aligned} \tag{5.87}$$

Substituting Eqs.(5.75)–(5.78) and (5.87) into Eq.(5.34), and equating the terms of the same order about ϵ and κ, we obtain from the lowest order,

$$q = p - \frac{4}{3}, \tag{5.88}$$

$$C_{\theta(0,0)} = -\frac{7C_{\rho(0,0)}\beta_\theta^{p-\frac{1}{3}}}{\tau_{R(1)}\beta_\rho^p(p+1)(3p-4)(6p-29)}, \tag{5.89}$$

and then from the next order

$$7(p+2)(3p-1)(6p-23)\frac{1}{\beta_\theta} - 21p(p+1)(6p-29)\frac{1}{\beta_\rho} = 2(78p^2-221p+107). \tag{5.90}$$

Further conditions are derived from the conservation law (5.32). By the same

procedure as in the above, and using Eqs.(5.88) and (5.89), we obtain

$$6(6p^2-23p-28)\beta_\theta = 7p(p+1)(3p-4)(6p-29)\frac{1}{\beta_\rho}, \tag{5.91}$$

$$8(6p^2-17p-336)\beta_\theta = 49p(p+1)^2(3p-4)(6p-29)\frac{1}{\beta_\rho^2} - 14(3p-4)(6p^2-11p-45). \tag{5.92}$$

By the numerical investigation, we find a ser of positive roots for (p, β_ρ, β_θ) of Eqs.(5.90)–(5.92) as follows;

$$p = 1.65752, \qquad \beta_\rho = 1.66227 \qquad \text{and} \qquad \beta_\theta = 1.15420 \tag{5.93}$$

Now we consider the quadrupole moment $Q(T)$ and its time-derivatives d^mQ/dT^m Note that hereafter we do not assume Eq.(5.74). In order to observe the contribution of the central singularity to d^mQ/dT^m, we consider the integrand in the right hand side of Eq.(5.62). Using Eq.(5.66), we obtain

$$\frac{\partial^m}{\partial\tau^m}\left(F'\Delta_\rho R^2\right) = I^{(m)}(\tau,x) \equiv \left(\frac{9}{4}F\right)^{\frac{2}{3}} x^4 \sum_{i=0}^{m}\binom{m}{i}\frac{\partial^i C_\rho}{\partial\tau^i}\sum_{j=0}^{m-i} C(m-i,j) \times (\tau_R-\tau)^{\frac{1}{3}(4-3j)}(\tau_\rho-\tau)^{-(p+m-i-j)}, \tag{5.94}$$

where

$$C(r,s) \equiv \frac{1}{3^s}\binom{r}{s}\prod_{k=0}^{s-1}(3k-4)\prod_{l=0}^{r-s-1}(p+l), \tag{5.95}$$

and we adopt the convention

$$\prod_{l=0}^{-1} g(l) = 1. \tag{5.96}$$

From Eq.(5.94), we find that the following relation satisfies at the moment of the central singularity formation;

$$I^{(m)}(1,x) \longrightarrow \frac{C_{\rho(0,0)}}{\tau_{R(1)}^{p+m-\frac{4}{3}}\beta_\rho^p x^{2p+2m-\frac{26}{3}}}\sum_{n=0}^{m} C(m,n)\beta_\rho^{n-m} \quad \text{for} \quad x \longrightarrow 0. \tag{5.97}$$

By Eq.(5.93), we find that $I^{(m)}$ diverges for $x \to 0$ if m is larger than or equal to three. $I^{(3)}$ is proportional to $x^{-0.65}$ near the origin and hence the integral (5.62) converges. On the other hand, since $I^{(4)}$ is proportional to $x^{-2.65}$ for $x \to 0$, the integral (5.62) becomes infinite. This means that the forth order time derivative of the quadrupole moment diverges for $\tau \to 1$ due to the central singularity formation, and is consistent with the relativistic perturbation analysis. By the quadrupole formula (5.59), the metric perturbation and the energy flux of the gravitational radiation do not diverge but the Weyl tensor due to the gravitational radiation

diverges by the central singularity formation.

In order to see the time-dependence of d^4Q/dT^4, leaving only the $i = 0$ term in the summation of Eq. (5.94), we approximate $I^{(4)}$ as

$$I^{(4)} \sim I(\tau, w) \equiv \frac{C_{\rho(0,0)}}{\tau_{R(1)}^3 \Delta\tau^{p-\frac{1}{3}}} w^6 \sum_{n=0}^{4} C(4,n)(w^2+1)^{\frac{4}{3}-n}(\beta_\rho w^2+1)^{-p-4+n} \tag{5.98}$$

The function I has a maximum absolute value at

$$w = w_{\rm m} \sim 1.3100. \tag{5.99}$$

Here it should be noted that by Eq.(5.73), the radial coordinate $x_{\rm m}$ at the maximum absolute value of I is of the order $\epsilon^{\frac{1}{2}}$ and hence our approximation (5.98) is valid at the maximum absolute value of I. From Eq.(5.98), we find

$$I(\tau, w_m) = I_{max} \equiv O(\epsilon^{\frac{1}{3}-p}) \longrightarrow \infty \quad \text{for} \quad \Delta\tau \longrightarrow 0. \tag{5.100}$$

The above result implies that the integral (5.62) is mainly determined by the contribution around $w = w_{\rm m}$. Hence we can estimate d^4Q/dT^4 by

$$\begin{aligned} \frac{d^4Q}{dT^4} &\sim \frac{1}{8\pi}\left(\frac{\Delta\tau}{\tau_{R(1)}}\right)^{\frac{1}{2}} \int_0^{w_c} I(\tau, w) dw \\ &= \frac{C_{\rho(0,0)}\Delta\tau^{\frac{5}{6}-p}}{8\pi\tau_{R(1)}^{\frac{7}{2}}} \sum_{n=0}^{4} C(4,n) \int_0^{w_c} dw w^6 (w^2+1)^{\frac{4}{3}-n}(\beta_\rho w^2+1)^{-p-4+n} \\ &\propto \Delta\tau^{-0.8242}, \end{aligned} \tag{5.101}$$

where w_c is a constant sufficiently larger than $w_{\rm m}$. The above result is also similar to the relativistic perturbation analysis.

In summary, the perturbations in the Newtonian analysis behave similar to the ones in the relativistic analysis. We summarize the power indices of the perturbation variables in Table 5.1. This similarity suggests that, at the globally naked case, the relativistic effect is not considerable until the formation of central naked singularity and Cauchy horizon.

Table 5.1: Power indices for Newtonian analysis (left column) and for relativistic numerical analysis (right column).

	$(1-\tau)^{-m}$		Δt^{-n}, $(u_0-u)^{-n}$
$\hat{\Delta}_\rho$	$m = 1.6572$	$\frac{\delta\rho}{\bar{\rho}}$	$n = 1.6$
$\hat{U}_x$	0.3239	V_1	0.4
$\hat{U}_\theta$	0.3239	V_2	0.4
$\frac{d^4Q}{dT^4}$	0.8242	Ψ_4	0.88

Chapter 6

Conclusions

The occurrence of singularity is believed to be inevitable at the final stage of the gravitational collapse. It is accepted that the singularities are not the results of assumptions of symmetries. These facts were proved by Penrose and Hawking in their singularity theorems developed between 1965 and 1970. The singularity theorems state only the existence of the singularity. We can not derive the information about the properties of the singularities from these theorems, for example, where they exist, how strong they are, and so on. Anyway, the standard understanding about singularity would be that classical general relativity is violated there. Penrose considered such a singularity should be covered by event horizon and not be visible. Then he proposed the so-called "Cosmic Censorship Hypothesis." No one has ever succeeded in the proof of this hypothesis. In such a difficult situation for proof it is worth trying to obtain counterexamples. The Lemaître-Tolman-Bondi (LTB) solution is one of the most tractable solution in the suggested counterexamples. Therefore many researchers have investigated the properties of this solution.

The LTB spacetime denotes the spherically symmetric inhomogeneous dust collapse. It seems that the LTB spacetime is unrealistic because of the assumptions of exact spherical symmetry and of the dust fluid as its matter content. In this thesis we have concerned the significance of the spherical symmetry for the naked singularity formation. We have inspected the stability of nakedness of naked singularity against the linear non-spherical perturbation of the LTB spacetime. At the same time we have paid attention to the generation of the gravitational radiation from the naked singularity.

The odd-parity perturbations have been investigated in Chap. 3. The numerical analysis for the pure gravitational-wave case shows that, outside of the Cauchy horizon associated with the globally naked singularity, the propagation of this mode is similar to that of Minkowski spacetime. Including the matter perturbations in the analysis, we have concluded that the Cauchy horizon is not destroyed by the gravitational waves while the shell-focusing naked central singularity may change its properties, for example, the divergence of the magnetic part of the Weyl curvature tensor.

In Chap. 4, we have investigated the behavior of the even-parity perturbations in the LTB spacetime. In contrast to the results of the odd-parity mode, the numerical analysis for the even-parity perturbations shows that the Cauchy horizon

should be destroyed by the even-parity gravitational radiation. The energy flux of this radiation, however, is finite for an observer at constant circumferential radius outside of the dust cloud. Therefore the inhomogeneous aspherical dust collapse is not expected to the strong source of gravitational wave burst.

The difference between the odd and even modes seems to originate from the properties of matter perturbations. The odd-parity matter perturbations are produced by the rotational motion of the dust cloud and the evolution of them decouples from the evolution of metric perturbations. On the other hand, the even-parity matter perturbations contain the radial motion of dust fluids and the evolution of them couple to the metric perturbations. These two modes, the odd and even-parity, couple to each other when we consider the second order perturbations.

Newtonian approximation analysis has been performed in Chap. 5. We estimate the even-parity gravitational waves and Weyl scalar by the quadrupole formula. The results have significant similarity to the relativistic analysis. This fact suggests that relativistic effects are not effective for the behavior of perturbations outside of the Cauchy horizon of the globally naked LTB spacetime.

The main conclusion of this thesis is that the spherically symmetric collapse is insufficient for the counterexample of CCH. Non-sphericity has ability to change drastically the final fate of the gravitational collapse from that of the spherically symmetric collapse. Therefore we should consider well the significance of the investigations into the spherical collapse in the context of the counterexample to the CCH. The possibility of gravitational wave burst from the naked singularity cannot be supported by our perturbation analysis. The non-linear or full-relativistic analysis of the non-spherical collapse is important to get more deep insight into the above problems. Unfortunately, we cannot answer the problem how do we see a naked singularity. There are other channels to investigate the observational effects of the naked singularity, e.g., electro-magnetic radiation, emission due to quantum effects, and so on.

Appendix A

Gauge-Invariant Perturbations

In this appendix we give a brief introduction to the formalism of Gerlach and Sengupta [84, 85] for perturbations around the most general spherically symmetric spacetime.

We consider the general spherically symmetric spacetime with a metric

$$g_{\mu\nu}dx^\mu dx^\nu \equiv g_{ab}(x^d)dx^a dx^b + R^2(x^d)\gamma_{AB}(x^D)dx^A dx^B, \tag{A.1}$$

and stress-energy tensor

$$t_{\mu\nu}dx^\mu dx^\nu \equiv t_{ab}(x^d)dx^a dx^b + \frac{1}{2}t_A{}^A R^2(x^d)\gamma_{AB}(x^D)dx^A dx^B, \tag{A.2}$$

where $\gamma_{AB}dx^A dx^B = d\theta^2 + \sin^2\theta d\phi^2$. Lower-case latin indices refer to radial and time coordinate, while capital latin indices refer to θ and ϕ.

Now we introduce an arbitrary perturbation of this spacetime. The angular dependence of perturbations is decomposed into series of tensorial spherical harmonics. The scalar spherical harmonics are $Y_l^m(x^A)$. A basis of vector harmonics is formed by $Y_{l:A}^m$ and $S_l^m{}_A \equiv \epsilon_A{}^B Y_{l:B}^m$. A basis of symmetric rank-two tensor harmonics is formed by $Y_l^m\gamma_{AB}$, $Z_l^m{}_{AB} \equiv Y_{l:AB}^m + \frac{l(l+1)}{2}Y_l^m\gamma_{AB}$ and $S_l^m{}_{A:B} + S_l^m{}_{B:A}$. For $l = 0, 1$ the last two tensors vanish identically. Linear perturbations with different l and m decouple. In the following we consider one value of l and m, and we suppress these indices. We also suppress the explicit summation over them. Perturbations with different values of m for the same l have the same dynamics on a spherically symmetric background, so that m will never appear in the field equations. Spherical harmonics are called even if they have parity $(-1)^l$ under spatial inversion and odd if they have parity $(-1)^{l+1}$. Even and odd perturbations decouple each other.

The odd-parity perturbations are expressed in the form

$$h_{\mu\nu}dx^\mu dx^\nu = h_a^{(o)}(x^c)S_B(dx^a dx^B + dx^B dx^a) + h^{(o)}(x^c)S_{(A:B)}dx^A dx^B, \tag{A.3}$$

for metric and

$$\Delta t_{\mu\nu}dx^\mu dx^\nu = \Delta t_a^{(o)}(x^c)S_A(dx^a dx^A + dx^A dx^a) + \Delta t^{(o)}(x^c)S_{(A:B)}dx^A dx^B, \tag{A.4}$$

for matter. The even-parity perturbations are

$$\begin{aligned} h_{\mu\nu} &= h_{ab}(x^d)Y dx^a dx^b + h_a(x^d)Y_{:B}(dx^a dx^B + dx^B dx^a) \\ &\quad +[K(x^d)R^2\gamma_{AB}Y + G(x^d)R^2 Z_{AB}]dx^A dx^B, \end{aligned} \tag{A.5}$$

for metric and

$$\begin{aligned} \Delta t_{\mu\nu} &= \Delta t_{ab}(x^d)Y dx^a dx^b + \Delta t_a(x^d)Y_{:B}(dx^a dx^B + dx^B dx^a) \\ &\quad +[\Delta t^3(x^d)R^2\gamma_{AB}Y + \Delta t^2(x^d)R^2 Z_{AB}]dx^A dx^B, \end{aligned} \tag{A.6}$$

for matter where $Y \equiv Y_l^m(x^D)$ are the scalar spherical harmonics and $Z_{AB} = Y_{:AB} + \frac{l(l+1)}{2}Y\gamma_{AB}$. Here covariant derivatives are distinguished as follows:

$$\gamma_{AB:C} \equiv 0, \qquad g_{ab|c} \equiv 0. \tag{A.7}$$

For the convenience of expression, we introduce

$$v_a \equiv R_{,a}/R, \tag{A.8}$$

and

$$p_a \equiv h_a - \frac{1}{2}R^2 G_{,a}. \tag{A.9}$$

We then introduce the gauge-invariant variables to eliminate gauge ambiguities in perturbations. The gauge transformation is induced by the infinitesimal vector fields:

$$\xi_\mu dx^\mu = M(x^c)S_A dx^A, \tag{A.10}$$

for odd-parity and

$$\xi_\mu dx^\mu = \xi_a(x^c)Y dx^a + \xi(x^c)Y_{:A}dx^A, \tag{A.11}$$

for even-parity. The odd-parity metric variables are given by

$$k_a \equiv h_a^{(o)} - \frac{1}{2}R^2\partial_a\left(\frac{h^{(o)}}{R^2}\right) \tag{A.12}$$

The odd-parity matter variables are given by the combinations

$$L_a \equiv t_a^{(o)} - \frac{1}{2}\bar{T}_B{}^B h_a^{(o)}, \tag{A.13}$$

$$L \equiv t^{(o)} - \frac{1}{2}\bar{T}_B{}^B h^{(o)} \tag{A.14}$$

A set of even-parity gauge-invariant metric perturbations is defined as

$$k_{ab} \equiv h_{ab} - (p_{a|b} + p_{b|a}), \tag{A.15}$$

$$k \equiv K + \frac{l(l+1)}{2}G - 2v^a p_a. \tag{A.16}$$

A set of even-parity gauge-invariant matter perturbations is defined as

$$
\begin{aligned}
T_{ab} &\equiv \Delta t_{ab} - t_{ab|c}p^{c} - t_{a}{}^{c}p_{c|b} - t_{b}{}^{c}p_{c|a}, && \text{(A.17)}\\
T_{a} &\equiv \Delta t_{a} - t_{a}{}^{c}p_{c} - R^{2}(t_{A}{}^{A}/4)G_{,a}, && \text{(A.18)}\\
T^{3} &\equiv \Delta t^{3} - (p^{c}/R^{2})(R^{2}t_{A}{}^{A}/2)_{,c} + l(l+1)(t_{A}{}^{A}/4)G, && \text{(A.19)}\\
T^{2} &\equiv \Delta t^{2} - (R^{2}t_{A}{}^{A}/2)G. && \text{(A.20)}
\end{aligned}
$$

The linearized Einstein equations, expressed only in gauge-invariant perturbations, are

$$
k^{a}{}_{|a} = 16\pi L \qquad (l \geq 2), \tag{A.21}
$$

$$
-\left[R^{4}\left(\frac{k_{a}}{R^{2}}\right)_{|c} - R^{4}\left(\frac{k_{c}}{R^{2}}\right)_{|a}\right]^{|c} + (l-1)(l+2)k_{a} = 16\pi R^{2}L_{a} \ (l \geq 1), \tag{A.22}
$$

for odd-parity, and

$$
\begin{aligned}
&2v^{c}\left(k_{ab|c} - k_{ca|b} - k_{cb|a}\right) - \left[\frac{l(l+1)}{R^{2}} + G_{c}{}^{c} + G_{A}{}^{A} + 2\mathcal{R}\right]k_{ab}\\
&-2g_{ab}v^{c}\left(k_{ed|c} - k_{ce|d} - k_{cd|e}\right)g^{ed} + g_{ab}\left(2v^{c|d} + 4v^{c}v^{d} - G^{cd}\right)k_{cd}\\
&+g_{ab}\left[\frac{l(l+1)}{R^{2}} + \frac{1}{2}\left(G_{c}{}^{c} + G_{A}{}^{A}\right) + \mathcal{R}\right]k_{d}{}^{d} + 2\left(v_{a}k_{,b} + v_{b}k_{,a} + k_{,a|b}\right)\\
&-g_{ab}\left[2k_{,c}{}^{|c} + 6c^{c}k_{,c} - \frac{(l-1)(l+2)}{R^{2}}k\right] = -16\pi T_{ab},
\end{aligned} \tag{A.23}
$$

$$
k_{,a} - k_{ac}{}^{|c} + k_{c}{}^{|}{}_{|a} - v_{a}k_{c}{}^{c} = -16\pi T_{a}, \tag{A.24}
$$

$$
\begin{aligned}
&-\left(k_{,c}{}^{|c} + 2v^{c}k_{,c} + G_{A}{}^{A}k\right) + \left[k_{cd}{}^{|c|d} + 2v^{c}k_{cd}{}^{|d} + 2(v^{c|d} + v^{c}v^{d})k_{cd}\right]\\
&-g_{ab}\left[k_{c}{}^{c}{}_{|d}{}^{|d} + v^{c}k_{d}{}^{d}{}_{|c} + \mathcal{R}k_{c}{}^{c} - \frac{l(l+1)}{R^{2}}k\right] = -16\pi T^{3},
\end{aligned} \tag{A.25}
$$

$$
k_{c}{}^{c} = -16\pi T^{2}, \tag{A.26}
$$

for even-parity where $\mathcal{R}$ is the Gaussian curvature of the 2-dimensional submanifold M^{2} spanned by x^{a} and

$$
G_{ab} \equiv -2\left(v_{a|b} + v_{a}v_{b}\right) + g_{ab}\left(2v_{a}{}^{|a} + 3v_{a}v^{a} - \frac{1}{R^{2}}\right), \tag{A.27}
$$

$$G_A{}^A \equiv 2\left(v_a{}^{|a} + v_a v^a - \mathcal{R}\right) \tag{A.28}$$

The linearized conservation equation ($\delta(T^{\mu\nu}{}_{\nu}) = 0$) reduce to

$$\left(R^2 L^a\right)_{|a} = (l-1)(l+2)\,L \qquad (l \geq 1), \tag{A.29}$$

for odd-parity and

$$\frac{(R^2 T^a)_{|a}}{R^2} + T^3 - \frac{(l-1)(l+2)}{2R^2} T^2 = \frac{1}{2} t_A{}^A \left(k - \frac{1}{2} k_c{}^c\right) + \frac{1}{2} t^{ab} k_{ab}, \tag{A.30}$$

$$\begin{aligned} \frac{(R^2 T_{ab})^{|b}}{R^2} - \frac{T_a l(l+1)}{R^2} - 2v_a T^3 = {} & \frac{1}{2} k_{bc|a} t^{bc} + k_{cb}^{|b} t^c{}_a - \frac{1}{2} k_c{}^c{}_{|b} t^b{}_a \\ & - k_{,c} t^c{}_a + \frac{1}{2}(k_{,a} - k v_a)\, t_A{}^A \\ & + 2v^b k_{bc} t^c{}_a + k^b{}_c t^c{}_{a|b}, \end{aligned} \tag{A.31}$$

for even-parity.

Appendix B

Power of Gravitational Radiation

In this appendix we examine the asymptotic behavior of the gauge-invariant variables in the asymptotically flat spacetime with out-going wave condition. Then we can calculate the radiated power of the gravitational waves and thereby we grasp the physical meaning of the gauge-invariant quantities.

Note that in vacuum at large distance, the spherically symmetric background metric is identical to the Schwarzschild solution, where hereafter we adopt the Schwarzschild coordinates,

$$ds^2 = -\left(1-\frac{2M}{R}\right)d\tau^2 + \left(1-\frac{2M}{R}\right)^{-1} dR^2 + R^2\left(d\theta^2 + \sin^2\theta d\phi^2\right) \tag{B.1}$$

To relate the perturbation of the metric to the radiated gravitational power, it is useful to specialize to the radiation gauge, in which the tetrad components $h_{(\theta)(\theta)} - h_{(\phi)(\phi)}$ and $h_{(\theta)(\phi)}$ fall off as $O(1/R)$, and all other tetrad components fall off as $O(1/R^2)$ or faster w.r.t. the following background tetrad basis:

$$e^a_{(\tau)} = \left(1-\frac{2M}{R}\right)^{1/2}(d\tau)^a, \tag{B.2}$$

$$e^a_{(R)} = \left(1-\frac{2M}{R}\right)^{-1/2}(dR)^a, \tag{B.3}$$

$$e^a_{(\theta)} = R(d\theta)^a, \tag{B.4}$$

$$e^a_{(\phi)} = R\sin\theta(d\phi)^a \tag{B.5}$$

In this radiation gauge, the metric perturbations in Eqs. (A.3) and (A.5) behave as

$$h_0, h_1 = O\left(\frac{1}{R}\right), \tag{B.6}$$

$$h_2 = w(\tau - R_*) + O(1), \tag{B.7}$$

for the odd-parity and as

$$h_{ab} = O\left(\frac{1}{R^2}\right), \tag{B.8}$$

$$h_a = O\left(\frac{1}{R}\right), \tag{B.9}$$

$$K = O\left(\frac{1}{R^2}\right), \tag{B.10}$$

$$G = \frac{g(\tau - R_*)}{R} + O\left(\frac{1}{R^2}\right), \tag{B.11}$$

for the even-parity where

$$R_* = R + 2M \ln\left(\frac{R}{2M} - 1\right) + \text{const}, \tag{B.12}$$

and the out-going wave condition is respected. Then, the gauge-invariant metric perturbations (A.15) and (A.16) are calculated as

$$k_0 = -\frac{1}{2} w^{(1)} R + O(1), \tag{B.13}$$

$$k_1 = \frac{1}{2} w^{(1)} R + O(1), \tag{B.14}$$

for odd-parity, and

$$k_{\tau\tau} = g^{(2)} R + O(1), \tag{B.15}$$

$$k_{\tau R} = -g^{(2)} R + O(1), \tag{B.16}$$

$$k_{RR} = g^{(2)} R + O(1), \tag{B.17}$$

$$k = -g^{(1)} + O\left(\frac{1}{R}\right), \tag{B.18}$$

for even-parity, where $w^{(n)}$ and $g^{(n)}$ denotes the nth derivative of$w$ and g with respect to its argument, respectively.

In this radiation gauge, the radiated power P per unit solid angle is given by the formula derived by Landau and Lifshitz [88] from their stress-energy pseudo-tensor:

$$\frac{dP}{d\Omega} = \frac{R^2}{16\pi}\left[\left(\frac{\partial h_{(\theta)(\phi)}}{\partial \tau}\right)^2 + \frac{1}{4}\left(\frac{\partial h_{(\theta)(\theta)}}{\partial \tau} - \frac{\partial h_{(\phi)(\phi)}}{\partial \tau}\right)^2\right] \tag{B.19}$$

For the axisymmetric mode, i.e. $m = 0$, the above formula is reduced to

$$\frac{dP}{d\Omega} = \frac{1}{64\pi}(w^{(1)})^2 A_l(\theta), \tag{B.20}$$

for the odd-parity, and

$$\frac{dP}{d\Omega} = \frac{1}{64\pi}(g^{(1)})^2 A_l(\theta), \tag{B.21}$$

for the even-parity, where

$$A_l(\theta) \equiv \frac{2l+1}{4\pi} \sin^4\theta \left(\frac{d^2 P_l(\cos\theta)}{(d\cos\theta)^2} \right)^2 \tag{B.22}$$

It is found that, for the monopole and dipole modes, the radiate power exactly vanishes. By using the gauge-invariant quantities and integrating over all solid angles, the formula for the power of the gravitational radiation of $l \geq 2$ is obtained in the following form:

$$\frac{dP}{d\Omega} = \frac{1}{16\pi}\frac{k_0^2}{R^2} A_l(\theta) = \frac{1}{16\pi}\frac{k_1^2}{R^2} A_l(\theta), \tag{B.23}$$

$$P = \frac{1}{16\pi} B_l \frac{k_0^2}{R^2} = \frac{1}{16\pi} B_l \frac{k_1^2}{R^2}, \tag{B.24}$$

for the odd-parity, and

$$\frac{dP}{d\Omega} = \frac{1}{64\pi} k^2 A_l(\theta), \tag{B.25}$$

$$P = \frac{1}{64\pi} B_l k^2, \tag{B.26}$$

for even-parity, where

$$B_l \equiv \frac{(l+2)!}{(l-2)!}. \tag{B.27}$$

Appendix C

Equations and Coefficients

C.1 Even-Parity Equations of Marginally Bound LTB Spacetime

For marginally bound LTB spacetime linearized quadrupole Einstein equations are

$$\begin{aligned} &\frac{4}{R^2}q + \frac{1}{RR'}q' + \frac{\dot{R}}{R}\dot{q} \\ -\frac{6}{R^2}k + \left(\frac{2}{RR'} - \frac{R''}{R'^3}\right)k' - \left(2\frac{\dot{R}}{R} + \frac{\dot{R}'}{R'}\right)\dot{k} + \frac{1}{R'^2}k'' \\ +2\left(\frac{\dot{R}}{R^2R'} - \frac{\dot{R}R''}{RR'^3} + \frac{\dot{R}'}{RR'^2}\right)k_{01} + 2\frac{\dot{R}}{RR'^2}k_{01}' &= -8\pi\delta\rho, \end{aligned} \tag{C.1}$$

$$-\frac{\dot{R}}{R}q' + \frac{R'}{R}\dot{q} + \left(2\frac{\dot{R}}{R} - \frac{\dot{R}'}{R'}\right)k' + \dot{k}' - \frac{3}{R^2}k_{01} = -8\pi\bar{\rho}V_1, \tag{C.2}$$

$$\begin{aligned} 2\frac{R'^2}{R^2}q - \frac{R'}{R}q' - \frac{R'^2\dot{R}}{R}\dot{q} + 4\frac{R'^2\dot{R}}{R}\dot{k} + R'^2\ddot{k} \\ -2\frac{R'\dot{R}}{R^2}k_{01} - 2\frac{R'}{R}k_{01} &= 0, \end{aligned} \tag{C.3}$$

$$-2\frac{\dot{R}'}{R'}q - \dot{q} + 2\frac{\dot{R}'}{R'}k + 2\dot{k} + \frac{R''}{R'^3}k_{01} - \frac{1}{R'^2}k_{01}' = -16\pi\bar{\rho}V_2, \tag{C.4}$$

$$q' + k_{01} + \frac{\dot{R}'}{R'}k_{01} = 0, \tag{C.5}$$

$$\left(\frac{R^2R''}{R'^3} - 2\frac{R}{R'}\right)q' - \left(2R\dot{R} + 3\frac{R^2\dot{R}'}{R'}\right)\dot{q} - \frac{R^2}{R'^2}q'' - R^2\ddot{q}$$

$$+4\left(R\dot{R}+\frac{R^2\dot{R}'}{R'}\right)\dot{k}+2R^2\ddot{k}+2\left(\frac{RR''\dot{R}}{R'^3}-\frac{R\dot{R}'}{R'^2}\right)k_{01}$$
$$-2\frac{R\dot{R}}{R'^2}k_{01}{}'+2\left(\frac{R^2R''}{R'^3}-\frac{R}{R'}\right)k_{01}-2\frac{R^2}{R'^2}\dot{k_{01}'} = 0, \quad \text{(C.6)}$$

$$-k_{00}+\frac{1}{R'^2}k_{11} = 0. \quad \text{(C.7)}$$

Here we use Eq. (C.7) to eliminate k_{11} in Eqs. (C.1)–(C.6).

C.2 Coefficients of Differential Equations

The coefficients of Eqs. (4.16)–(4.20) are

$$a_1 = \frac{1}{R}-\frac{\dot{R}}{R}-4\frac{R''}{R'^2}+\frac{5}{2}\frac{\dot{R}'}{R'}, \quad \text{(C.8)}$$
$$a_2 = 2\frac{R'^3}{R^2}\left(R\dot{R}'-R'\dot{R}\right), \quad \text{(C.9)}$$
$$a_3 = 3\frac{R'^2\dot{R}^2}{R^2}-3\frac{R'\dot{R}\dot{R}'}{R}, \quad \text{(C.10)}$$
$$a_4 = -4\frac{R'^4\dot{R}^2}{R^3}+12\frac{R'^3\dot{R}\dot{R}'}{R^2}-8\frac{R'^2\dot{R}'^2}{R}, \quad \text{(C.11)}$$
$$a_5 = -3\frac{R'}{R}-\frac{1}{4}\frac{R'\dot{R}^2}{R}+\frac{1}{2}\dot{R}\dot{R}', \quad \text{(C.12)}$$
$$b_1 = -\frac{1}{R'^4}, \quad \text{(C.13)}$$
$$b_2 = -8\frac{\dot{R}}{R}+8\frac{\dot{R}'}{R'}, \quad \text{(C.14)}$$
$$b_3 = 0, \quad \text{(C.15)}$$
$$b_4 = -7\frac{\dot{R}^2}{R^2}+28\frac{\dot{R}\dot{R}'}{RR'}-20\frac{\dot{R}'^2}{R'^2}, \quad \text{(C.16)}$$
$$b_5 = -\frac{3}{R'^3}-4\frac{\dot{R}}{R'^3}-\frac{9}{2}\frac{\dot{R}^2}{R'^3}+4\frac{R\dot{R}'}{R'^4}+4\frac{R\dot{R}\dot{R}'}{R'^4}, \quad \text{(C.17)}$$
$$c_1 = -\frac{1}{R'^2}, \quad \text{(C.18)}$$
$$c_2 = 0, \quad \text{(C.19)}$$
$$c_3 = -5\frac{\dot{R}}{R}+6\frac{\dot{R}'}{R'}, \quad \text{(C.20)}$$
$$c_4 = 0, \quad \text{(C.21)}$$
$$c_5 = -\frac{1+\dot{R}}{R'}, \quad \text{(C.22)}$$

$$d_1 = 0, \tag{C.23}$$
$$d_2 = 1, \tag{C.24}$$
$$d_3 = 0, \tag{C.25}$$
$$d_4 = 0, \tag{C.26}$$
$$d_5 = \frac{R\left(1+\dot{R}\right)}{R'^3}, \tag{C.27}$$
$$e_1 = \frac{1}{R}, \tag{C.28}$$
$$e_2 = 0, \tag{C.29}$$
$$e_3 = 2\frac{R'}{R^2}\left(R'\dot{R} - R\dot{R}'\right), \tag{C.30}$$
$$e_4 = 0, \tag{C.31}$$
$$e_5 = 7\frac{R''}{R'} - 3\frac{R'}{R}\left(1+\dot{R}\right) + 5\dot{R}'. \tag{C.32}$$

Bibliography

[1] C. W. Misner, K. S. Thorne, and J. A. Wheeler, *Gravitation*, W. H. Freeman and Company, 1973.

[2] A. Einstein, Die Grundlage der allgemeinen Relativitatstheorie (Foundation of the General Theory of Relativity), Annalen Phys. **49**, 769–822 (1916).

[3] C. J. S. Clarke, *The Analysis of Space-Time Singularities*, Cambridge University Press, Camgridge, England, 1993.

[4] R. Penrose, Gravitational collapse and space-time singularities, Phys. Rev. Lett. **14**, 57–59 (1965).

[5] S. W Hawking, The occurence of singularity in cosmology. III. Causality and singularities, Proc. Roy. Soc. Lond. **A300**, 187–201 (1967).

[6] S. W. Hawking and R. Penrose, The Singularities of gravitational collapse and cosmology, Proc. Roy. Soc. Lond. **A314**, 529–548 (1970).

[7] S. W Hawking and G. F. Ellis, *The large scale structure of space-time*, Cambridge, 1973.

[8] R. Penrose, Gravitational collapse: The role of general relativity, Riv. Nuovo Cim. **1**, 252–276 (1969).

[9] R. Penrose, Singularities and Time Asymmetry, In Hawking, S.W., Israel, W.: General Relativity, 581- 638.

[10] R. M. Wald, *General Relativity*, The University of Chicago Press, Chicago USA, 1984.

[11] C. J. S. Clarke, A title of cosmic censorship, Classical and Quantum Gravity **11**(6), 1375–1386 (1994).

[12] P. S. Joshi, Gravitational collapse, gr-qc/9702036 (1997).

[13] T. P. Singh, Gravitational collapse, black holes and naked singularities, gr-qc/9805066 (1997).

[14] R. M. Wald, Gravitational collapse and cosmic censorship, gr-qc/9710068 (1997).

[15] T. Harada, *Final Fate of Generic Gravitational Collapse – Is Shell-Focusing Naked Singularity Realized?* –, PhD thesis, Kyoto University, 1999.

[16] C. V Vishveshwara, Stability of the Schwarzschild Metric, Phys. Rev. **D1**, 2870–2879 (1970).

[17] R. H. Price, Nonspherical perturbations of relativistic gravitational collapse. 1. Scalar and gravitational perturbations, Phys. Rev. **D5**, 2419–2438 (1972).

[18] R. M. Wald, Gedanken Experiments to Destroy a Black Hole, Annals Phys. **82**, 548–556 (1974).

[19] I. Semiz, Dyon black holes do not violate cosmic censorship, Class. Quant. Grav. **7**, 353 (1990).

[20] M. Simpson and R. Penrose, Internal instability in a Reissner-Nordström black hole, Int. J. Theor. Phys. **7**, 183–197 (1973).

[21] J. M. McNamara, Instability of black hole inner horizon, Proc. Roy. Soc. Lond. **A358**, 499–515 (1978).

[22] J. M. McNamara, Behaviour of scalar perturbations of a Reissner-Nordström black hole inside the event horizon, Proc. Roy. Soc. Lond. **A364**, 121 (1978).

[23] S. Chandrasekhar and J. B. Hartle, On Crossing the Cauchy Horizon of a Reissner-Nordström Black Hole, Proc. Roy. Soc. Lond. **A384**, 301–315 (1982).

[24] E. Poisson and W. Israel, Internal structure of black holes, Phys. Rev. **D41**, 1796 (1990).

[25] A. Ori, Evolution of scalar field perturbations inside a Kerr black hole, Phys. Rev. **D58**, 084016 (1998).

[26] K. S. Thorne, Nonspherical Gravitational Collapse: A Short Review, In *J R Klauder, Magic Without Magic*, San Francisco 1972, 231-258.

[27] R. Schoen and S. T. Yau, The Existence of a Black Hole Due to Condensation of Matter, Commun. Math. Phys. **90**, 575 (1983).

[28] J. R. Oppenheimer and H. Snyder, On Continued gravitational contraction, Phys. Rev. **56**, 455–459 (1939).

[29] G. Lemaître, L'universe en expansion, Ann. Soc. Sci. Bruxelles **A53**, 51–85 (1933).

[30] R. C. Tolman, Effect of inhomogeneity on cosmological models, Proc. Natl. Acad. Sci. **20**, 169–176 (1934).

[31] H. Bondi, Spherically Symmetric Models in General Relativity, Mon. Not. R. Astron. Soc. **107**, 410–425 (1999).

[32] P. Yodzis, H. J. Seifert, and H. Müller zum Hagen, On the occurrence of naked singularities in general relativity, Commun. Math. Phys. **34**, 135–148 (1973).

[33] H. Müller zum Hagen, P. Yodzis, and H. J. Seifert, On the occurence of naked singularities in general relativity II, Commun. Math. Phys. **37**, 29–40 (1974).

[34] D. M. Eardley and L. Smarr, Time function in numerical relativity. Marginally bound dust collapse, Phys. Rev. **D19**, 2239–2259 (1979).

[35] D. Christodoulou, Violation of Cosmic Censorship in the Gravitational Collapse of a Dust Cloud, Commun. Math. Phys. **93**, 171–195 (1984).

[36] R. P. A. C. Newman, Strengths of naked singularities in Tolman-Bondi spacetimes, Classical and Quantum Gravity **3**(4), 527–539 (1986).

[37] P. S. Joshi and I. H. Dwivedi, Naked singularities in spherically symmetric inhomogeneous Tolman-Bondi dust cloud collapse, Phys. Rev. **D47**, 5357–5369 (1993).

[38] S. Jhingan and P S. Joshi, The Structure of singularity in spherical inhomogeneous dust collapse, in *Internal structure of Black holes and singularities*, edited by L. M. Burko and A. Ori, page 357, 1997.

[39] A. Ori and T. Piran, Naked Singularities in Selfsimilar Spherical Gravitational Collapse, Phys. Rev. Lett. **59**, 2137 (1987).

[40] A. Ori and T. Piran, Naked Singularities and Other Features of Selfsimilar General Relativistic Gravitational Collapse, Phys. Rev. **D42**, 1068–1090 (1990).

[41] P. S. Joshi and I. H. Dwivedi, The Structure of Naked Singularity in Self-Similar Gravitational Collapse, Commun. Math. Phys. **146**, 333–342 (1992).

[42] T. Harada, Final fate of the spherically symmetric collapse of a perfect fluid, Phys. Rev. **D58**, 104015 (1998).

[43] B. K. Datta, Non-Static Spherically Symmetric Clusters of Particles in General Relativity: I, Gen. Rel. Grav. **1**, 19 (1970).

[44] H. Bondi, On Datta's Spherically Symmetric Systems in General Relativity, Gen. Rel. Grav. **2**, 321 (1971).

[45] A. B. Evans, Relativistic Dynamics of Spherical Counter-Rotating Dust Bodies, Gen. Rel. Grav. **8**, 155 (1976).

[46] T. Harada, H. Iguchi, and K. Nakao, Naked singularity formation in the collapse of a spherical cloud of counterrotating particles, Phys. Rev. **D58**, 041502 (1998).

[47] G. Magli, Gravitational collapse with non-vanishing tangential stresses: a generalization of the Tolman Bondi model, Classical and Quantum Gravity **14**(7), 1937–1953 (1997).

[48] G. Magli, Gravitational collapse with non-vanishing tangential stresses: II. A laboratory for cosmic censorship experiments, Classical and Quantum Gravity **15**(10), 3215–3228 (1998).

[49] T. P. Singh and L. Witten, Cosmic censorship and spherical gravitational collapse with tangential pressure, Class. Quant. Grav. **14**, 3489 (1997).

[50] S. Barve, T. P. Singh, and L. Witten, Spherical gravitational collapse: Tangential pressure and related equations of state, gr-qc/9901080 (1999).

[51] T. Harada, K. Nakao, and H. Iguchi, Nakedness and curvature strength of shell focusing singularity in the spherically symmetric space-time with vanishing radial pressure, Class. Quant. Grav. **16**, 2785 (1999).

[52] I. H. Dwivedi and P S. Joshi, On the occurrence of naked singularity in spherically symmetric gravitational collapse, Commun. Math. Phys. **166**, 117–128 (1994).

[53] P. S. Joshi and I. H. Dwivedi, Initial data and the end state of spherically symmetric gravitational collapse, Class. Quant. Grav. **16**, 41 (1999).

[54] D. Christodoulou, The Problem of a Selfgravitating Scalar Field, Commun. Math. Phys. **105**, 337 (1986).

[55] D. Christodoulou, Global Existence of Generalized Solutions of the Spherically Symmetric Einstein Scalar Equations in the Large, Commun. Math. Phys. **106**, 587 (1986).

[56] D. Christodoulou, The Formation of Black Holes and Singularities in Spherically Symmetric Gravitational Collapse, Commun. Pure Appl. Math. **44**, 339 (1991).

[57] D. Christodoulou, Bounded Variation Solutions of the Spherically Symmetric Einstein-Scalar Field Equations, Commun. Pure Appl. Math. **46**, 1131 (1993).

[58] D. Christodoulou, Examples of naked singularity formation in the gravitational collapse of a scalar field, Annals Math. **140**, 607 (1994).

[59] M. W. Choptuik, Universality and scaling in gravitational collapse of a massless scalar field, Phys. Rev. Lett. **70**, 9–12 (1993).

[60] P. S. Joshi and A. Krolak, Naked strong curvature singularities in Szekeres space- times, Class. Quant. Grav. **13**, 3069–3074 (1996).

[61] S. S. Deshingkar, S. Jhingan, and P. S. Joshi, On the global visibility of singularity in quasispherical collapse, Gen. Rel. Grav. **30**, 1477 (1998).

[62] S. L. Shapiro and S. A. Teukolsky, Formation of naked singularities: The violation of cosmic censorship, Phys. Rev. Lett. **66**, 994 (1991).

[63] S. L. Shapiro and S. A. Teukolsky, Gravitational collapse of rotating spheroids and the formation of naked singularities, Phys. Rev. **D45**, 2006 (1992).

[64] R. M. Wald and V. Iyer, Trapped surfaces in the Schwarzschild geometry and cosmic censorship, Phys. Rev. **D44**, R3719–R3722 (1991).

[65] C. Barrabès, W. Israel, and P. S. Letelier, Analytic models of nonspherical collapse, cosmic censorship and the hoop conjecture, Phys. Lett. **A160**, 41–44 (1991).

[66] M. A. Pelath, K. P. Tod, and R. M. Wald, Trapped surfaces in prolate collapse in the Gibbons-Penrose construction, Class. Quant. Grav. **15**, 3917 (1998).

[67] T. Nakamura, M. Shibata, and K. Nakao, Naked Singularity Dries Up?, Prog. Theor. Phys. **89**, 821–832 (1993).

[68] T. A. Apostolatos and K. S. Thorne, Rotation halts cylindrical, relativistic gravitational collapse, Phys. Rev. **D46**, 2435–2444 (1992).

[69] F Echeverria, Gravitational collapse of an infinite, cylindrical dust shell, Phys. Rev. **D47**, 2271 (1993).

[70] T. Chiba, Cylindrical Dust Collapse in General Relativity —*Toward Higher Dimensional Collapse* —, Prog. Theor. Phys. **95**, 321–338 (1996).

[71] C. W. Misner and D. H. Sharp, Relativistic Equations for Adiabatic, Spherically Symmetric Gravitational Collapse, Phys. Rev. **136**, B571–B576 (1964).

[72] T. P. Singh and P. S. Joshi, The Final fate of spherical inhomogeneous dust collapse, Class. Quant. Grav. **13**, 559–572 (1996).

[73] S. Jhingan, P. S. Joshi, and T. P. Singh, The Final fate of spherical inhomogeneous dust collapse. 2. Initial data and causal structure of singularity, Class. Quant. Grav. **13**, 3057–3068 (1996).

[74] S. Barve, T. P. Singh, C. Vaz, and L. Witten, Particle creation in the marginally bound, selfsimilar collapse of inhomogeneous dust, Nucl. Phys. **B532**, 361 (1998).

[75] C. T. Cunningham, R. H. Price, and V Moncrief, Radiation from Collapsing Relativistic Stars. II. Linearized Odd-Parity Radiation, Astrophys. J. **224**, 643 (1978).

[76] C. T. Cunningham, R. H. Price, and V Moncrief, Radiation from Collapsing Relativistic Stars. II. Linearized Even-Parity Radiation, Astrophys. J. **230**, 870 (1979).

[77] C. T. Cunningham, R. H. Price, and V. Moncrief, Radiation from Collapsing Relativistic Stars. III Second Order Perturbations of Collapse with Rotation, Astrophys. J. **236**, 674 (1980).

[78] E. Seidel and T. Moore, Gravitational radiation from realistic relativistic Stars: Odd-parity fluid perturbations, Phys. Rev. **D35**, 2287 (1987).

[79] E. Seidel, E. S. Myra, and T. Moore, Gravitational radiation from type-II supernovae: The effect of the high-density equation of state, Phys. Rev. **D38**, 2349 (1988).

[80] E. Seidel, Gravitational radiation from even parity perturbations of stellar collapse: Mathematical formalism and numerical methods, Phys. Rev. **D42**, 1884 (1990).

[81] M. M. May and R. H. White, Hydrodynamic Calculations of General-Relativistic Collapse, Phys. Rev. **141**, 1232–1241 (1966).

[82] H. Iguchi, K. Nakao, and T. Harada, Gravitational waves around a naked singularity: Odd parity perturbation of Lemaître-Tolman-Bondi space-time, Phys. Rev. **D57**, 7262–7273 (1998).

[83] H. Iguchi, T. Harada, and K. Nakao, Gravitational Radiation from a Naked Singularity — Odd-Parity Perturbation —, Prog. Theor. Phys. **101**, 1235–1252 (1999).

[84] U. H. Gerlach and U. K. Sengupta, Gauge Invariant Perturbations on Most General Spherically Symmetric Space-Times, Phys. Rev. **D19**, 2268 (1979).

[85] U. H. Gerlach and U. K. Sengupta, Gauge Invariant Coupled Gravitational, Acoustical, and Electromagnetic Modes on Most General Spherical Space-Times, Phys. Rev. **D22**, 1300 (1980).

[86] J. M. Bardeen and T. Piran, General Relativistic Axisymmetric Rotating System: Coordinates and Equations, Phys. Rept. **205**, 205 (1983).

[87] S. Chandrasekhar and S. Detweiler, The quasi-normal modes of the Schwarzschild black hole, Proc. Roy. Soc. Lond. **344**, 441–452 (1975).

[88] L. D. Landau and E. M. Lifshitz, *The Classical Theory of Fields*, Pergamon, London, 4th edition, 1975.

[89] H. Iguchi, T. Harada, and K. Nakao, Gravitational Radiation from a Naked Singularity — Even-Parity Perturbation —, Prog. Theor. Phys. **103** (2000).